

**ANTI-TUMOR ACTIVITY, PHARMACOLOGY AND
TOXICOLOGY OF EPCAM/CD3-BISPECIFIC SIN-
GLE-CHAIN ANTIBODIES**

Dissertation der

**Fakultät für Biologie der
Ludwig-Maximilians-Universität
München**

Vorgelegt von

**Diplom-Biologin
Maria Amann**

Ehrenwörtliche Erklärung

Hiermit erkläre ich, dass ich die vorliegende Dissertation selbständig und ohne unerlaubte Hilfe angefertigt habe. Ich habe weder anderweitig versucht, eine Dissertation einzureichen oder eine Doktorprüfung durchzuführen, noch habe ich diese Dissertation oder Teile derselben einer anderen Prüfungskommission vorgelegt.

München,

Die vorliegende Arbeit wurde zwischen Juli 2005 und Februar 2009 unter der Anleitung von Prof. Dr. Patrick A. Bäumler in der Firma Micromet AG, München, durchgeführt.

Wesentliche Teile dieser Arbeit sind veröffentlicht in:

Amann M, Brischwein K, Lutterbuese P, et al. Therapeutic window of MuS110, a single-chain antibody construct bispecific for mouse EpCAM and mouse CD3. *Cancer Res.* 2008; 68: 143-51.

Amann M, Friedrich M, Lutterbuese P, et al. Therapeutic window of an EpCAM/CD3-specific BiTE antibody in mice is determined by a subpopulation of EpCAM-expressing lymphocytes that is absent in humans. *Cancer Immunol Immunother.* 2009; 58: 95-109.

Amann M, d'Árgouges S, Lorenczewski G, et al. Anti-tumor activity of an EpCAM/CD3-bispecific BiTE antibody during long-term treatment of mice in the absence of T cell anergy and cytokine release. *J Immunother.* in press.

Teile dieser Arbeit (Text und Abbildungen) sind daher diesen Veröffentlichungen entlehnt.

Promotionsgesuch eingereicht am:	23.05.2009
Tag der mündlichen Prüfung:	15.12.2009
Erster Gutachter:	Prof. Dr. Elisabeth Weiß
Zweiter Gutachter:	Prof. Dr. Berit Jungnickel
Sondervotum:	Prof. Dr. A. Patrick Bäumler

CONTENTS

1	SUMMARY	1
2	INTRODUCTION	3
2.1	Epithelial Cell Adhesion Molecule (EpCAM) and its role in cancer.....	3
2.1.1	Structure and tissue distribution.....	3
2.1.2	Biological functions of EpCAM	4
2.1.3	EpCAM as a prognostic carcinoma marker and its role in cancer	7
2.1.4	Therapeutic antibodies targeting EpCAM in cancer	8
2.2	The concept of bispecific T cell engagers (BiTEs)	10
2.2.1	Structure of BiTEs.....	10
2.2.2	Mode of action of BiTEs	11
2.2.3	MT110 and muS110	13
3	AIM OF THIS STUDY	17
4	MATERIAL AND METHODS	18
4.1	Material.....	18
4.1.1	Cell lines	18
4.1.2	Mouse strains	20
4.1.3	Reagents, media and enzymes.....	20
4.1.4	Kits.....	22
4.1.5	Buffer.....	23
4.1.6	Antibodies	23
4.1.7	BiTEs.....	24
4.1.8	Equipment	25
4.1.9	Software.....	26
4.2	Methods	27
4.2.1	Cell culture.....	27
4.2.2	Preparation of leukocytes.....	27
4.2.2.1	Isolation of PBMC from human and mouse blood	27
4.2.2.2	Isolation of mouse leukocytes from spleen and lymph nodes	28
4.2.2.3	Enrichment of CD3 cells	28
4.2.2.4	Negative isolation of CD3 cells	28
4.2.2.5	Stimulation of T cells	29
4.2.3	Cell staining and FACS analysis.....	29
4.2.3.1	FACS analysis of cell surface proteins	30
4.2.3.2	FACS analysis of intracellular proteins	30
4.2.3.3	FACS analysis of whole blood	31
4.2.4	Labeling of target cells	31
4.2.4.1	PKH staining	31
4.2.4.2	CFSE labeling	31
4.2.5	Cytotoxicity assay	32
4.2.5.1	ToxiLight assay	32
4.2.5.2	Caspase assay	33
4.2.5.3	FACS based assay	34
4.2.6	Determination of cytokine concentration	35

4.2.7	TGF- β enzyme linked immuno sorbent assay (ELISA)	36
4.2.8	Determination of whole blood cell count	36
4.2.9	Depletion of EpCAM ⁺ cells from mouse splenocytes and PBMC	37
4.2.10	Analysis of BiTE serum concentrations	38
4.2.10.1	Bioassay based BiTE quantification	38
4.2.10.2	BiTE quantification with Meso Scale Discovery (MSD)	39
4.2.11	Saturation binding analysis and calculation of receptor occupancy.....	39
4.2.12	Histopathology	40
4.2.13	Mouse models and <i>in vivo</i> work.....	41
4.2.13.1	Housing	41
4.2.13.2	Monitoring of health, body weight and temperature	41
4.2.13.3	Application techniques	42
4.2.13.4	Blood sampling	42
4.2.13.5	Tumor models	43
4.2.13.6	Dissection, isolation of organs and fixation	44
5	RESULTS.....	46
5.1	<i>In vitro</i> characterization of muS110	46
5.1.1	Binding affinities of muS110 to CD3 and EpCAM	46
5.1.2	Redirected lysis of respective target cells mediated by muS110	47
5.1.3	T cell activation mediated by muS110	49
5.1.3.1	Cell proliferation in cytotoxicity assays	49
5.1.3.2	Up-regulation of T cell activation marker induced by muS110	51
5.1.3.3	Cytokine release induced by muS110	55
5.2	Pharmaco-toxicological effects of muS110 <i>in vivo</i>	57
5.2.1	Characterization of single dose administration	57
5.2.1.1	Adverse effects induced by a single dose of muS110	57
5.2.1.2	Systemic T cell activation induced by a single dose of muS110	58
5.2.1.3	Transient systemic cytokine release induced by a single dose of muS110	59
5.2.1.4	Peripheral lymphocytopenia induced by a single dose of muS110	61
5.2.1.5	Comparison of pharmaco-toxicological effects of muS110, KT3 and 145-2C11	63
5.2.2	Histopathological analysis of mice repeatedly treated with muS110....	66
5.2.3	EpCAM ⁺ mouse lymphocytes.....	67
5.2.3.1	Presence of EpCAM ⁺ cells in mouse but not in human lymphocytes	67
5.2.3.2	Dependence of muS110-induced T cell activation on EpCAM ⁺ lymphocytes	69
5.2.4	Characterization of multiple dose administrations	72
5.2.4.1	Adverse effects induced by repetitive doses of muS110	72
5.2.4.2	Cytokine release induced by repetitive muS110 treatment	73
5.2.4.3	Cytotoxic T cells induced by repetitive doses of muS110	76
5.2.5	Increased muS110 tolerability and immune modulation	78
5.2.5.1	Tolerability increase of muS110 after <i>in vivo</i> depletion of EpCAM ⁺ lymphocytes	78
5.2.5.2	<i>Ex vivo</i> T cell activation after repeated administration of muS110	82
5.2.5.3	Cytotoxic and proliferative capacity of T cells after repeated administration of muS110	84
5.2.6	Impact of glucocorticoids on muS110 tolerability <i>in vivo</i>	87
5.3	<i>In vivo</i> efficacy	92
5.3.1	MuS110 efficacy and toxicity in mouse pulmonary metastasis models	92
5.3.2	MuS110 efficacy and toxicity in an orthotopic 4T1 breast cancer model	97
6	DISCUSSION.....	100

6.1	The bioactivity of muS110.....	100
6.2	MuS110 as murine surrogate of MT110.....	101
6.3	The therapeutic window of muS110.....	103
6.3.1	First dose response to muS110.....	103
6.3.2	Adaptation to repeated injections of muS110.....	108
6.3.3	Efficacy.....	115
7	ABBREVIATIONS	117
8	ACKNOWLEDGEMENTS.....	121
9	CURRICULUM VITAE	122

1 SUMMARY

The Epithelial Cell Adhesion or Activating Molecule (EpCAM, CD326) was selected as a target for a multitude of immunotherapeutic approaches treating human malignancies. However, EpCAM is also expressed on various non-malignant cells. So far, all well tolerated drug candidates suffer from weak efficacy, whereas severe systemic side effects accompany more potent immunotherapies. Thus, to prevent clinical failure, a new systemic immunotherapy targeting EpCAM requires adequate pre-clinical models to study the efficacy in the face of systemic tolerability.

MT110 is an antibody of the BiTE format and represents a new systemic immunotherapeutic approach targeting EpCAM⁺ tumors. BiTEs are bispecific single chain antibodies recruiting the high cytotoxic potential of T cells to eradicate cancer cells. With one of its two specific binding sites MT110 attaches to the pan T cell antigen CD3 ϵ and with the other one to the EpCAM antigen present on tumor cells. This physical link induces an immunological synapse, leading to the death of the adjacent cancer cell.

MT110 promises good potency in clinical use, as it shows high anti-tumor efficacy in xenograft models established in immune deficient NOD/SCID mice grafted with human T cells. However, due to its species-specific reactivity mouse models are not adequate to directly evaluate toxicological effects of MT110 in immune competent hosts. This demanded the development of the mouse specific surrogate muS110. Analogous to MT110, muS110 redirects mouse T cells to lyse mouse EpCAM positive tumor cells. The following study describes the *in vitro* characterization of muS110 as well as the *in vivo* evaluation of its efficacy and tolerability. The primary and secondary pharmacology of muS110 were analyzed with special emphasize on its influence on T cell functions.

In the presence of target cells muS110 led *in vitro* to a dose dependent proliferation of T cells, cytokine secretion, up-regulation of activation markers, and a transformation of resting to cytotoxic effector T cells, resulting in the specific elimination of EpCAM positive target cells. In quality and quantity muS110 mediated T cell activation was similar to that obtained by a full anti-CD3/CD28 stimulation in the presence of IL-2.

To the extent possible, muS110 was constructed to yield structural and biological characteristics similar to those of drug candidate MT110. MuS110 has comparable affinity to the EpCAM antigen and binds to the orthologous epitope in mouse as MT110 does in human. With

respect to EpCAM expression, a significant overlap was found between mouse and human tissues. However, a key difference was EpCAM expression on mouse lymphocytes, which was not seen on human lymphocytes.

In vivo muS110 induced a dose dependent onset of side effects including hemoconcentration, hypomotility, piloerection, body weight reduction, hypothermia and diarrhea up to 24 hours after injection. Most probably, these adverse side effects were caused by a transient release of inflammatory cytokines through T cells, systemically activated by an encounter with EpCAM⁺ lymphocytes and muS110. No lesions were found in healthy EpCAM⁺ tissue, which seemed to be non-accessible for BiTE induced lysis. All observed clinical signs were previously described for mice in response to agonistic anti-CD3 monoclonal antibodies and termed anti-CD3-induced acute syndrome.

All dose-dependent side effects were self-limiting and animals adapted to repetitive treatment with muS110. This phenomenon was already observed after treatment with anti-CD3 antibodies. However, the cause of adaptation was different for BiTE and conventional anti-CD3 antibodies.

MuS110 induced only very transient lymphocytopenia but most probably no T cell depletion, no down-modulation of the TCR/ CD3 complex, no immune deviation to a TH₂ immune response and no anergy of T cells. However, it led to a transient, not IL-2 reversible block of cytokine secretion upon *in vitro* re-stimulation in T cells. *In vivo* administration led to a persistent release of IL-10, an expansion of CD4⁺CD25⁺FoxP3⁺ regulatory T cells in the spleen and an increase of the CD8⁺/CD4⁺ ratio in the blood. This might be indicative for the involvement of regulatory cells in the adaptation to muS110, which, however, had no negative impact on muS110 mediated lysis of EpCAM⁺ target cells. These immune modulating effects together with the elimination of EpCAM⁺ lymphocytes over time might be the reason for adaptation to repeated treatment with muS110.

The adaptation to muS110 was implemented in a dose escalation scheme to improve the anti-tumor efficacy. Thus, a higher, but still well tolerated drug load was achieved in mice. Thereby, muS110 showed an exceptionally good efficacy against solid 4T1 tumors. It led to a 99% reduction of these rapid and aggressive tumors in immune competent mice and prevented outgrowth in five of six mice totally. This might resemble the assumable therapeutic window of MT110 in humans and would promise high clinical potential.

2 INTRODUCTION

2.1 Epithelial Cell Adhesion Molecule (EpCAM) and its role in cancer

2.1.1 Structure and tissue distribution

The Epithelial Cell Adhesion or Activating Molecule (EpCAM, CD326) was not only the first human tumor-associated antigen discovered, but also the target of the first monoclonal antibody (mAb17-1A, later named edrecolomab and Panorex[®]) applied in cancer therapy (1-4). Identification of closely related sequences in all mammalian and avian genomes indicates an important functional role of EpCAM (5). Due to its versatile functions and its status as pan-carcinoma marker it was independently discovered several times and is known under many synonyms as 17-1A, 323/A3, AUA1, CD326, CO-17A, EGP2, EGP34, EGP40, Ep-CAM, ESA, GA733-2, HEA125, KSA, KS1/4, MH99, MK-1, MOC31, TACST-1, Trop1, amongst others (2, 6, 7). A recently revised structure model is shown in Figure 1 (2).

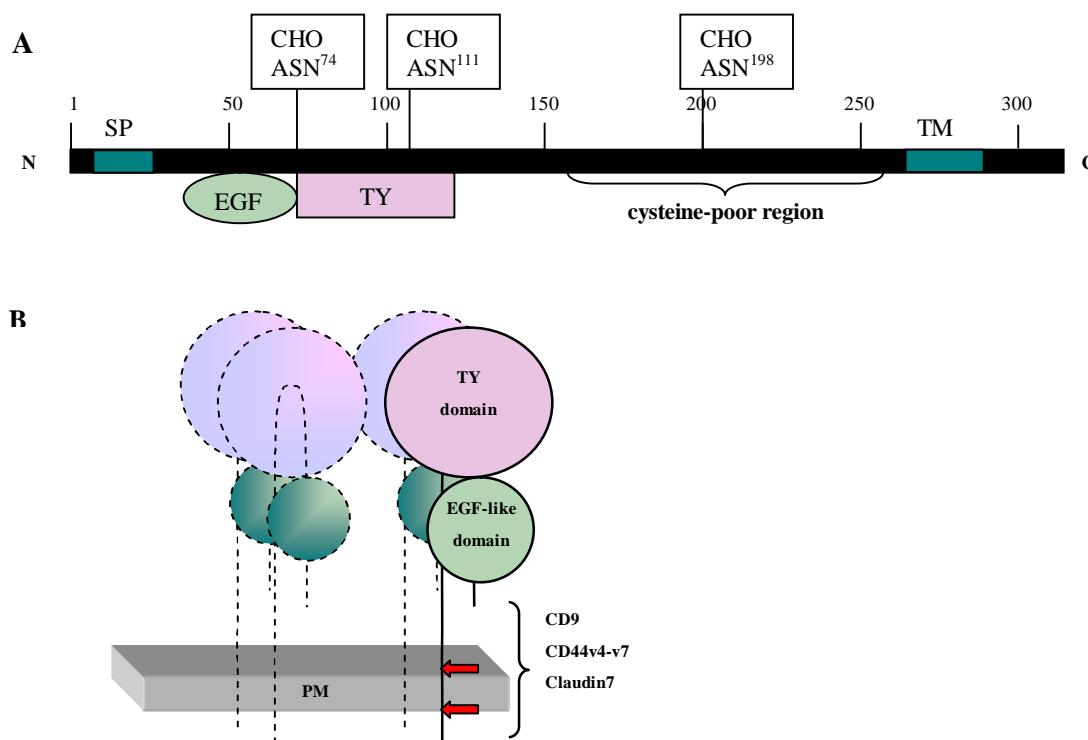


Figure 1: Structural model of EpCAM (according to Baeuerle and Gires (2))

(A) EpCAM is shown with N- (N) and C-terminus (C), signal peptide (SP), transmembrane domain (TM), N-linked carbohydrates (CHO), EGF-like domain (EGF) and thyroglobulin repeat domain (TY). (B) EpCAM is depicted as a tetramer showing three additional subunits with dotted lines. Cleavage sites for two proteases releasing the intracellular portion of EpCAM are indicated by red arrows, and the domain of EpCAM interacting with the listed proteins is shown with a bracket. Plasma membrane (PM)

EpCAM is a 40 kDa transmembrane glycoprotein (314 aa) located in the basolateral plasma membrane of epithelial cells. It consists of a short cytoplasmatic domain (26 aa) containing two α -actinin binding sites, a single transmembrane domain (23 aa) and three extracellular domains (242 aa; SP=23 aa) with three N-glycosylation sites (8). The external portion consists of an epidermal growth factor (EGF) like repeat and a thyroglobulin (TY) repeat domain followed by a cysteine-poor domain (2, 5, 9). Most likely EpCAM forms dimers and tetramers at the cell surface (9).

In healthy individuals, EpCAM is expressed in almost all simple, pseudo stratified and transitional epithelial cells but not in mature squamous epithelia. It is considered to be a marker for cells of epithelial lineage (10). Exceptions are some fully differentiated epithelial derived cell types, like keratinocytes, hepatocytes, thymic cortical epithelia, gastric parietal cells and myoepithelial cells. EpCAM is not expressed by mesodermal or neural cell membranes, neurons, stromal cells, endothelial cells, syncytiotrophoblasts and bone marrow derived cells (except on plasma B cells and thymic T cells in mice) (6).

2.1.2 Biological functions of EpCAM

Initially, EpCAM was described as a Ca^{2+} -independent homophilic cell adhesion molecule (CAM) of the group of type 1 transmembrane proteins (11). It can form homophilic cell-cell interactions with molecules on surrounding epithelial cells via its EGF-like domain. The TY-like domain mediates lateral interactions of EpCAM molecules (12). The short cytoplasmic tail links EpCAM to the actin cytoskeleton (8, 13).

However, EpCAM is structurally not related to any of the four archetypal families of CAMs, the cadherines, the selectins, the integrins or the immunoglobulin (Ig) cell adhesion molecule superfamily (7). EpCAM is distributed equally on the basolateral plasma membrane of polarized epithelial cells. It is neither enriched in any of the major types of cell adhesion structures, like tight junctions, adhesive junctions, desmosomes or hemidesmosomes, nor does it form any structures similar to those mentioned above (8). The cell-cell adhesion mediated by EpCAM is weak in comparison to that of other CAMs, and there is not sufficient evidence that EpCAM mediated adhesion is required for epithelial cell support (8, 11).

Beside their direct mechanical role as interconnectors of cells, CAMs also constitute an important group of signal-transducing molecules. They are responsible for a variety of dynamic processes in cell proliferation, migration and differentiation (14). It has been shown that EpCAM is strongly associated with cellular proliferation and inhibition of terminal epithelial

differentiation in developing pancreatic islet cells and a transformed keratinocyte cell line (14-18). However, the current knowledge of EpCAM's function in tissue morphogenesis and morphogenetic movements of cells is still incomplete. Identified ligands and possible EpCAM related functions are summarized in Figure 2 after Trzpis et al. (7).

EpCAM seems to play a morphoregulatory role in embryogenesis, as it is already expressed in the first developmental stages (19). It is detected in fetal lung, kidney (proximal tubes), liver, pancreas, skin, and germ cells (8). In the initial phases of morphogenesis it is expressed by epithelial precursor cell as well as by cells not yet assigned to a certain cell fate. In later stages of epithelial development, EpCAM acquires a strictly epithelial specific expression, whereas in terminally differentiated cells EpCAM expression is lost (7). Small bile duct canaliculi in the adult liver express EpCAM, whereas hepatocytes and large bile ducts are negative for EpCAM (15). The germinal regions of the colonic mucosal lining in colonic crypts display high EpCAM expression, which steadily decreases as cells differentiate and migrate to the top of the villi (20). Progenitor cells of skin epithelium express EpCAM, whereas differentiated cells do not (21).

One mode of EpCAM's function in morphogenesis might be its negative impact on E-cadherin, one of the major morphoregulatory molecules in epithelia (14). EpCAM is thought to affect the connection between the cadherin adhesion complexes and the cytoskeleton, as it binds to p85, the regulatory subunit of the Phosphatidylinositol 3 kinase (PI3K) (14, 22). PI3K is known to bind to α -actin and down-regulate cadherin-mediated cell adhesion (10). Consequently, upon EpCAM induction, cadherin-mediated adhesion is replaced by the weaker EpCAM-mediated adhesion. Inhibition of cadherin-mediated adhesion, however, is associated with poor differentiation, increased invasiveness and metastasis formation of tumors. In contrast, silencing of EpCAM expression by small interfering RNA rescued functionality of E-cadherin, α and β -catenin in different breast cancer cell lines. The increased cadherin-mediated cell-to-cell adhesion correlated well with a decrease in proliferation, cell migration and invasion (23).

Thus, EpCAM can weaken tight cell-cell adhesions and modulate proliferation, differentiation and migration. A disturbed regulation of these processes in neoplastic cells could result in an increased metastatic capacity. Hence, it might explain the promotional effect of EpCAM overexpression upon metastasis, although its nature as CAM would rather argue for a negative impact (24).

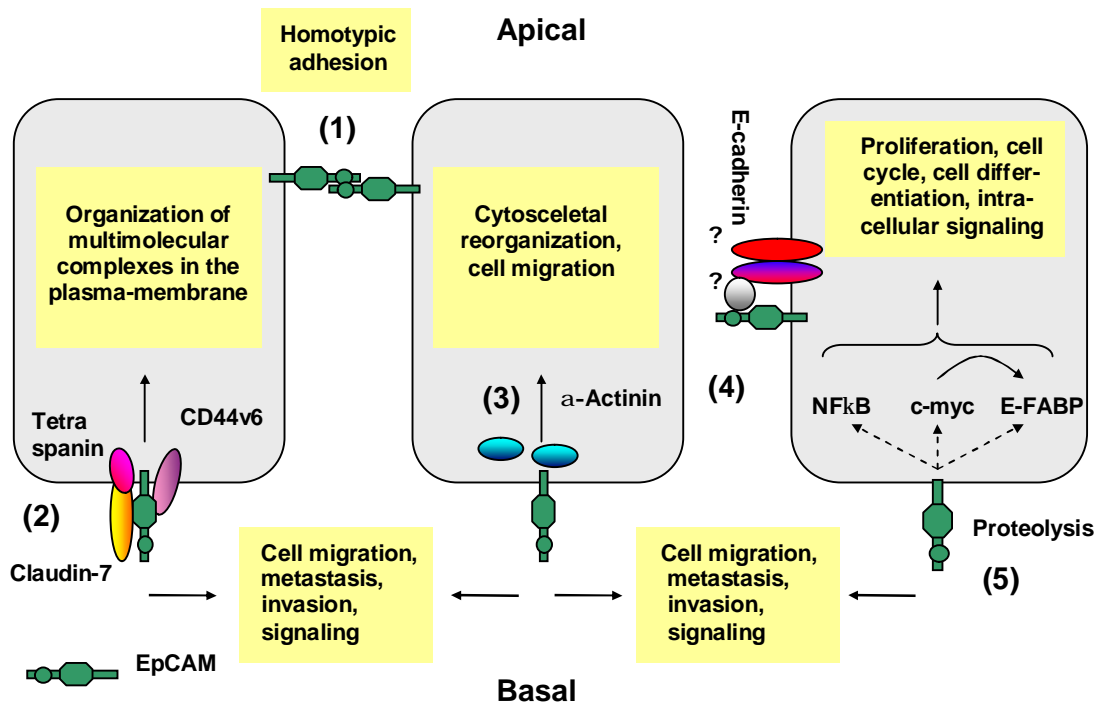


Figure 2: Schematic representation of identified EpCAM ligands and their possible functions (according to Trzpis et al. (7))

(1) The extracellular domain of EpCAM interacts with a second EpCAM molecule resulting in homotypic cell-cell adhesion. (2) EpCAM forms a complex with tetraspanins, e.g. CD9 or D6.1A, with CD44v4-v7 (carcinoma associated variants of CD44) and with claudin-7, a protein required for the formation of tight junctions. This complex is recruited to tetraspanin enriched membrane domains and promotes apoptosis resistance and enhanced metastasis. (3) (4) Direct interactions of α -actinin with the intracellular domain of EpCAM links this molecule to the cytoskeletal organization. (4) EpCAM indirectly associates with E-cadherin. The adaptor proteins that facilitate this complex formation are yet to be identified (5) EpCAM modulates the expression of NF- κ B, c-myc, and E-FABP. The interplay of EpCAM with E-cadherin (4) and the CD9/CD44v4-v7/claudin-7 complex (2), as well as the influence of EpCAM on NF- κ B, c-myc, and E-FABP (5) provides a link for its involvement in cell migration, metastasis, and cell signaling. E-FABP, epidermal fatty acid-binding protein.

EpCAM can act as a signaling molecule on its own as well. Signaling was found to be induced either by soluble EpCAM or through zones of cell-cell contact, suggesting that its own oligomerisation might be a trigger. These signals led to a cleavage of EpCAM, releasing an intracellular protein termed EpIC. EpIC in turn binds to intracellular adaptor molecules, forming a multi-protein signaling complex translocated to the nucleus. This complex is involved in target gene induction and growth-promoting effects (2). Consistent with its role as an oncogene, overexpression of EpCAM can induce upregulation of the proto-oncogene c-myc and promote cell proliferation via upregulated synthesis of cyclin A and E (25). It was also shown that upregulation of EpCAM decreased growth factor requirement and enhanced the colony

forming capacity of cells, which are prerequisites for cancer stem cells (25, 26). Interestingly, EpCAM surface expression is enhanced upon cell cycle arrest by various chemotherapeutics (27). Immunotherapy targeting EpCAM⁺ cells might therefore address chemotherapy resistant, slowly dividing cancer stem cells.

2.1.3 EpCAM as a prognostic carcinoma marker and its role in cancer

EpCAM is not only present on cancer stem cells, but high levels of EpCAM are found in most of the major human malignancies, i.e. epithelial carcinomas of colon, lung, prostate, liver, pancreas, breast and ovary as summarized in Table 1 according to Balzar et al. (8, 28, 29).

However, EpCAM expression in tumors itself can be heterogeneous, and is probably negatively affected by a shift from tumor cell differentiation to either mesenchymal or squamous cell phenotypes (8). EpCAM is not expressed on neurogenic tumors, sarcomas, lymphomas or melanomas (30).

Table 1: EpCAM expression in human malignancies (according to Balzar et al. (8, 28, 29))

Most carcinomas express EpCAM whereas tumors derived from non-epithelial tissues are EpCAM negative. The level of EpCAM expression is indicated by (–) for no expression, (+) for low expression levels, (++) for intermediate expression levels and (+++) for high expression levels. Data on distribution and expression levels was obtained from multiple studies using different EpCAM specific monoclonal antibodies (mAb).

Type of Tumor	EpCAM Expression
Carcinoma of small intestine, colorectal adenocarcinoma, lung carcinoma, adenocarcinoma of cervix	+++
Oral mucosal basal cell carcinoma, gastric adenocarcinoma, pancreatic carcinoma, cholangiocarcinoma (liver), biliary duct carcinoma, basal cell carcinoma of skin, renal cell carcinoma, transitional cell carcinoma of bladder, thyroid carcinoma, prostate carcinoma, ovarian carcinoma, endometrium carcinoma, squamous cell carcinoma of cervix, mammary carcinoma, epithelioid mesotheliomas	++
Oral mucosal squamous cell carcinoma, laryngeal (squamous cell) carcinoma, esophageal (squamous cell) carcinoma,	+
Germ cell tumor, Wilm's tumor (epithelial component)	+/-
Melanom, sarcoma, lymphoma, meningioma, non-epithelioid mesotheliomas, squamous cell carcinoma of skin, hepatocellular carcinoma (liver)	-

Tumors originating from epithelial cells over-express EpCAM, e.g. gastric carcinoma, or express it *de novo*, e.g. hepatocellular carcinoma. *De novo* expression can be detected already in precursors of carcinomas of squamous epithelia and serves as an early marker for (pre-) malignancies (17, 31). The number of EpCAM expressing cell and the grade of EpCAM (over)expression increases with the grade of neoplasia and dysplasia. Its overexpression usually correlates with poor prognosis for instance in ampullary carcinoma of the pancreas, squamous cell cancer of head and neck, squamous cell carcinoma of the esophagus, breast cancer, gall bladder cancer and ovarian cancer (32-36). However, some patients over-expressing EpCAM show prolonged survival in clear cell renal cell carcinoma and in gastric carcinoma (37-40). Finally, in prostate and lung cancers intensity of EpCAM expression has no impact on prognosis (41, 42). Therefore, the prognostic value of EpCAM is still controversial although it is clearly considered to be a pan-carcinoma marker.

Experiments addressing the role of EpCAM in metastasis reveal contradictory results. Surface expression of EpCAM on disseminated tumor cells was shown to be increased. EpCAM overexpression promotes metastasis in fibrosarcomas (24) and is required for proliferation, migration and invasiveness of breast cancer cell lines (23, 43). Additionally, a complex formed by EpCAM with the CD44 isoform v6, the tetraspanins CO-029 or CD9, and the tight junction protein claudin-7 facilitates metastasis formation in colorectal cancer cells (Figure 2) (12, 44, 45). The presence of this complex also correlated inversely with disease free survival and directly with apoptosis resistance. On the other hand, carcinoma cells disseminated from their primary tumor and circulating in the blood stream had ten times reduced EpCAM expression in comparison to cells within the primary tumor (43, 46). Furthermore, Songun et al. found a correlation between a loss of EpCAM expression in stomach cancer and enhanced malignancy. They consider this to be due to enhanced metastasis of carcinoma cells upon loss of EpCAM (37). Went et al. argue that similarly to the CAM CD44, both, tumor environment and expression level of EpCAM, might determine the outcome of its adhesive or anti-adhesive and mitogenic effects and either block or facilitate metastasis (47, 48).

2.1.4 Therapeutic antibodies targeting EpCAM in cancer

EpCAM is a prime target for immunotherapies in the major human malignancies. The most common human cancers show a low frequency of EpCAM negative tumors and mostly an insignificant influence of tumor staging on EpCAM expression. In an EpCAM⁺ tumor, EpCAM expressing cells represent normally a high percentage of resident cells (49). EpCAM was selected as a target antigen in a multitude of immunotherapeutic approaches. This in-

cludes vaccines, mouse and human mAbs and antibody conjugates with bacterial toxins and chemotherapeutics (8). Currently, a number of EpCAM specific immunotherapies are in phase I and II clinical trials. These are the anti-EpCAM antibodies ING-1, adecatumumab, and edrecolomab, as well as the locally applied immunotoxin proxinium and some locally applied tri-specific approaches recruiting cytotoxic cells to EpCAM⁺ tumor cells (50-56).

Edrecolomab is a well-tolerated low affinity mouse antibody against EpCAM, which was temporarily marketed in Germany. A significant increase in overall survival of colorectal cancer patients was found in the adjuvant setting in two of four trials. But the short half-life, the rapid neutralization of the drug by a humoral immune response against the mouse antibody, and a borderline clinical activity asked for further development (57-60). Administration of this antibody induced the production of neutralizing anti-idiotypic antibodies. Their efficacy was analyzed in clinical trials using small amounts of edrecolomab as a subcutaneously administered vaccine called IGN101. Only in a subgroup of stage IV rectal cancer patients a significant survival benefit was observed. No significant impact was observed in the majority of patients in a double-blind placebo controlled phase II trial in several carcinoma indications (2). ING-1 is a high-affinity monoclonal antibody. A phase I trial in patients with advanced adenocarcinoma caused acute pancreatitis with severe abdominal pain, nausea, and vomiting. The risk of pancreatitis and the marginal anti-tumor effect precluded further monotherapy studies (50, 61). Adecatumumab (MT201) is a fully human anti-EpCAM antibody, currently analyzed in two phase II studies with metastatic breast cancer and early-stage prostate cancer, as well as in a phase I study testing the safety of a combination with the chemotherapeutic agent docetaxel (Taxotere®). So far the human antibody was well tolerated and no signs of pancreatitis were found (51).

Catumaxomab is a hybrid mouse/rat antibody, generated by the hybrid-hybridoma technique. It is tri-specific for EpCAM, CD3 and via its Fc portion for antigen-presenting cells as well as NK cells. Phase I clinical trials analyzing intraperitoneal administration to ovarian cancer patients suffering from ascites and peritoneal carcinomatosis, showed profound clinical activity. Catumaxomab appears to be a promising agent for the local treatment of peritoneal carcinomatosis, but systemic treatment was hampered by systemic intolerability (2, 55). This was also observed for the hybrid antibodies HEA125xCD3, recruiting CD3 positive T cells, and HEA125x197, recruiting activated neutrophils and monocytes, using a similar tri-specific approach to kill EpCAM positive cancer cells. HEA125xCD3 showed an inhibition of ascites

production in 8 of 10 patients in ovarian cancer patients. A dramatic, 1000 fold increase of local TNF- α concentration indicated a very strong local inflammatory response (2, 56).

Proxinium is a stability-engineered, single-chain humanized anti-EpCAM antibody fused to a subunit of the bacterial *Pseudomonas* exotoxin. It is currently in a phase II/III trial for local treatment of head and neck cancer. In former phase I/II phase trials in head and neck cancer proxinium had positive impact on overall survival and showed 88% response rate. Currently an improved immunotoxin is under development with a replacement of the furin cleavage site by a metalloproteinases-2 and -9 cleavage site. These metalloproteinases are selectively expressed by tumor cells and might improve the therapeutic window of the immunotoxin (2, 53).

EpCAM is expressed on various sides on normal epithelial tissue as well as on cancer cells. Low affinity EpCAM binders showed only a borderline clinical activity (57-60). High affinity EpCAM binders induced pancreatitis, gastrointestinal toxicity and collateral damage of normal EpCAM-expressing tissues (61, 62). Systemic intolerability of tri-specific formats and immunotoxins led to mostly local usage in cancer therapy (2). Therefore, finding a therapeutic window of EpCAM specific drugs with profound clinical activity and good systemic tolerability is still a major concern for researchers. Thus, appropriate pre-clinical models are mandatory, to evaluate the efficacy and toxicity of newly developed systemic immunotherapies targeted against EpCAM.

2.2 The concept of bispecific T cell engagers (BiTEs)

2.2.1 Structure of BiTEs

BiTE antibodies are designed to direct cytotoxic T cells against tumor cells and represent a different therapeutic approach in cancer immunotherapy. The BiTE protein consists of a single polypeptide chain of approximately 55 kDa length, which is folded into two tandemly arranged single-chain antibody fragments (scFv). These are of different specificity and connected by a flexible peptide linker. The scFv is build up by a variable domain of a heavy chain (V_H) linked by a stretch of synthetic peptides to a variable domain of a light chain (V_L) and resemble a truncated Fab fragment of a conventional antibody. One scFv recognizes CD3 ϵ , which is a common T cell signaling molecule and part of the T cell receptor (TCR). The other scFv shows specificity for the tumor cell antigen of interest. The basic design of a BiTE antibody and its structural relationship to its two parental mAb molecules is depicted in Figure 3 (63).

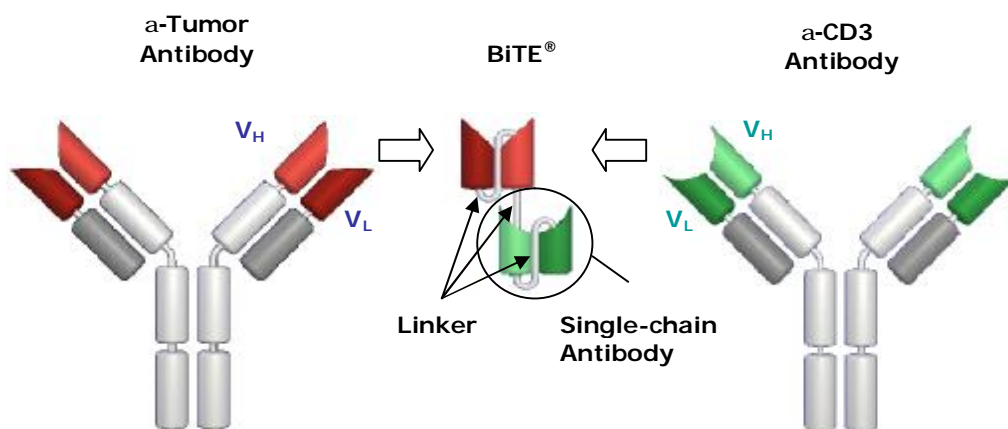


Figure 3: Structural relationship of BiTE antibody to its parental monoclonal antibodies

Generation of a BiTE antibody is principally shown. Note that only variable V_H and V_L domains of antibodies are used and all other non-binding parental antibody parts are spared. Linkers connect V_H and V_L domains to create single chain antibody fragments (scFv). A second linker joins two scFv of different specificity to form a BiTE antibody. The flexible linkers enable free rotation and kinking of the two scFv arms to bind to two epitopes on different cells at once. Recombinant DNA technology is used to combine the four different gene products into one gene coding for a single, bispecific protein.

The scFv consist only of the variable regions of the heavy and the light chain domains of their respective parental antibodies. Any other part that is not necessary for antigen binding is avoided to minimize immunogenicity (64). The scFv are joined by a short linker that allows for a much closer approximation of opposing cells than it is possible with larger bispecific formats such as quadroma antibodies (65). The flexible linkage is expected to enable free rotation and kinking of the two scFv arms. Thus, simultaneous recognition of two epitopes present on two opposing cell membranes is possible (66). The low molecular mass of bispecific antibodies might facilitate penetration into tumors, as it has been shown for Fab or Fv antibody fragments (67, 68).

2.2.2 Mode of action of BiTEs

Cytotoxic T lymphocytes (CTL) are the most abundant and powerful specific effector cells in the adaptive immune response and eliminate virus-infected or cancerous target cells (69, 70). Thereby, an individual T cell clone finds its specific target cell via its unique TCR, recognizing only a distinctive combination of peptide antigen and major histocompatibility complex (MHC) I. In concert with other stimulating signals, this binding leads to the formation of a cytolytic synapse. There, delivery of the cytotoxic proteins perforin and granzymes B is triggered, mediating target cell apoptosis (71-73). Tumor cells can interfere at each level with this target cell recognition and destruction process. They can lose MHC I expression, or modu-

late the occurrence of T cell stimulating or suppressing molecules, like members of the B7 family, tumor growth factor- β (TGF- β) and interleukin (IL)-10 (74-78). This immune-editing enables tumor cells to finally grow out into a large tumor mass, as they escape from an adaptive immune response, surviving in the presence of T cells.

BiTEs leverage the high cytotoxic potential of T cells without the many restrictions imposed by specific T cell recognition and counter-acting tumor evasion mechanisms (79). They provide a temporary physical link between any T cell and a tumor cell independently of MHC-peptide restrictions of T cells or altered MHC I expression of tumor cells. With one of its two specific binding sites the BiTE antibody attaches to the pan T cell antigen CD3 (ϵ -subunit), whereas the other one binds to a selected surface antigen on tumor cells. This transient T cell/target cell binding induces a fully functional cytolytic synapse between T cells and tumor cells, eliciting a polyclonal T cell response against tumor cells. Interestingly, activation can occur independent of normally required co-stimulating molecules, like CD28 or IL-2, even in previously un-stimulated naive T cells (Figure 4) (80, 81).

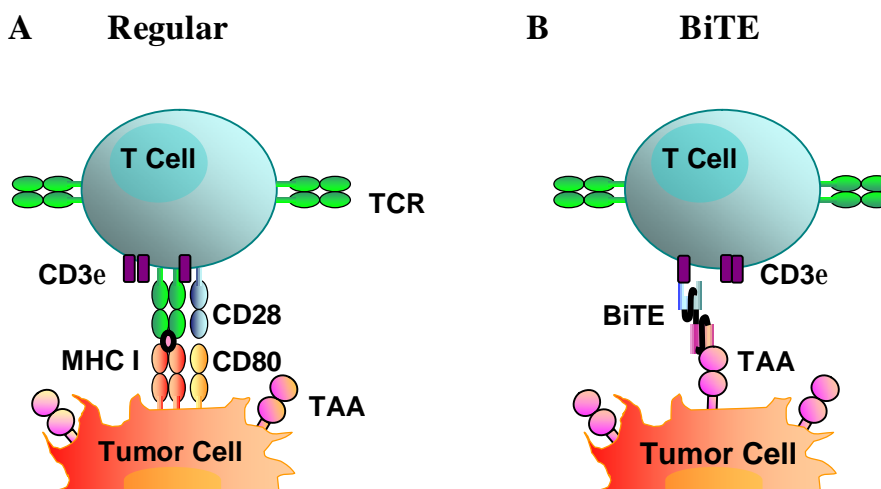


Figure 4: BiTEs bypass elements of regular T cell activation

(A) Via its unique T cell receptor (TCR) a T cell recognizes its target cell through specifically binding to the major histocompatibility complex (MHC) I loaded with a foreign peptide. In concert with other stimulating signals, like CD28, this binding leads to the formation of a cytolytic synapse that mediates apoptosis of the tumor cell by the release of toxins. (B) BiTEs bypass the MHC-peptide restriction of T cells and provide a link between any T cell and a tumor cell via binding to the CD3 ϵ antigen and a selected tumor surface antigen. This induces the formation of a functional cytolytic synapse indistinguishable from a physiologically induced one and leads to target cell lysis. TAA: Tumor associated antigen

Offner et al. showed that the BiTE-induced cytolytic immunological synapse was indistinguishable in composition, sub-domain arrangement and size from regular MHC I-peptide (erBB2) induced synapses and was formed even with MHC I negative cells. Granules with the typical signaling molecules Phosphokinase C θ (PKC θ), Leukocyte specific protein tyrosine kinase (Lck), CD3 and secretory molecules granzyme A, B and perforin were distributed to the immunological synapse. Markers of the immunological synapses like CD3, intracellular adhesion molecule-1 (ICAM-1), leukocyte functional antigen 1 (LFA1), VAV1 and talin showed similar surface distribution. In both cases, CD45 was excluded from the synapse (82). Of note, no activation of T cells by BiTEs was seen in the absence of target cells, implying that for TCR mediated activation binding to a second binding partner was crucial. Elimination of target cells was shown to be restricted only to cells expressing the selected antigen (79). Hoffmann et al. demonstrated that BiTEs recruit T cells to multiple rounds of target cell elimination, which might explain the high biological activity of BiTE antibodies already at very low concentrations [10-100 pg/ml] and at very low ratios of T cells to target cells (1:10) (66).

The binding affinities of BiTEs to CD3 ϵ have dissociation constants (KD) of approximately 10^{-7} M whereas the affinity to the tumor antigen is >10-100 times higher with KD in the nanomolar range. This means that BiTEs cover the surface of antigen positive target cells and turn them to a T cell activating matrix rather than “arming” polyclonal T cells with single chain antibodies specific for the tumor antigen (66). The clustering of BiTEs on the target cell surface results in gain of avidity for subsequent CD3 binding.

With their properties, BiTE antibodies are a new class of bispecific antibodies that could effectively perform in the conditions typically found in the *in vivo* tumor environment such as low T cell numbers, immune-suppression and low drug concentrations (83). First clinical data of phase I/II clinical trials in Non-Hodgkin’s lymphoma patients with MT103, a BiTE recognizing CD19 positive lymphoma cells, confirm the potency of the BiTE format. Partial or complete tumor regression was found in all seven patients treated at a dose level of 0.06 mg/m²/day (84).

2.2.3 MT110 and muS110

MT110 is a bispecific single chain antibody of the BiTE format, recognizing the tumor antigen EpCAM. The KD for human EpCAM is 13 +/- 0.25 nM and 100 +/-15 nM for human CD3 ϵ (85). It is constructed to redirect T cells to lyse EpCAM positive tumor cells. *In vitro*,

MT110 shows specific lysis of a large panel of EpCAM positive human target cell lines, e.g. KatoIII or SW480, over a low nanomolar range. The half maximal lysis [EC₅₀] of target cells by human peripheral blood mononuclear cells (PBMC) is at a concentration of 0.65 +/- 0.5 ng/ml (85). MT110 mediates target cell death independent from co-stimulatory signals, as it was able to redirect unstimulated human PBMC to lyse rodent cells transfected with human EpCAM. The same cells transfected with the mouse orthologue were not killed, which demonstrates the high specificity of the MT110-induced anti-tumor activity (79). In the presence of appropriate target cells MT110 induces polyclonal T cell activation, resulting in a dose dependent up-regulation of the activation marker CD69 and CD25, T cell proliferation, induction of cytokine release and granzyme synthesis (79). Although all CD4⁺ and CD8⁺ T cells were redirected to lyse target cells, closer analysis revealed a major contribution of CD8⁺ effector memory cells.

The *in vivo* anti-tumor capacity of MT110 was tested in immune deficient NOD/SCID mice. Its mode of action relies completely on the presence of human T cells, and tumor cells as well as human T cells can be grafted to these mice. However, unlike tumor cells, T cells have only a limited life span in these animals, which handicaps the evaluation of MT110's efficacy against established tumors. In a model inoculating subcutaneously a mixture of SW480 cells and naive human PBMCs (effector to target = 1:1), as few as five daily intravenous injections of 1 µg MT110 per animal were sufficient, to completely prevent tumor outgrowth. Five daily doses of 10 µg per animal were able to eradicate already established tumors of ~ 0.1 mm³. In a more physiological model pieces of metastatic tumor tissue from ovarian cancer patients were transplanted to NOD/SCID mice. Schlereth et al. showed that using solely the tumor-resident T cells as effector cells five daily doses of 5 µg per animal MT110 prevented or at least slowed down the growing of the tumor grafts (86).

MT110 is specific for human targets and has no cross-reactivity to other species except chimpanzee. Therefore, toxicological studies would be only possible in chimpanzees, which are limited due to strict animal protection rights, ethical considerations and huge costs. Development of the mouse specific surrogate muS110 for extended animal toxicology and efficacy studies in immune competent animals was therefore mandatory. MuS110 binds to the mouse orthologues of EpCAM and CD3 and mediates death of mouse tumor cells. A prerequisite to this attempt was the good comparability of mouse and human. A histo-pathological analysis of multiple mouse and human tissues revealed largely overlapping expression patterns of EpCAM, which was primarily seen on epithelial cells (Table 2).

Table 2 Comparison of EpCAM staining patterns of human and mouse tissues (Amann et al. (85))

Sections of fresh frozen mouse and human tissues were stained. All slides were evaluated by a certified pathologist to ensure that the quality of staining was sufficient for interpretation. The relative density of positive cells and the intensity of staining was graded on the following scale: 0 = no labeled cells; 1+ = light staining and/or occasional cells/types of cells “Minimal”; 2+ = light-medium staining and/or small numbers of cells/types of cells “Mild”; 3+ = moderate staining and/or medium numbers of cells/types of cells “Moderate” and 4+ = dark staining and/or large numbers of cells/types of cells “Marked”. Mouse and human tissues both expressing EpCAM are highlighted by mint color; unique EpCAM staining is highlighted in pink.

Antibodies Concentration	Mouse Tissues		Human Tissues	
	Anti-murine EpCAM	Isotype Control	Anti-human EpCAM	Isotype Control
	1 µg/mL	1 µg/mL	1 µg/mL	1 µg/mL
Pos. ctrl [CHO/Ep-CAM]	4	0	4	0
Neg. ctrl [CHO]	0	0	0	0
Adrenal	0	0	1	0-1
Bladder	2	0	3	0
Bone Marrow	2	2	2	2
Breast/Skin	2	1	2-3	0
Cerebellum	0	0	0-1	0
Cerebral cortex	0	0	0-1	0
Colon	4	0-1	3	0-2
Endothelium	0	0	0	0
Eye	2	0	2	0
Fallopian Tube	3	0-1	2-3	0-1
GI Tract	4	2	3	0-1
Heart	0	0	0-1	0
Kidney	3	2	4	1
Liver	3	2	3	0-1
Lung	2	1	4	0-1
Lymph Node	2	1	1-2	0-1
Ovary	0	0	0-1	0-1
Pancreas	3	0	4	0-1
Pituitary	2-3	0	4	0
Prostate	3	0	3	0
Spinal Cord	0	0	0-1	0
Spleen	1	1	1-2	1-2
Striated muscle	0	0	0	0
Testes	0	0	3	0
Thymus	2	1	2-3	0-1
Thyroid	3-4	0	4	0-1
Tonsil	-	-	2-3	1
Ureter/uterine Horn	3	1	1-2	0-1
Vagina/cervix	3	1-2	1-2	0-1

In both species, EpCAM was largely confined to the cell surface, showed no difference with respect to polarized expression on epithelial cells, and stained a similar proportion of cells in tissues. Human epithelia of breast, bladder, colon, intestine, kidney, bile ducts, lung, pancreas, pituitary, prostate, thyroid and uterus expressed EpCAM, and so did all respective mouse tissues. Likewise, certain tissues were not stained with either human or mouse EpCAM-specific mAbs, including bone marrow, cerebellum, cerebral cortex, endothelium, heart, ovary, spinal cord, spleen and striated muscle. The only differences in EpCAM expression between man and mouse were noted for adrenal gland and testis tissues, which were stained in human but apparently not in mouse tissue samples (85). The amino acid sequence homology between human and mouse EpCAM is 82 % (87).

3 AIM OF THIS STUDY

As MT110 is only specific for human targets, the mouse specific surrogate muS110 was developed for extended toxicology and efficacy studies in immune-competent animals. MuS110 binds to the mouse orthologues of EpCAM and CD3 and mediates death of mouse EpCAM positive tumor cells.

The following study describes first the *in vitro* characterization of muS110 and thereafter the *in vivo* evaluation of its efficacy and tolerability. Thereby, the impact of muS110 on healthy EpCAM⁺ tissues, EpCAM⁺ tumor cells and T cells was addressed in immune-competent mice. Special emphasize was laid on the analysis of immediate effects on T cells, but also on its impact on T cell effector functions after repeated and prolonged administration. Additionally, glucocorticoids were tested as a way to increase the therapeutic window of muS110. Thereby, potential changes in systemic tolerability as well as T cell effector functions were analyzed after glucocorticoid co-treatment. Lastly, these findings were implemented in different *in vivo* tumor models, to evaluate the anti-tumor efficacy of muS110 and improve its therapeutic window.

The outread of all described experiments was used for the pre-clinical development of MT110, which was finally allowed to enter phase I clinical trials in April, 2008.

4 MATERIAL AND METHODS

4.1 Material

4.1.1 Cell lines

All non-transfected cell lines were either obtained by the American type culture collection (ATCC, Manassas, USA) or from “Deutsche Sammlungen von Mikroorganismen und Zellkulturen GmbH (DMSZ, Braunschweig, Germany). All transfected cell lines were provided by the department for BiTE research. Cells were either transfected with full length mouse EpCAM (NCBI entrez Nucleotide, <http://www.ncbi.nlm.nih.gov/sites/entrez>, NM_008532) or full length human EpCAM (NCBI entrez Nucleotide, <http://www.ncbi.nlm.nih.gov/sites/entrez>, NM_002354).

CHO dHFR⁻ (ATCC)

CHO dHFR⁻ cells are Chinese hamster ovary cells isolated from healthy *cricetulus griseus*. They are of epithelial origin and grow semi-adherent. These cells are deficient in dihydrofolate reductase (dHFR) and die in the absence of adenosine and thymidine. Cells were cultivated in HyQ PF CHO liquid soy medium (Thermo Scientific) supplemented with 10 µg/ml adenosine (Sigma-Aldrich), 10 µg/ml 2'-deoxyadenosine (Sigma-Aldrich) and 10 µg/ml thymidine (Sigma-Aldrich) at 37°C, 95% humidity and 5% CO₂.

CHOmuEpCAM⁺, CHOhuEpCAM⁺

CHOmuEpCAM⁺ cells are CHO dHFR⁻ cells (ATCC) transfected with the eukaryotic expression vector pEF-dHFR containing full length mouse EpCAM. CHOhuEpCAM⁺ are CHO dHFR⁻ cells (ATCC) transfected with the eukaryotic expression vector pEF-dHFR containing full length human EpCAM. The pEF-dHFR vector encodes the dihydrofolate reductase and enables successfully transfected CHO dHFR⁻ cells to grow without exogenous nucleoside supply (68). These semi-adherent cells were cultivated in pure HyQ PF CHO liquid soy medium (Thermo Scientific) for selection. For gene amplification 20 mM of the dHFR inhibitor methotrexate (MTX, Sigma-Aldrich) was added. Cells were grown at 37°C, 95% humidity and 5% CO₂.

4T1 (ATCC)

4T1 cells were established of the 410.4 mammary gland tumor from *mus musculus* (BALB/c). These cells of epithelial origin are tumorigenic in NOD/SCID and BALB/c mice and produce

highly metastatic tumors that can metastasize to lung, liver, lymph nodes and brain while the primary tumor is growing *in situ*. The resulting disease closely mimics human breast cancer and is an animal model for stage IV human breast cancer. The cells show a natural expression of mouse EpCAM. The adherent cells were cultivated in RPMI 1640 medium w 2.0 g/l NaHCO₃ (Biochrome AG) supplemented with 10% FCS (Gibco) and 1% penicillin/streptomycin (Biochrome AG) at 37°C, 95% humidity and 5% CO₂.

B16F10muEpCAM⁺

B16F10muEpCAM⁺ cells are B16F10 cells (ATCC) transfected with the eukaryotic expression vector pEFNEO containing full length mouse EpCAM. The B16F10 cell line was established of skin melanoma from *mus musculus* (C57BL/6). The fibroblast-like cell line shows adherent growth and is tumorigenic in NOD/SCID and C57BL/6 mice. The cells were cultivated in RPMI 1640 medium w 2.0 g/l NaHCO₃ (Biochrome AG) supplemented with 10% FCS (Gibco) and 1 mg/ml G418 (PAA) for selection at 37°C, 95% humidity and 5% CO₂.

CT26muEpCAM⁺

CT26muEpCAM⁺ cells are CT26.WT cells (ATCC) transfected with the eukaryotic expression vector pEFNEO containing full length mouse EpCAM. The CT26.WT cell line was established of an N-nitroso-N-methylurethane induced, undifferentiated colon carcinoma from *mus musculus* (BALB/c). The adherent growing cells are tumorigenic in NOD/SCID and BALB/c mice. The cells were cultivated in RPMI 1640 medium w 2.0 g/l NaHCO₃ (Biochrome AG) supplemented with 10% FCS (Gibco) and 1 mg/ml G418 (PAA) for selection at 37°C, 95% humidity and 5% CO₂.

CTLL-2 (ATCC)

The CTLL-2 cell line was established of a clone of CTLs derived from *mus musculus* (C57BL/6). The suspension cells were cultivated in ISCOVE medium (Biochrome AG) supplemented with 10% FCS (Gibco), 0.1 mg/l penicillin/ streptomycin (Sigma-Aldrich), 50 nM 2-mercaptoethanol (Invitrogen) and 5.5 ng/l recombinant human IL-2 (Chiron Corp. Lim.) at 37°C, 95% humidity and 5% CO₂.

Kato III (DSMZ)

The Kato III cell line was established of gastric carcinoma cells from pleural effusion, supraclavicular and axillary lymph nodes and Douglas cul-de-sac from a 55 year old Asian male. The cells show adherent growth and natural expression of human EpCAM. They were culti-

vated in RPMI 1640 medium w 2.0 g/l NaHCO₃ (Biochrome AG) supplemented with 10% FCS (Gibco) and 1% penicillin/streptomycin (Biochrome AG) at 37°C, 95% humidity and 5% CO₂.

4.1.2 Mouse strains

All animals were between 6 to 12 weeks of age and were obtained either from Charles River Laboratories (Sulzfeld, Germany) or the Institut for Immunology (Munich, Germany).

BALB/c (Charles River Laboratories and Institute for Immunology)

BALB/c mice are immune-competent, inbred laboratory mice that develop preferentially T helper cell type 2 (TH₂) responses with release of typical TH₂ cytokines like IL-4 and IL-10, are more susceptible to intracellular parasite infection, have a higher tumor incidence and are more resistant to the induction of autoimmune diseases compared to C57BL/6 mice.

C57BL/6N (Charles River Laboratories and Institute for Immunology)

C57BL/6N mice are immune-competent, inbred laboratory mice which show preferentially TH₁ dominated cellular immune response and release of typical TH₁ cytokines like IFN- γ and IL-2 upon challenge with pathogens.

C3H/HeJ (Charles River Laboratories)

The inbred strain shows resistance to endotoxin due to a mutation of the toll-like receptor 4 gene. This impairs the activation of cells of the innate immunity by lipopolysaccharide. C3H/HeJ mice are highly susceptible to infection by gram-negative bacteria and show delayed chemokine production, impaired nitric oxide generation and attenuated cellular immune responses.

CD-1 (Charles River Laboratories)

The CD-1 strain is an outbreed mouse line derived from Swiss mice and has a high degree of genetic variation. They are most often used in toxicology and carcinogenicity bioassays.

4.1.3 Reagents, media and enzymes

2 Desoxyadenosine	Sigma-Aldrich
2 Mercaptoethanol (50 mM)	Gibco
Adenosine	Sigma-Aldrich
Ammonium Chloride (NH ₄)	Sigma-Aldrich
Biocoll Separating Solution ($\rho = 1.079$ g/ml)	Biochrome AG

Bovine Serum Albumine (BSA) V	Paessel & Lorei
Brefeldin A (<i>Penicillium Brefeldianum</i>)	Sigma-Aldrich
Cell Dissociation Solution	Sigma-Aldrich
DELFLIA [®] BATDA Solution	Wallac Oy
DELFLIA [®] Europium Solution	Wallac Oy
DELFLIA [®] Lysis Buffer	Wallac Oy
Dexamethasone	Sigma-Aldrich
Disodium Hydrogenphosphate ($\text{Na}_2\text{HPO}_4 \cdot (\text{H}_2\text{O})_2$)	Merck
Eosin G	Roth
Etylene-di-nitro-tetra-acetic-acid (EDTA)	Sigma-Aldrich
G418 Sulphate	PAA
Heat inactivated Fetal Calf Serum (FCS)	Gibco
Hepes Buffer (1 M)	Sigma-Aldrich
Human soluble EpCAM	Micromet AG
Hydrochlorid Acid 1 M (HCl)	Merck
HyQ PF CHO Liquid Soy	Thermo Scientific
Ionomycin, Calcium salt	Sigma-Aldrich
Iscove medium	Biochrome AG
Isoflurane	CP Pharma
Isotonic NaCl solution	Freeflex
Para-nitro-phenyl-phosphate substrate	Sigma-Aldrich
Phosphate Buffered Saline (PBS), Dulbecco's	Gibco/ Invitrogen
Phorbol Myristate Acetate (PMA)	Sigma-Aldrich
Potassium-di-hydrogen-phosphate (KH_2PO_4)	Merck
Methotrexate	Sigma-Aldrich
Methylprednisolone (mPDS)	Sigma-Aldrich
MSD Blocker A	MSD
MSD Reading buffer	MSD
Mouse soluble EpCAM	Micromet AG
Neutral buffered Formalin (10%)	Sigma-Aldrich
Non Essential Amino Acids (NEA)	Biochrome AG
Penicillin/ Streptomycine (10.000 U/l)	Biochrome AG
Phenol Red (0.5% (w/v))	Biochrome AG
Potassium Chloride (KCl)	Merck
Propidium Iodide (PI)	Sigma-Aldrich
Sodium Azide (NaN_3)	Merck
Sodium Chloride (NaCl)	Merck

Sodium Heparin (25000 I.E./5ml)	Braun
Sodium Hydroxide (1 M; NaOH)	Merck
Sodium Pyruvat (100 mM)	Sigma-Aldrich
Sulfuric Acid (2M, H ₂ SO ₄)	Merck
Recombinant human IL-2 (rhuIL-2)	Chiron Corp. Lim.
RPMI 1640 medium	Gibco
RPMI 1640 medium + L-GLN + 25 mM Hepes	Gibco
RPMI 1640 medium w 2.0 g/l NaHCO ₃ low endotoxin	Biochrome AG
Thymidine	Sigma-Aldrich
Tissue Tek O.C.T. Compound	Sakura
Trypsin/EDTA	Gibco
Tween 20	Sigma-Aldrich
Xylazine Hydrochloride (2%)	CP Pharma

4.1.4 Kits

BD Cytotfix/Cytoperm Kit	BD Bioscience
Caspase-Glo 3/7 Assay	Promega
Dynabeads Mouse CD3/CD28 T Cell Expander	Invitrogen (Dyna)
Dyna Mouse T Cell Negative Isolation Kit	Invitrogen (Dyna)
Dyna T Cell Negative Isolation Kit Ver. II	Invitrogen (Dyna)
Human T Cell Enrichment Column	R&D Systems
Human TH ₁ /TH ₂ CBA Kit	BD Bioscience
Human/mouse TGF-β1 ELISA Ready Set Go!	Natutec (eBioscience)
Mouse GM-CSF CBA Flex- Set (Bead A4)	BD Bioscience
Mouse IFN-γ CBA Flex- Set (Bead A4)	BD Bioscience
Mouse IL-2 CBA Flex- Set (Bead A5)	BD Bioscience
Mouse IL-3 CBA Flex- Set (Bead A4)	BD Bioscience
Mouse IL-4 CBA Flex- Set (Bead A7)	BD Bioscience
Mouse IL-6 CBA Flex- Set (Bead B4)	BD Bioscience
Mouse IL-10 CBA Flex- Set (Bead C4)	BD Bioscience
Mouse Inflammation CBA Kit	BD Bioscience
Mouse Regulatory T Cell Staining Kit#2	Natutec (eBioscience)
Mouse/Rat Soluble Protein Master Buffer Kit	BD Bioscience
Mouse T Cell Enrichment Columns	R&D Systems
Mouse TH ₁ /TH ₂ CBA Kit	BD Bioscience
Mouse TNF CBA Flex- Set (Bead C8)	BD Bioscience
PKH-26 Red Fluorescent Cell Linker Kit	Sigma

ToxiLight Bioassay Kit	Cambrex
TruCount Tubes	BD Bioscience
Vybrant CellTracer™ CFSE Cell Proliferation Kit	Molecular Probes

4.1.5 Buffer

Erythrolysis buffer

155 mM	NH ₄
10 mM	KHCO ₃
100 µM	EDTA

In ddH₂O

FACS Buffer

1% (v/v) (v/v)	FCS
0.05% (w/v)	NaN ₃

In PBS

PBS (pH = 7.4)

150 mM	NaCl
3 mM	KCl
8 mM	Na ₂ HPO ₄
2 mM	KH ₂ PO ₄

In ddH₂O

Cytotoxicity Media

1 mM	NEA
10 mM	Hepes Buffer
50 µM	2-β-Mercaptoethanol
1% (v/v)	Sodium Pyruvate
100 U/ml	Penicillin/ Streptomycin

In RPMI 1640 w 2.0g/l NaHCO₃

4.1.6 Antibodies

For FACS analysis

Rat anti-mouse CD3 e (KT3; #CBL1317)	Cymbus Biotech.
Hamster anti-mouse CD3 e (145/2C11; #553063, #553058)	BD Bioscience
Rat anti-mouse CD4 (RM4-5; #553051, #553046)	BD Bioscience
Rat anti-mouse CD4 (RM4-5; #35-0042-82)	Natutec
Rat anti-mouse CD4 (H129.19; #553653)	BD Bioscience
Rat anti-mouse CD4 (GK1-5; #11-0041-86)	Natutec
Rat anti-mouse CD8a (53-6.7; #553030, #553032, #553034, #553035)	BD Bioscience
Rat anti-mouse CD11b (M1/70; #550993)	BD Bioscience
Rat anti-mouse CD11b (M1/70; #25-0112-82)	Natutec
Hamster anti-mouse CD11c (HL3; #553802)	BD Bioscience
Hamster anti-mouse CD11c (N418; #27011482)	Natutec
Rat anti-mouse CD19 (1D3; #557398, #557399)	BD Bioscience
Rat anti-mouse CD19 (MB19-1; #17-0191)	Natutec
Rat anti-mouse CD25 (3C7; #553075)	BD Bioscience
Rat anti-mouse CD25 (PC61, #557192)	BD Bioscience
Rat anti-mouse CD25 (PC61.5; #25-0251)	Natutec
Rat anti-mouse CD44 (IM7; #553134)	BD Bioscience
Rat anti-mouse CD45 (30-F11; #559864, #553082)	BD Bioscience

Rat anti-mouse CD45R/B220 (RA3-6B2, #553091, #553092)	BD Bioscience
Rat anti-mouse CD45R/B220 (RA3-6B2, #25-0452)	Natutec
Rat anti-mouse CD49b/Pan-NK Cells (DX5; #553857, #553858)	BD Bioscience
Hamster anti-mouse CD62L (MEL-14; #553150)	BD Bioscience
Hamster anti-mouse CD69 (MEL-14; #55237, #553236, #552879)	BD Bioscience
Hamster anti-mouse CD127 (SB/199, #552543)	BD Bioscience
Rat anti-mouse CD152 (UC10-4F10-11; #12-1522-81)	Natutec
Rat anti-mouse EpCAM (G8.8; #552370, #624048)	BD Bioscience
Rat anti-mouse FoxP3 (FJK-16s, #11-5773-82, #2528545)	Natutec
Rat anti-mouse Granzyme B (16G6; #2528545)	Natutec
Rat anti-mouse IFN- γ (XMG1.2; #554412)	BD Bioscience
Rat anti-mouse IL-10 (JES5-16E3; #1899932)	Natutec
Rat anti-mouse Ly-6C (AL-21; #553104)	BD Bioscience
Rat anti-mouse Ly-6G (RB6-8C5, #553126)	BD Bioscience
Isotype controls	
Hamster IgG1 κ (A19-3; #553971, #553972)	BD Bioscience
Hamster IgG1 λ (G2352356; #554711)	BD Bioscience
Rat IgG1 (R3-34; #554686)	BD Bioscience
Rat IgG1 (A110-1; #554684)	BD Bioscience
Rat IgG2a κ (R35-95; #554688, #555844, #554690)	BD Bioscience
Rat IgG2b κ (A95-1; #553988, #553989, #553991)	BD Bioscience
Rat IgM (pooled mouse Ig; #553943)	BD Bioscience
Blocking antibodies	
Rat anti-Mouse CD16/CD32/Fcg III/II Receptor Block	BD Bioscience
For ELISA	
Mouse anti-Pentahistidine conjugated with Biotin (#3440)	Qiagen
Streptavidin conjugated with Horse Radish Peroxidase (#P0397)	Dako
Streptavidin conjugated with Phycoerythrin (#554061)	BD
Streptavidin conjugated with MSD SULFO-TAG (#R32AD-1)	MSD

4.1.7 BiTEs

All BiTEs were provided by the department of BiTE research (Micromet).

MT110 was engineered by recombinant DNA technology using the gene sequence of an antibody specific for human EpCAM (clone 5-10) and human CD3 (clone diL2K) (88). To generate muS110, the gene sequence of an antibody specific for mouse CD3 (clone CD3-1) and an antibody specific for mouse EpCAM (clone G8.8) was used. To generate the hyS110 con-

trol antibody, gene sequences of antibodies specific for mouse CD3 (clone CD3-1) and human EpCAM (clone 5-10) were used. For engineering of the muMEC14 control BiTE, the gene sequence of an antibody specific for mouse CD3 (clone CD3-1) was used as effector cell recognizing scFv. The target cell binding moiety was directed against the herbicide Mecoprop comprising of a structure completely absent in the human or mouse system. However, the control BiTE was proven to be fully functional in the respective setting. The specificity and parental offspring of all used BiTEs is summarized in Table 3.

The hybridoma producing rat anti-mouse EpCAM mAb was obtained from the Developmental Studies Hybridoma Bank, developed under the auspices of the NICHD and maintained by the Department of Biological Sciences (University of Iowa). The mouse variable domains recognizing human EpCAM were obtained by phage display. The gene sequence for the scFv binding moiety to Mecoprop (clone Mec14) was retrieved from Li et al.(89). Human T helper cell epitopes and MHC class II anchor amino acids were removed from the anti-human CD3 antibody (L2K) resulting in a deimmunized antibody (diL2K) (90).

The arrangement of the variable domains for all used BiTEs is $V_L - V_H$ for the N-terminal scFv and $V_H - V_L$ for the C-terminal scFv. All used BiTEs are equipped with a HIS-6 Tag on the C-terminal end of the protein for purification and detection. Sequences encoding the variable domains of the respective antibodies were amplified and modified as described by Mack et al. (68). Expression plasmids were transfected into dhFR-deficient CHO cells and protein expression was performed as described by Kaufman et al. (91). All BiTEs were purified from cell culture supernatants as described by Kufer et al. (80).

Table 3: Specificity and parenteral offspring of used BiTEs

Name	Target	Target Reactivity		CD3 Reactivity	
		Parent	Specificity	Parent	Specificity
MT110	huEpCAM	5-10	Human	diL2K	Human
muS110	muEpCAM	G8.8	Murine	CD3-1	Murine
HyS110	huEpCAM	5-10	Human	CD3-1	Murine
muMec14	Mecoprop	Mec14	Herbicide	CD3-1	Murine
huMec14	Mecoprop	Mec14	Herbicide	diL2K	Human

4.1.8 Equipment

Axiovert 25 microscope
DAS-6007 scanner

Carl Zeiss
PLEXX

DM-FZ 30eGLumix digital camera	Panasonic
Dynal MPC-1 magnetic separator	Invitrogen (Dynal)
ELISA reader PowerWave select X	Bio Tek Instruments Inc.
ELISA washer	Molecular Devices
FACS Calibur 4CA	Becton Dickinson
FACS Canto II	Becton Dickinson
Heating box	VetTech solution
Hemocytometer	Marienfeld
Hematokrit sealing kit	Heiland
Heraeus Heracell incubator	Kendro Laboratory Products GmbH
Heraeus Herasafe HS 12 flow	Kendro Laboratory Products GmbH
Heraeus Multifuge 3 S	Kendro Laboratory Products GmbH
IPTT-300 transponder	PLEXX
Isotec3 isoflurane evaporator	Völker GmbH
Spectra Fluor Plus Fluorometer	Tecan
MiniCAPS capillaries (NaHep 5 µl)	Hirschmann Laborgeräte
Microtainer SST tubes	BD Bioscience
Micro hematocrit centrifuge	Hawksley
Mikro hematokrit capillaries (NaHep, 50 µl)	Heiland
Mikro 20 Typ: 2004 centrifuge	Hettich
MoFlo high performance cell sorter	DAKO
MS1 minishaker	IKA® Werke GmbH
MSD high bind plate	MSD
MXX - 212 balance	Denver instruments
Leucosept tubes	Greiner
Omnican 0.3x12mm 0.01-1 ml syringe	Braun
Sektor imager 2400	MSD
Sterican100 0.05x16mm 25Gx5/8“ syringe needle	Braun
Victor Multilabel counter	Wallac Oy
WB4 45 waterbath	Memmert GmbH+Co.KG

4.1.9 Software

DAS Host software	PLEXX
Prism 4	GraphPad Software
Cell Quest Pro	Becton Dickinson
FACS Diva software	Becton Dickinson
FCAP Array software	SoftFlow
WinNonlin Professional 4.1	Pharsight Corporation

4.2 Methods

4.2.1 Cell culture

All cells were maintained at 37°C in an atmosphere containing 5% CO₂ in the indicated media. The cell count was determined using a hemacytometer (Marienfeld). The vitality of cells was determined using 0.5 % (v/v) isotonic EosinG solution (Roth). All cells were split three times a week 1:4 to 1:10. The suspension cells CHO dHFR⁻, CHOmuEpCAM⁺, CHOhuEpCAM⁺ and CTLL-2 were split by replacing the excess amount of cell suspension with fresh media. To detach the adherent cell lines 4T1, B16F10muEpCAM⁺, CT26muEpCAM⁺ and KatoIII, the supernatant was removed, the cell culture flask was rinsed with PBS (Gibco) and cells were incubated for 5 to 10 minutes in PBS (Gibco) containing 1% (v/v) Trypsin/EDTA solution (Gibco) at 37°C. Cells were detached by gently tapping the flask. Excess Trypsin was inactivated by addition of FCS (Gibco). Cells were washed with media and spun down by centrifugation in a Heraeus Multifuge 3 (Kendro Laboratory Products GmbH) at 300xg for 5 minutes at room temperature (RT). The cell pellet was resolved in media and the respective amount was transferred back into the cell culture flask containing fresh media.

4.2.2 Preparation of leukocytes

In general, centrifugation was performed at 500xg for 5 min at RT using a Heraeus Multifuge 3 (Kendro Laboratory Products GmbH). If not otherwise indicated samples were filled up with indicated media for washing and supernatant was discarded after centrifugation. The cell count was determined using a hemacytometer (Marienfeld). The vitality of cells was determined using 0.5 % (v/v) isotonic EosinG solution (Roth).

4.2.2.1 Isolation of PBMC from human and mouse blood

PBMCs were isolated by Ficoll density gradient centrifugation with leucosept tubes (Greiner Bio one). Leucosept tubes, containing a porous high-density polyethylene barrier or "frit", were used to facilitate the layering process. The Biocoll separation solution (Biochrome AG) containing Ficoll in a density of 1.079 g/ml was spun down under the frit. Heparinized blood was diluted 1:1.5 with PBS (Invitrogen) to optimize separation efficacy. The Biocoll was over-laid by diluted blood. Centrifugation for 30 minutes at 400xg and RT in a Heraeus Multifuge 3 (Kendro Laboratory Products GmbH) led to the formation of following layers (from top to bottom): plasma and other constituents, a "buffy coat" containing PBMC, the Ficoll-

plaque, and an erythrocyte/granulocyte pellet. The buffy coat fraction was transferred to a new tube and washed three times with cytotoxicity media (see 4.1.5).

4.2.2.2 Isolation of mouse leukocytes from spleen and lymph nodes

Isolation was performed in cytotoxicity media (see 4.1.5). The spleen or respective lymph nodes were removed and stored in cytotoxicity media on ice until usage. The organs were homogenized grinding them through a cell strainer (70 μm , BD) with a plunger of a syringe. The cell suspension was washed once with media and the pellet was resolved in erythrolysis buffer (see 4.1.5). Erythrolysis was performed for 10 min at 37°C in a water bath. Afterwards cells were washed twice and filtered through a cell strainer (70 μm , BD) to remove conglomerated, dead cell debris.

4.2.2.3 Enrichment of CD3 cells

For enrichment of untouched T cells mouse T cell enrichment columns (R&D Systems) were used with splenocytes. The T cell enrichment column contains glass beads covered with anti-IgG antibodies, to retain B cells, and with an IgG cocktail to retain monocytes binding to their Fc receptors. The resulting column eluate contains highly enriched CD3⁺ T cells with a purity of 81-88%. Of note, NK cells were not removed by this method.

0.5 to 2*10⁸ cells were resolved in provided washing buffer and were loaded onto columns pre-equilibrated with washing buffer. To allow adherence of B cells and monocytes, cells were incubated for 10 min at RT followed by elution with washing buffer. The resulting enriched T cell fraction was washed twice with cytotoxicity media (see 4.1.5).

4.2.2.4 Negative isolation of CD3 cells

To obtain more pure untouched T cells, Dynal negative T cell isolation kit ver II for the human setting and Dynal mouse T cell negative isolation kit (both Invitrogen) for the mouse setting were used. In a first step all cells with exception of T cells were labeled with a cocktail of monoclonal antibodies. In a second step all labeled cells were bound with antibodies to magnetic beads. And in a third step all magnetic beads and therefore also bound non-T cell were removed using the MPC-1 magnetic separator (Dynal). The resulting bead free supernatant contains T cells in a purity of > 99 %.

The isolation was performed in PBS (Gibco) containing 1% FCS (Invitrogen) and 2 mM EDTA (Sigma Aldrich), which is further termed Dynal buffer. Prior to usage Dynal magnetic depletion beads were washed with Dynal buffer. For that the recommended amount of beads

was transferred to a 15 ml tube (Greiner), which was filled up with Dynal buffer. The tube was incubated for 2 minutes on the MPC-1 magnetic separator (Dyna), the supernatant was removed and the beads were solved with Dynal buffer in the initial bead volume. Each 1×10^7 cells were resolved in 100 μ l Dynal buffer and stained with 20 μ l provided antibody cocktail in the presence of 20 μ l FCS (Invitrogen) for 20 minutes at 4°C. Cells were washed twice with Dynal buffer to remove excess antibodies. Afterwards cells were resuspended in 200 μ l (human setting) and 100 μ l (mouse setting) provided magnetic depletion beads, respectively, and samples were filled up to 1 ml total volume with Dynal buffer. Antibodies were allowed to bind to Dynal beads for 15 minutes at RT. Samples were filled up to 10 ml with Dynal buffer and were incubated for 2 minutes on the MPC-1 magnetic separator (Dyna). The supernatant containing untouched T cells was transferred to another tube and the magnetic separation was repeated once again to improve purity. Afterwards cells were washed once with cytotoxicity media (see 4.1.5).

4.2.2.5 Stimulation of T cells

T cells were *in vitro* stimulated using the Dynabeads mouse CD3/CD28 T cell expander (Invitrogen). Anti-CD3 and anti-CD28 antibodies are coupled to the same Dynabeads, mimicking *in vivo* stimulation by antigen presenting cells. The simultaneous presentation of optimal stimulatory signals to the T cells in culture allows their full activation and expansion.

The stimulation was conducted in cytotoxicity media containing 10 - 100 U/ml rhIL-2. T cells were seeded with a density of 1×10^6 T cells/ml. 10 μ l washed bead solution per each 1×10^6 T cells was added to the T cell culture. Cells were incubated at 37°C, 5%CO₂ for 3 to 4 days whereby 10-100 U/ml rhIL-2 was added daily. Stimulation of T cells with IL-2 and anti-CD3 antibodies led to internalization of surface CD3. To guaranty proper CD3 surface expression, T cells were therefore washed with cytotoxic media and were allowed to recover overnight in a density of 0.5×10^6 cells/ml prior to cytotoxicity assays.

4.2.3 Cell staining and FACS analysis

In general, centrifugation of cells was performed at 500xg for 5 min at RT using a Heraeus Multifuge 3 (Kendro Laboratory Products GmbH). If not otherwise indicated samples were filled up with indicated media for washing and supernatant was discarded after centrifugation. For compensation single stains of each antibody present in the staining cocktail were performed. After staining cells were washed once with FACS buffer and were either resolved in 60 μ l FACS buffer for analysis on a FACSCantoII™ flow cytometer running FACSDiva™

Software (all BD Bioscience) or they were resolved in 200 μ l FACS buffer and were transferred to U tubes (Micronics) for analysis on a FACSCaliburTM flow cytometer running Cell Quest Pro Software (all BD Bioscience). To determine cell vitality 1 μ g/ml PI (Sigma) was added to samples directly before measurement.

4.2.3.1 FACS analysis of cell surface proteins

0.5 – 1*10⁵ cells/well were spun down in a 96 well V bottom plate (Hartenstein). Cells were resolved in 25 μ l FACS buffer (see 4.1.5) containing the antibody cocktail of choice and were then incubated for 20 minutes at 4°C in the dark.

4.2.3.2 FACS analysis of intracellular proteins

The Cytofix/ Cytoperm Kit (BD Bioscience) was used for intracellular staining. The provided BD Cytofix/Cytoperm fixation/ permeabilization solution contains 0.1 % of the detergent saponin and 4% formaldehyde. Saponin perforates the cell membrane; formaldehyde fixates proteins via cross-linking of amides and side chains of arginine and aromatic amino acids. The provided permeabilization/ washing solution contains additionally to saponin 1% FCS, which reduces unspecific staining.

To enhance signal to noise ratio, cells were activated by PMA / ionomycin treatment in the presence of Brefeldin A prior to intracellular staining of cytokines. The phorbol ester PMA activates protein kinase C whereas the calcium ionophore ionomycin leads to an intracellular rise of Ca²⁺. This mimics a full blown T cell activation via the TCR and up-regulates cytokine secretion. Brefeldin A prevents the transport of proteins to the cell surface, enriching secreted proteins in the cell. Briefly, PBMC or splenocytes were incubated at a density of 2-4 * 10⁶ cells/ml at 37°C in an incubator for 4 to 6 hours in pre-warmed cytotoxicity media (see 4.1.5) containing 20 ng/ml PMA (Sigma-Aldrich), 1 μ g/ml ionomycin (Sigma-Aldrich) and 10 μ g/ml Brefeldin A (Sigma Aldrich).

0.5-1*10⁶ cells/well were seeded in a 96-well V-bottom plate (Hartenstein). To identify cell types surface stain was performed as described in 4.2.3.1. Afterwards, cells were fixed and permeabilized by addition of 100 μ l fixation/ permeabilization solution and a subsequent incubation for 20 min at 4°C. Cells were washed twice with permeabilization/ washing solution. Unspecific staining was blocked additionally by incubation with a 1:100 dilution of anti-mouse CD16/CD32 FC γ Block (BD Bioscience) for 15 min at 4°C. Afterwards, the recommended amount of intracellular antibody was given directly into the blocking solution and the

incubation was prolonged for another 30 minutes to allow intracellular staining. Cells were washed once with permeabilization/ washing buffer.

4.2.3.3 FACS analysis of whole blood

20 μ l of blood was transferred to a 96 well V bottom plate (Hartenstein). Erythrolysis was performed for 7 minutes at 37°C in an incubator after addition of 200 μ l erythrolysis buffer (see 4.1.5). Cells were spun down and erythrolysis was repeated a second time. Cells were washed once and normal surface stain was performed as described in 4.2.3.1. The FACSCantoII™ flow cytometer allows the concrete event count of any stained cell type in a precise sample volume. Therefore, it was possible to calculate the blood cell count of any identified cell type. To ensure precise numbers the method of reverse pipetting was used.

4.2.4 Labeling of target cells

In general, centrifugation of target cells was performed at 300xg for 5 min at RT using a Heraeus Multifuge 3 (Kendro Laboratory Products GmbH). If not otherwise indicated samples were filled up with indicated media for washing and supernatant was discarded after centrifugation. The cell count was determined using a hemacytometer (Marienfeld). The vitality of cells was determined using 0.5 % (v/v) isotonic EosinG solution (Roth).

4.2.4.1 PKH staining

Target cells were stained using the PKH-26 Red Fluorescent Cell Linker Kit (Sigma). PKH is an aliphatic reporter molecules stably incorporated into the cell membrane. The excitation and emission maxima lay at 490 nm and 504 nm, respectively.

Briefly, $1 \cdot 10^7$ cells were washed twice with PBS (Invitrogen). Cells were re-suspended in 500 μ l provided Solution C (Sigma), and 500 μ l Solution C containing 16 μ l PKH dye (Sigma) was added. Cells were incubated for 5 min at 37°C and afterwards 1 ml FCS (Gibco) was added to stop the reaction. Cells were washed twice with cytotoxicity media (see 4.1.5). Correct labeling was approved by flow cytometry.

4.2.4.2 CFSE labeling

To track proliferation, lymphocytes were labeled with 50 nM Carboxy-Fluorescein diacetate, Succinimidyl Ester (CFSE) using the Vybrant CFDA SE Cell Tracer Kit (Invitrogen). CFDA-SE diffuses passively into cells where it becomes membrane impermeable and fluorescent when it is cleaved by intracellular esterases to CFSE. It is equally distributed to daughter cells

during cell division. The intensity of the fluorescent signal is reduced by half with each subsequent generation, giving a possibility to track cell proliferation. The CFSE excitation and emission maxima lay at 490 nm and 518 nm, respectively.

The staining was performed in PBS (Gibco). 1×10^5 T cells were incubated with 50nM CFDA-SE (Molecular Probes) for 15 min at 37°C. The reaction was stopped by addition of excess amount of cytotoxicity media and cells were washed twice. The cells were allowed to recover for 30 min at 37°C to ensure complete conversion of the dye by esterases. Correct labeling was approved by flow cytometry.

4.2.5 Cytotoxicity assay

The aim of a cytotoxicity assays is to determine the amount of redirected lysis or apoptosis of target cells mediated by the BiTE of interest. Apoptosis or redirected lysis of target cells was induced by incubating them with effector cells in the presence of different concentrations of BiTE. If not otherwise indicated, a 10fold dilution row ranging from [1 pg/ml] to [1 µg/ml] and a blank sample as reference was prepared for that purpose. Each set was performed in duplicates or triplicates. Used effector cells were PBMCs, splenocytes, leukocytes isolated from lymph nodes and naive or activated T cells. The cytotoxic bioactivity of BiTEs was analyzed determining the ability to induce apoptosis (caspase assay) or cell lysis (ToxiLight assay and FACS based assay). The index of apoptose or the specific lysis was plotted against the logarithm of antibody concentration using Prism software (Graph Pad Software Inc., version 4.02). The resulting dose-response curves were analyzed with the integrated four-parameter nonlinear fit model accepting only series with R^2 values >0.9 . Calculated concentrations of the half-maximal kill (EC_{50}) were used as indicator for specific bioactivity.

4.2.5.1 ToxiLight assay

The redirected lysis of target cells was determined using the ToxiLight Bioassay Kit combined with the ToxiLight 100% Lysis Control Set (both Cambrex). The kit is based on the bioluminescent measurement of the adenylate kinase (AK) which is present in all cells. A loss of cell integrity through damages to the plasma membrane results in leakage of AK from cells into the surrounding medium. External added adenosindiphosphate (ADP) can be converted to adenosintriphosphate (ATP) by the present AK. The emerging ATP is utilized by added luciferase to catalyze the reaction of luciferin and O_2 to form oxyluciferin and CO_2 . During this reaction light is emitted in a stoichiometrical manner. The intensity of the emitted light is

proportional to the AK concentration in the supernatant and therefore to the redirected lysis of cells present in the sample and can be determined with a luminometer.

The assay was conducted in pure RPMI1640 (Gibco) containing 10% FCS (Invitrogen). 1×10^4 target cells/well and 1×10^5 effector cells/well were plated to a white flat-bottom 96-well plate (Nunc) in 50 μ l media and different concentrations of BiTE antibody in 50 μ l media or pure media as blank sample were added. Each set was performed in triplicates. Samples were incubated for 48 hours at 37°C, 5% CO₂. Spontaneous lysis was determined in samples containing only target cells and effector cells (blank sample). Maximal lysis was determined adding 25 μ l Toxilight 100% Lysis reagent (Cambrex) to blank samples followed by incubation for 10 min at RT. The same volume of medium was added to all other samples to ensure equal volumes. 100 μ l of ToxiLight reagent (Cambrex) was added to all samples and the plate was incubated at RT for 5 minutes in the dark. Thereafter luminescence was read out in a Spectra Fluor Plus Fluorometer (Tecan) using the luminescence mode (Gain 150, Integration time 1000 ms). Background luminescence was measured of pure cell culture medium (RLU_M) and was subtracted from luminescence of samples (RLU_S) and blank value before and after maximal lysis (RLU_B and RLU_{Max}). The specific lysis was calculated according to following mathematical equation:

$$\text{Specific Lysis [\%]} = 100\% * \left[\frac{(\text{RLU}_S - \text{RLU}_M) - (\text{RLU}_B - \text{RLU}_M)}{(\text{RLU}_{\text{Max}} - \text{RLU}_M) - (\text{RLU}_B - \text{RLU}_M)} \right]$$

4.2.5.2 Caspase assay

The Caspase-Glo 3/7 Assay (PROMEGA) is a luminescent assay that measures the activity of caspase 3 and 7, which are known to play a key role in apoptosis in mammalian cells. The assay provides a proluminescent caspase-3/7 substrate, which contains the tetrapeptide sequence DEVD. Addition of the Caspase-Glo 3/7 reagent results in cell lysis and therefore in release of intracellular caspase 3 and 7. These enzymes cleave in turn the substrate, generating a luciferase mediated luminescent signal. This is proportional to the amount of caspase-3 and -7 present and thus also to the number of apoptotic cells.

The assay was performed in pure RPMI1640 (Gibco) containing 10% FCS (Invitrogen). 1×10^4 target cells/well and $0.5 - 1 \times 10^5$ effector cells/well were plated to a white flat-bottom 96-well plate (Nunc) in 50 μ l media and different concentrations of BiTE in 50 μ l media or pure media as reference were added. Each set was performed in duplicates. Samples were incubated for 48 hrs at 37°C, 5% CO₂. Caspase-Glo 3/7 reagent (Promega) was added in a

volume ratio of 1:1 and samples were incubated at RT for 45 minutes. Thereafter luminescence was read out in a Spectra Fluor Plus Fluorometer (Tecan) using the luminescence mode (Gain 150, Integration time 1000 ms). Background luminescence was measured of pure medium (RLU_M) and was subtracted from luminescence of samples (RLU_S) and the blank value (RLU_B). The index of apoptosis was evaluated calculating the ratio of caspase activity of samples versus the blank value with following mathematical equation:

$$\text{Index of Apoptosis} = \left[\frac{RLU_S - RLU_M}{RLU_B - RLU_M} \right]$$

4.2.5.3 FACS based assay

The vitality of target cells was determined via PI (Sigma-Aldrich) exclusion in a FACS based assay. PI is a fluorescent, DNA intercalating molecule that is membrane impermeable. As it can only pass the disintegrated membrane of necrotic cells, its exclusion can be used to differentiate between viable and non-viable cells. Once the dye has bound to nucleic acids, its fluorescence is enhanced 20 to 30fold which can be measured by flow cytometry.

The assay was performed in cytotoxicity media (see 4.1.5). In some cases target cells were labeled in advance with the PKH-26 Red Fluorescent Cell Linker (Sigma-Aldrich) as described in 4.2.4.1. Then, 1×10^5 target and 1×10^6 effector cells/well were plated to an U-bottom 96-well plate (Greiner) in 100 μ l media and different concentrations of BiTE in 50 μ l media or pure media as blank control were added. Samples were incubated for 24, 48 or 72 hrs at 37°C, 5% CO₂. After incubation cells were stained with antibodies against EpCAM, CD3 or CD4/CD8, to identify unlabeled target and effector cells. The number of living target cells (n) was evaluated by flow cytometry on a FACSCantoII™ and FACSCalibur™ flow cytometer, respectively, running FACSDiva™ or Cell Quest Pro Software (all BD Bioscience), respectively. The vitality of cells was determined via PI (Sigma-Aldrich) exclusion. The specific lysis was calculated as:

$$\text{Specific Lysis [\%]} = 100 * \left(1 - \frac{n_{\text{Sample}}}{n_{\text{Blank}}} \right)$$

4.2.6 Determination of cytokine concentration

The cytometric bead array (CBA) technology uses the method of a bead - based immunoassay. Each bead is identifiable by discrete fluorescence intensity and provides a capture surface for a specific cytokine via coupled cytokine specific antibodies. Bead bound cytokine is then detected with a secondary phycoerythrin (PE) - labeled cytokine specific antibody. The amount of bound secondary PE – labeled antibody, and therefore the emitted red fluorescence, is directly proportional to the amount of a specific cytokine and can be determined with flow cytometry. For the detection of cytokines two different CBA assays were used. The used CBA kits, e.g. human and mouse Th1/Th2 CBA kit and the mouse inflammatory CBA kit (all BD Bioscience), allow analysis of an already preformed set of cytokines. The CBA flex sets offers the analysis of up to 89 freely combinable cytokines at once. Beads used in the preformed CBA kits are identified with one distinct fluorescent signal whereas two are used for this purpose in the CBA flex set system giving a greater combinatorial possibility. CBA Flex sets used were mouse IL-2 CBA Flex set, mouse IL-6 CBA Flex set, mouse IL-10 CBA Flex set, mouse TNF CBA Flex set, mouse IFN- γ CBA Flex set, mouse IL-3 CBA Flex set, mouse GM-CSF CBA Flex set and mouse IL-4 CBA Flex set (all BD Bioscience).

The assay was conducted in a 96-well V bottom plate (Hartenstein). All washing steps were accomplished by centrifugation at 200xg for 5 min at RT. The cocktails containing the different Flex set beads and Flex set secondary detection antibodies, respectively, were prepared in accordance to the manufacturer's instructions. A twofold serial dilution row ranging from 20 to 5000 pg/ml of provided cytokines was prepared as standard. Serum samples or cell culture supernatants were diluted with provided assay diluent if recommended. Serum or cell culture supernatants were incubated with the bead cocktail and thereafter with secondary antibody cocktail, each for one hour at RT in the dark. Samples were washed once and the bead pellet was solved in provided wash buffer for analysis on a FACSCantoII™ and FACSCalibur™ flow cytometer, respectively, running FACSDiva™ and Cell Quest Pro Software (all BD Bioscience), respectively. The cytometer was calibrated for analysis using the cytometer setup beads as described in the manufacturer's instructions. The data was analyzed by the FCAP Array™ Software (V 1.0, SoftFlow Inc. Hungary). The lower limit of quantification for each analyte was below 20 pg/ml. Concentrations calculated below this value were reported as zero.

4.2.7 TGF- β enzyme linked immuno sorbent assay (ELISA)

Mouse serum concentrations of TGF- β were determined using the human/mouse TGF- β ELISA ready set Go! (Natutec). The provided anti-TGF- β capture and detection antibodies (#eB-461/25D8) recognize only the active form of TGF- β . This molecule is secreted from cells predominantly in its latent form. It is converted to its active form by proteolytic cleavage and subsequent release of the resulting latency associated protein at the source and the target site. For measurement of complete TGF- β content, serum samples were treated with hyperchloric acid to convert all latent TGF- β to the immune-reactive form.

Between each antibody staining or blocking steps the plates were washed 5 times with 250 μ l/well PBS (Invitrogen) containing 0.05% (v/v) Tween 20 (Sigma) using the ELISA washer (molecular devices). All serum samples were diluted 1:5 with PBS (Invitrogen). For acid activation 100 μ l diluted sample was acidified with 20 μ l of 1 M HCl (Merck) for 10 minutes at RT. Samples were then neutralized with 20 μ l of 1 M NaOH (Merck). As standard a twofold serial dilution row of the provided recombinant active TGF- β [8000 pg/ml - 125 pg/ml, blank] was produced with the provided assay diluent. Maxisorp 96 well ELISA plates (NUNC) were coated with 100 μ l of the provided capture antibody mix at 4°C overnight. Plates were blocked with 200 μ l/well provided assay diluent for one hour at RT. For binding of TGF- β wells were incubated with 100 μ l standard, acid activated or normal diluted sample for two hours at RT. To allow the formation of the sandwich ELISA complex, samples were subsequently incubated with 100 μ l provided biotin conjugated detection antibody and 100 μ l provided streptavidin conjugated with horse radish peroxidase (Dako), each for one hour at RT. Finally, plates were incubated with 100 μ l provided tetramethylbenzidine substrate for 15 minutes at RT for detection. The reaction was stopped by the addition of 50 μ l 2N H₂SO₄ (Merck). Absorbance was read at 405 nm on a Power WaveX select (Bio-Tek instruments). Standard curves were fitted by four-parameter analysis. The corresponding OD values of the samples were used to calculate the concentration of active and total TGF- β , respectively.

4.2.8 Determination of whole blood cell count

If not otherwise indicated whole blood cell count was determined as described in 4.2.3.3. In some cases, however, the blood cell count was analyzed using BD TruCount tubes (BD) in accordance to the manufacturer instruction. To maximize accuracy of cell count, centrifugation was avoided and erythrolysis and antibody staining of whole blood cells took place in one provided tube, containing a concrete amount of lyophilized beads. These were distin-

guishable in the forward scatter and side scatter from blood cells. By comparing cellular events to bead events, the absolute number (cells/ μ l) of positive cells in the sample was calculated.

Prior to erythrolysis, 50 μ l of whole blood was directly stained with 20 μ l of the antibody cocktail of choice for 20 minutes at RT in the dark. Afterwards, erythrocytes were simultaneously lysed and stained cells were fixed by adding 350 μ l BD FACS lysing solution (BD Bioscience). After 20 minutes cells were analyzed with flow cytometry. CD45 positive cells were considered as leukocytes and subpopulations were defined by co-expression of surface markers CD19 (B cells) or CD3 (T cells). Total blood cell numbers were determined by following equation:

$$\text{Blood cell count [cell/ml]} = \left(\frac{n_{\text{double positive events}}}{n_{\text{beads in gate}}} \right) * \left(\frac{n_{\text{beads per Test}}}{V_{\text{Test}}} \right)$$

Additionally the hematokrit was determined to rule out injection induced volume effects on the blood cell count.

4.2.9 Depletion of EpCAM⁺ cells from mouse splenocytes and PBMC

In vitro depletion of EpCAM⁺ cells was achieved using a combination of depleting Dynabeads followed by fluorescence activated cell sorting. Briefly, mouse PBMC were labeled with rat anti-mouse EpCAM mAb (G8.8, BD Bioscience). Anti-rat IgG coated magnetic Dynabeads (Invitrogen) were added to bind selectively to cells coated with anti-mouse EpCAM mAbs. The Dynabeads with bound EpCAM⁺ cells were then removed using the MPC-1 magnetic separator (Dyna).

The isolation was performed in Dynal buffer (see 4.2.2.4). Prior to usage anti-rat IgG coated magnetic Dynabeads (Invitrogen) were washed with Dynal buffer as described in 4.2.2.4. $1 \cdot 10^6$ cells were resuspended in 100 μ l Dynal buffer containing 10 μ g/ml rat anti-mouse EpCAM mAb (G8.8, BD Bioscience) for 20 minutes at 4°C. Cells were washed twice with Dynal buffer to remove excess antibodies. Afterwards cells were resuspended in 100 μ l Dynal buffer and 6.25 μ l pre-washed anti-rat IgG coated magnetic Dynabeads (Invitrogen) were added. Antibodies were allowed to bind to Dynal beads for 30 minutes on ice. Separation was performed as described in 4.2.2.4. The magnetic separation was repeated twice to improve purity. The supernatant containing EpCAM depleted mouse PBMCs was subjected to further fluorescence activated cell sorting. Cells were stained with PE-conjugated anti-mouse EpCAM mAb

(BD Bioscience) as described in 4.2.3.1 and were then negatively sorted by a MoFlo High Performance Cell Sorter (DAKO).

4.2.10 Analysis of BiTE serum concentrations

All assays analyzing BiTE serum concentrations were performed and established by the bio-analytical department of Micromet AG (Munich, Germany).

4.2.10.1 Bioassay based BiTE quantification

The method is based on loading cells with a membrane permeable acetoxymethyl ester of a fluorescence enhancing ligand (BATDA). Within the cells its ester bonds are hydrolyzed to form a hydrophilic ligand (TDA), which is trapped in the cells. TDA released by dead cells can form a fluorescent chelate (EuTDA) in the presence of europium solution. The measured signal correlates directly with the amount of lysed cells.

MuS110 serum concentrations were quantified by a bioassay measuring the TDA release of BATDA-labeled CHOMuEpCAM⁺ cells lysed by muS110 redirected T cells. In general, centrifugation of cells was performed at 300xg for 5 min at RT using a Heraeus Multifuge 3 (Kendro Laboratory Products GmbH). If not otherwise indicated, samples were filled up with indicated media for washing and supernatant was discarded after centrifugation.

CHOMuEpCAM⁺ cells were labeled with the DELFIA[®] BATDA reagent (Wallac Oy) according to manufacturer instruction. $1 \cdot 10^6$ cells were incubated with 4 μ l BATDA reagent in cytotoxicity media (see 4.1.5) for 30 minutes at 37°C. Samples were washed four times afterwards with cytotoxicity media. Serum samples or control serum, BATDA-labeled target cells ($2.5 \cdot 10^3$ /well) and CTLL-2 effector cells ($1.5 \cdot 10^5$ /well) were incubated together for 3 hours at 37°C, 5% CO₂, to allow redirected lysis. 20 μ l supernatant containing TDA released by dead cells was incubated for 60 minutes at RT with 100 μ l DELFIA[®] Europium solution (Wallac Oy) to allow stable formation of EuTDA. The amount of EuTDA was quantified by analysis of the relative fluorescence intensity (RFU_S) at 520 nm with a Victor Multilabel Counter (Wallac Oy). Fluorescence intensity of background lysis (RFU_B) was determined in control serum samples. Fluorescence intensity of maximal lysis (RFU_M) was determined using DELFIA[®] lysis buffer (Wallac Oy) according to manufactures instructions. Standard samples were generated by a fourfold serial dilution of muS110 [2 μ g/ml – 7.6 pg/ml] and specific cell lysis was plotted against muS110 concentrations using Prism 4 (Graph Pad

Software). The limit of quantification was determined as 1 ng/ml. The percentage of specific cell lysis was calculated as:

$$\text{Specific Lysis [\%]} = \left[\frac{\text{RFU}_S - \text{RFU}_B}{\text{RFU}_M - \text{RFU}_B} \right]$$

4.2.10.2 BiTE quantification with Meso Scale Discovery (MSD)

The muS110 PK ELISA is based on the electrochemiluminescence detection technology developed and established from the company Meso Scale Discovery (MSD). This technology uses SULFO-TAGTM labels that emit light upon electrochemical stimulation initiated at the electrode surfaces of MULTI-ARRAY[®] micro plates. This signal is measured as a mean signal in the detector (emission at ~620 nm). Thus, the stimulation mechanism (electricity) is decoupled from the signal (light), leading to minimal background signals and high signal to background ratios. The procedure of the assay is based on the ELISA “sandwich” method.

According to manufactures’ instructions, a 96-well MSD High Bind Plate (MSD) was coated with 5 µl soluble mouse EpCAM ([64 µg/ml], Micromet AG) for 2 hours at RT and blocked with MSD Blocker A (MSD) for 1 hour at RT. 25 µl mouse serum was added and plates were incubated for 75 minutes at RT to capture muS110 present in the serum. This step was followed by a first incubation with 25 µl biotin-conjugated anti-pentahistidine antibody ([1 µg/ml], Qiagen) and a second incubation with 25 µl MSD SULFO-TAG labeled streptavidin ([2 µg/ml], MSD) to form a detectable sandwich complex. Both incubations were at 25°C for 30 minutes. Between each antibody staining or blocking steps the plates were washed 5 times with 250 µl/well PBS (Invitrogen) containing 0.05% (v/v) Tween 20 (Sigma) using the ELISA washer (molecular devices). After addition of 150 µl MSD Reading buffer the electrochemical signal of the bound ELISA sandwich was quantified with a SECTORTM Imager 2400 (MSD). For calibrations, a 4-fold serial dilution of muS110 [2 – 7.6 pg/ml] was performed. Unknown muS110 concentrations in mouse serum were back calculated with the help of the muS110 calibration curve using Prism 4 (Graph Pad Software). The limit of quantification was determined to be 0.2 ng/ml.

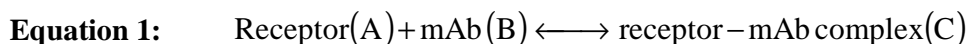
4.2.11 Saturation binding analysis and calculation of receptor occupancy

In general, centrifugation of cells was performed at 300xg for 5 min at RT using a Heraeus Multifuge 3 (Kendro Laboratory Products GmbH). If not otherwise indicated, samples were

filled up with indicated media for washing and supernatant was discarded after centrifugation. The cell count was determined using a hemacytometer (Marienfeld).

1×10^5 cells/well were incubated for 1 hour at RT with various concentrations of the respective BiTE antibody using a 4 fold serial dilution ranging from 1 $\mu\text{g/ml}$ to 0.24 ng/ml in FACS buffer. Cells were washed twice with FACS buffer to remove unbound BiTE. To detect bound BiTE antibody, cells were incubated first with a hexahistidine tag-specific secondary antibody labeled with biotin (Dianova) and then with PE-labeled streptavidin (BD Bioscience). Both incubation periods were at RT for 30 minutes and cells were washed twice with FACS buffer in between. Binding was analyzed by flow cytometry on a FACSCantoIITM device running FACS Diva software (both BD Biosciences). The mean fluorescence values of PE were plotted against the different BiTE concentrations. KD values were determined using the one site hyperbola fit function in Prism4 (Graph Pad Software).

At equilibrium condition the fraction of all receptor molecules that are bound to the antibody can be calculated if the concentration [mAb] and the dissociation constant KD of the respective antibody are known. The amount of a mAb bound to its receptor can be estimated from the following binding relationship:



The binding dissociation constant (KD) of the respective antibody is represented by:

Equation 2:
$$\text{KD} = \frac{[\text{receptor}] \times [\text{mAb}]}{[\text{receptor - mAb}]}$$

Finally the fractional occupancy, fraction (F) of all receptor molecules that are bound to the antibody can be calculated by:

Equation 3:
$$F = \frac{[\text{receptor - mAb}]}{[\text{receptor}] + [\text{receptor - mAb}]}$$

Formation of equation 2 and substitution in equation 3 results in:

Equation 4:
$$F = \frac{[\text{mAb}]}{[\text{mAb}] + \text{KD}}$$

4.2.12 Histopathology

Histological and pathological studies were contracted to Huntingdon Life Sciences Ltd (UK). Eyes were fixed in Davidson's fluid, testes and epididymides were fixed in Bouin's solution prior to transfer to 70% industrial methylated spirit. All other samples were fixed in 10% neutral buffered formalin (adrenals, brain, caecum, colon, duodenum, femurs, gall bladder,

harderian glands, heart, ileum, jejunum, kidney, lachrymal glands, larynx, liver, lungs, lymph nodes mandibular and mesenteric, mammary area (caudal), esophagus, optic nerves, ovaries, pancreas, pituitary, prostate, rectum, salivary glands, seminal vesicles, skeletal muscle, spinal cord, spleen, stomach, thymus, thyroid with parathyroid's, tongue, ureters, urinary bladder, uterus and cervix, vagina). Tissue samples were dehydrated, embedded in paraffin wax, sectioned at approximately 4-5 micron thickness and stained with haematoxylin and eosin. A reviewing pathologist undertook a peer review of the microscopic findings.

4.2.13 Mouse models and *in vivo* work

4.2.13.1 Housing

All experiments were performed according to the German Animal Protection Law with permission from the "Ethical Committee on Animal Care and Use" of the government of Bavaria, Germany. All efforts were made to keep their number and suffering limited to the minimum. Animals were kept in a temperature (25 ± 2 °C) and humidity ($50 \pm 5\%$) controlled room with an artificial 12 hour light-dark rhythm and rodent food pellets (Sniff, Soest) and autoclaved tap water available *ad libitum*. Animals were housed in standard Microloan type II - long cages (Beech) in individually ventilated cages to achieve specified pathogen - free conditions. Health status of animals was checked twice a year monitoring sentinels according to FELASA criteria. Commercially obtained animals were allowed to adapt to their surroundings at least 7 days before they were included to experiments.

4.2.13.2 Monitoring of health, body weight and temperature

Body weight was obtained with a MXX - 212 balance (Denver instruments). To measure body temperature, animals were chipped with temperature sensitive IPTT-300 transponders (PLEXX). The transponder was implanted subcutaneously between the two *scapulae*. Prior to implantation, mice were anaesthetized with 3-4% isoflurane (CP Pharma) for up to 1 minute using an Isotec3 isoflurane evaporator (Voelker GmbH). Chipped animals were allowed to recover for 4 days before they were included to experiments. The temperature was scanned with a DAS-6007 scanner running DAS Host software (both PLEXX). Animals were monitored prior and during experiments for the appearance of diarrhea, healthy fur appearance, relaxed posture, frequency of movements and breathing. Piloerection (ruffled fur), hypomotility, diarrhea, gasping and hunched posture was assessed as absent (-), mild (-/+) or strong (+). In some cases pictures and videos were made with a DM-FZ 30eGLumix digital camera (Panasonic) for documentation.

4.2.13.3 Application techniques

Used application techniques were intravenous (i.v.) injection via the tail vein, subcutaneous (s.c.) application under the skin of the left abdominal flank and intraperitoneal (i.p.) injection into the body cavity. For all injections Omnican syringes (0.3x12mm, 0.01-1 ml, Braun) were used.

The treatment dose was given in mg/kg. The agent was either injected according to individual mouse weight (10 µl agent per 1 g mouse), whereby the concentration of the injection solution ($C_{\text{Injection}}$) was always calculated as (dose * 0.02 kg/ 0.2 ml), or $C_{\text{Injection}}$ was calculated with the mean group body weight (m_{BW}) and a fixed injection volume ($V_{\text{Injection}}$) according to following equation:

$$C_{\text{Injection}} = \left[\frac{\text{Dose} \times \overline{m_{\text{BW}}}}{V_{\text{Injection}}} \right]$$

For s.c. application mice were first immobilized by grasping the excess skin over the animal's back between the thumb and forefinger and fixing the tail with the smallest finger. Whilst the mouse was lying on its back within the palm of the hand, the substance was applied in a volume of 50 µl under the skin in the lower left quadrant.

For i.p. application mice were restrained as described above and held with their ventrum exposed and head pointed downwards. This causes the freely moveable abdominal organs to move towards the animal's diaphragm, making accidental puncture of organs less likely. The needle was inserted into the abdominal cavity in the lower right quadrant to avoid the caecum and urinary bladder and the substance was applied in a volume of 200 µl.

For i.v. application animals were pre-warmed for 5 minutes using a heating box (VetTech Solutions) to increase visibility of the tail vein. Animals were fixed in a plexiglass restraining cylinder. The needle was inserted in the lateral tail vein by directing the needle with its bevel pointing upward at an angle of approximately 20 degrees. Once the vein's wall had been penetrated the needle was directed cranially and the substance was applied according to individual mouse weight (10 µl agent per 1 g mouse) or in a fixed volume of 200 µl within 15 seconds.

4.2.13.4 Blood sampling

Blood was obtained either via heart punctation or retro-orbital bleeding. For retro-orbital bleeding animals were anaesthetized with 3-4% isoflurane for up to 1 minute using an Isotec3

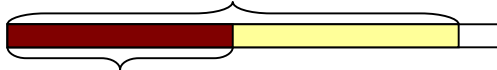
Isoflurane Evaporator (Voelker GmbH). Blood was taken from the ruptured peri-orbital sinus with heparinized MiniCAPS capillaries (5 μ l, Hirschmann Laborgeräte). Prior to heart punctation animals were euthanized on dry ice. The thorax was opened to expose the heart and venous blood was obtained from the right ventricle of the heart using a Sterican100 needle (0.05x16mm, 25Gx5/8“, Braun).

For serum preparation blood was collected in microtainer SST Tubes (BD Bioscience) and allowed to coagulate for 1 hour at RT. Samples were then spun down with 7000xg for 5 minutes at RT in a Mikro 20 centrifuge (Type 2004, Hettich) to separate serum from blood cells. Serum was stored at -80°C for subsequent cytokine analysis and at -20°C for determination of BiTE serum concentrations. In all other cases blood was collected in pre-heparinized containers and 5 μ l heparin was added to prevent coagulation. Samples were stored on ice until further usage.

In some experiments hematokrit of 50 μ l freshly sampled blood was determined with heparinized Mikro hematokrit capillaries (Heiland) using the hematokrit sealing kit (Heiland). Capillaries filled with blood were spun with 13.000xg for 2 minutes at RT in a hematokrit centrifuge to spin down all blood cells. The hematokrit was determined using following equation:

$$\text{Hematokrit [\%]} = 100 \times \frac{l_{\text{cell}}}{l_{\text{total}}}$$

Hematokrit capillary



4.2.13.5 Tumor models

Prior to tumor inoculation, respective exponential growing tumor cells were cultivated and harvested as described in 4.1.1. Mouse T cells were prepared as described in 4.2.2. Cells were washed with PBS and spun down by centrifugation in a Heraeus Multifuge 3 (Kendro Laboratory Products GmbH) at 300xg for 5 minutes at RT. The cell pellet was resolved in PBS and the cell count was determined using a hemacytometer (Marienfeld). The vitality of cells was determined using 0.5 % (v/v) isotonic EosinG solution (Roth). Cells were only used, if vitality was higher than 92%. Until inoculation cells were stored on ice. In solid tumor models lymphocytes were mixed to tumor cells prior to tumor inoculation, to resemble the physical situation of lymphocyte infiltrated human tumors. Cells were applied with a Sterican100 cannula (0.05x16mm 25Gx5/8, Braun) and syringes were loaded without a cannula to avoid cell disruption.

For the orthotopic 4T1 mouse breast carcinoma model, a mixture of 10^4 4T1 tumor cells and indicated amount of mouse T cells was injected in a final volume of 50 μ l PBS into the mammary fat pad of BALB/c mice. The solid 4T1 Tumors were measured on the indicated days with a caliper in two perpendicular dimensions and tumor volumes calculated according to the following equation. In compliance with the Animal Protection Law, mice had to be euthanized when tumor volumes exceeded 10% of their body weight.

$$\text{Tumor Volume [cm}^3\text{]} = \frac{\text{width}^2 \times \text{length}}{2}$$

For the CT-26 lung cancer model, 1×10^5 CT-26muEpCAM⁺ tumor cells were intravenously injected in the lateral tail vein of BALB/c mice in a final volume of 200 μ l PBS. For the B16F10 lung cancer model, 1×10^5 B16F10muEpCAM⁺ tumor cells were intravenously injected into the lateral tail vein of C57BL/6N mice in a total volume of 200 μ l PBS. CT-26muEpCAM⁺ or B16F10muEpCAM⁺ tumor cells were trapped in the small pulmonary venules around the alveoles of the lung, where they form small tumor colonies on the lung surface. The body weight was determined daily to check animal health status. The observation period was limited to 17 days for ethical reasons because of the severe effects of high lung tumor burden on respiration. Animals were sacrificed and the number of CT-26muEpCAM⁺ or B16F10muEpCAM⁺ tumor cell colonies on the lung surface was determined macroscopically.

Statistical analysis of the mean tumor volume or the lung metastasis burden of the corresponding treatment groups versus the vehicle control group was performed using the Student's t test.

4.2.13.6 Dissection, isolation of organs and fixation

Animals were sacrificed on frozen CO₂ or with cervical dislocation during isoflurane anesthesia. Gross pathology of animals was performed and abnormalities were noted. In some cases pictures were made with a DM-FZ 30eGLumix digital camera (Panasonic) for documentation. In some cases tumor tissue, lung, thyme, spleen, mesenterial lymph nodes, superficial cervical lymph nodes, inguinal lymph nodes or payers patches were isolated and stored in cytotoxicity medium (see 4.1.5) on ice until further *ex vivo* analysis. In some cases the brain, the gastrointestinal tract (caecum, colon, duodenum, ileum, jejunum, esophagus, and rectum), the heart, the kidney, the liver, the lungs, the cervical and mesenteric lymph nodes, the spleen and the thymus were removed and fixed in 10% neutral buffered formalin (Sigma-Aldrich) for further

histo-pathological analysis. Tumor tissue and organs infiltrated by tumor metastasis were embedded in tissue tec O.C.T compound (Sakura), frozen in liquid nitrogen and stored at -80°C until further histological analysis.

5 RESULTS

5.1 *In vitro* characterization of muS110

5.1.1 Binding affinities of muS110 to CD3 and EpCAM

Saturation binding assays were performed with CD3-enriched mouse T cells and CHOmuEpCAM⁺ cells. The cells were incubated with a 4-fold serial dilution row of muS110. Bound BiTE antibody was quantified by flow cytometry after staining with a hexahistidine tag-specific antibody labeled with biotin followed by streptavidin-PE. The equilibrium binding constants (KD) were obtained by computational analysis with Prism 4 (one side hyperbola fit) plotting the normalized binding signal against the various muS110 concentrations (Figure 5).

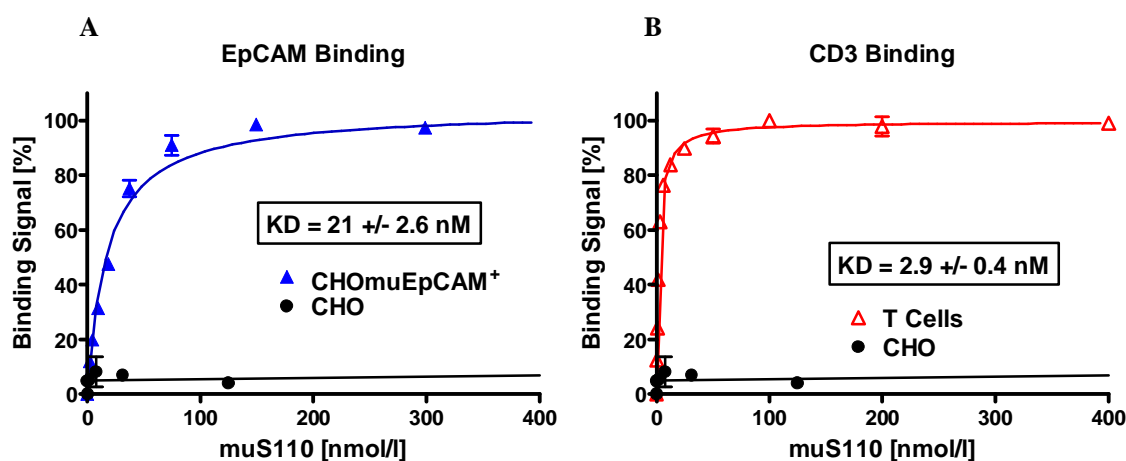


Figure 5: Saturation binding of muS110 to cells expressing EpCAM or CD3

Saturation binding assays were performed with CHO cells, (A) CHO cells transfected with mouse EpCAM antigen or (B) CD3 enriched mouse splenocytes. The cells were incubated with a 4-fold serial dilution row of muS110. Bound BiTE antibody was quantified with flow cytometry after staining with a hexahistidine tag-specific antibody labeled with biotin followed by streptavidin-PE. For saturation binding curves the mean fluorescence was normalized to the respective strongest signals and plotted against various muS110 concentrations. The KD values were obtained by computational analysis with Prism 4 (one side hyperbola fit) and are indicated in the corresponding graphs. Error bars indicate standard error of the mean (SEM) of triplicates.

MuS110 binds only to cells expressing either mouse CD3 ϵ or mouse EpCAM. No signal was detected with CHO cells lacking these antigens. The KD values for mouse EpCAM were 21 +/- 2.6 nM and 2.9 +/- 0.4 nM for CD3 ϵ . The binding affinities for EpCAM were comparable for muS110 and MT110 (21 +/- 2.6 nM to 13 +/- 0.25 nM). The binding affinity to the CD3 ϵ antigen was about 35 times stronger for muS110 than for MT110 (2.9 +/- 0.4 nM to 100 +/- 15 nM) (85).

5.1.2 Redirected lysis of respective target cells mediated by muS110

The potency of muS110 to mediate redirected lysis of mouse EpCAM positive target cells was tested for the mouse breast cancer cell line 4T1, naturally expressing EpCAM, and for CHO hamster cells, CT26 mouse colon carcinoma cells and B16F10 mouse skin melanoma cells, all transfected with mouse EpCAM. The respective target cells were incubated for 48 hours with CD3⁺-enriched mouse splenocytes at an effector to target (E:T) ratio of 10:1 in the presence of increasing concentrations of muS110. Similar assays were performed with the control BiTE hyS110 to assess the specificity of BiTE kill. HyS110 shares the CD3 binding part with muS110 but the target cell binding moiety is directed against human EpCAM instead of mouse EpCAM. The cytotoxic activity of muS110 was analyzed as the ability to induce apoptosis (caspase assay) or cell lysis (ToxiLight assay; FACS based assay) (Figure 6). The caspase index or the specific lysis was plotted against the antibody concentrations to obtain the half-maximal kill (EC_{50}) as indicator for specific bioactivity.

MuS110 was able to mediate lysis of all EpCAM expressing target cells by naive CD3-enriched splenocytes in a dose dependent fashion. The EC_{50} for all analyzed cell lines was over a range of 0.3 – 3 ng/ml muS110, namely 0.3 +/- 0.1 ng/ml for 4T1 cells, 1.6 +/- 0.7 ng/ml for CHOmuEpCAM⁺ cells, 1.1 +/- 0.9 ng/ml for CT26muEpCAM⁺ cells and 2.1 +/- 1.1 ng/ml for B16F10muEpCAM⁺ cells. However, the magnitude of the induced cytotoxic effect differed for each cell line and was additionally dependent on the test system. These differences most probably reflected individual sensitivity of each test system for the death of respective cell lines. Cell lines differ in the ability to produce adenylylase kinase, maintain enough cell integrity upon lysis for detectable PI incorporation, and the fraction played by apoptosis and lysis in their destruction. The control BiTE hyS110 did neither induce redirected lysis nor apoptosis in any of the tested cell lines with exception of B16F10muEpCAM⁺ cells analyzed by a FACS-based assay. However, this cell line seemed to be particularly sensitive to PI incorporation. The determined EC_{50} value for muS110 mediated re-directed lysis was also increased for more than an order of magnitude in comparison to all other assessed cell lines, which was not seen for the caspase or the ToxiLight assay. The unspecific lysis of B16F10muEpCAM⁺ target cells by hyS110 was clearly less pronounced and only detectable at high doses.

It was shown that the half-maximal lysis of CHO cells transfected with the respective target antigen was comparable for MT110 (0.65 +/- 0.5 ng/ml, n=5) and muS110 (2.51 +/- 1.2 ng/ml, n=10) (85).

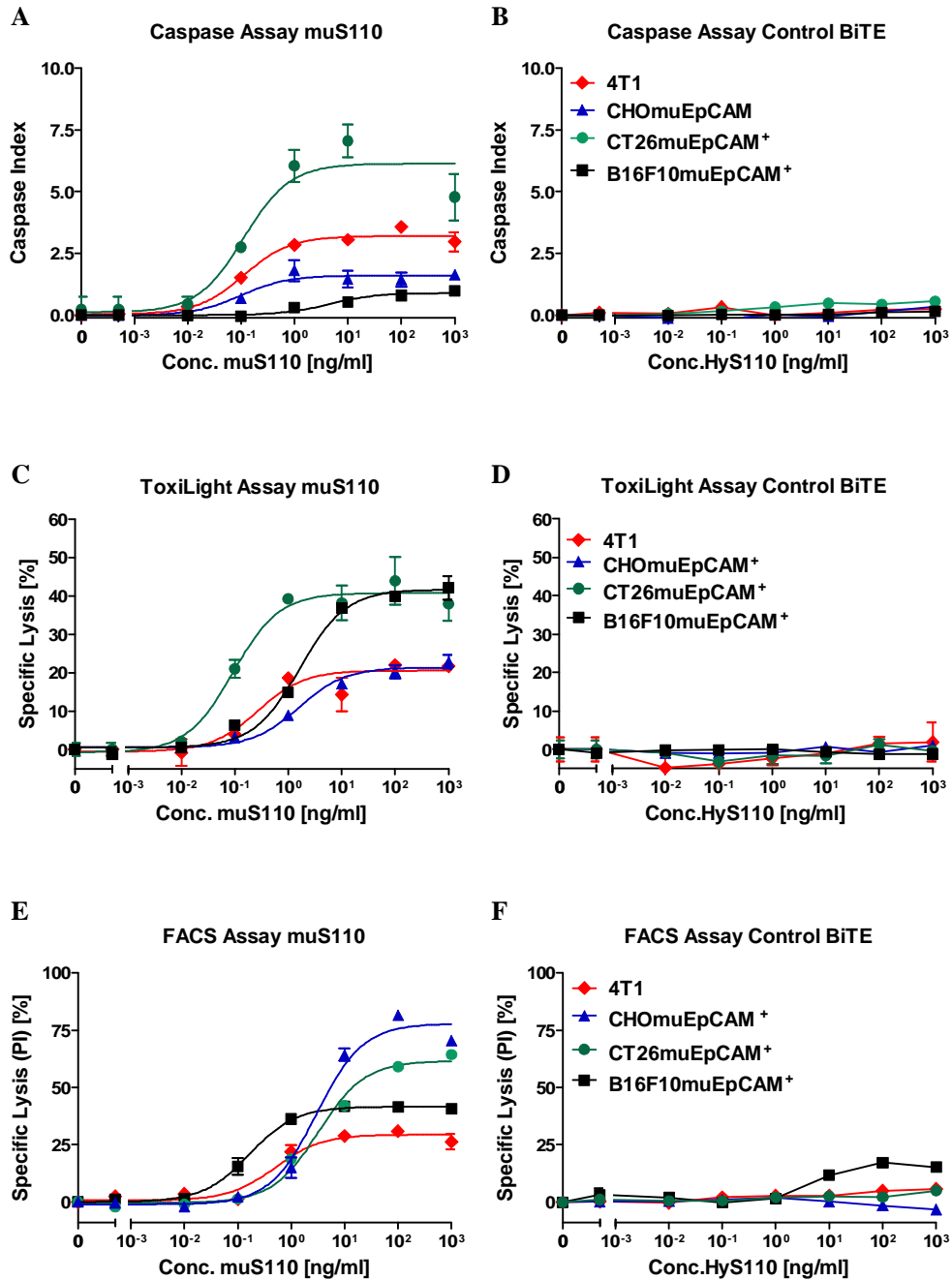


Figure 6: MuS110 redirected lysis of EpCAM⁺ target cells

The respective target cell line was incubated for 48 hours with CD3-enriched mouse splenocytes at an effector to target (E:T) ratio of 10:1 in the presence of increasing concentrations of muS110 (right side) or the control BiTE hyS110 (left side). (A, B) Potency to induce apoptosis was quantified with the caspase assay. (C - F) Potency to kill target cells was assessed with (C, D) the ToxiLight assay, or (E, F) the FACS based analysis of propidium iodide incorporation. Specific lysis was calculated as percentage of living cells in the sample corrected by that of the blank value. Dose response curves were obtained plotting the caspase index or the specific lysis against the antibody concentrations. Error bars indicate SEM of triplicates. Each cell line with each test system was tested at least three times.

5.1.3 T cell activation mediated by muS110

5.1.3.1 Cell proliferation in cytotoxicity assays

To assess muS110 induced T cell proliferation, PKH-26-labeled CHOmuEpCAM⁺ cells were incubated with mouse splenocytes at an E:T ratio of 10:1 in the presence of increasing concentrations of muS110 or the control BiTE hyS110. After 48 and 72 hours cells were stained for CD4 and CD8 to identify effector cells. The absolute number of alive T cells and target cells was determined by PI exclusion using flow cytometry (Figure 7).

MuS110 induced T cell proliferation in a dose dependent way and led to a 3-fold increase after 48 hours and a 5-fold increase in T cell numbers after 72 hours. However, the highest dose of muS110 led in some cases to a strong reduction of T cell vitality. The EC₅₀ values of proliferation were an order of magnitude lower than that observed for target cell lysis. The control BiTE hyS110 was not mitogenic (Figure 7A). Target cell numbers increased over time as well and almost doubled every 24 hours in the blank values and for the control BiTE. However, the total number of alive and dead target cells decreased in a reverse, concentration dependent way and decreased at high muS110 concentrations far below the initial applied numbers (Figure 7B). Dead target cells lost their cell integrity already after 48 hours and could not be detected by PI inclusion anymore. Therefore, the percentage of PI positive dead cells in a sample underestimated the percentage of cells killed by muS110-mediated redirected lysis. As a result specific lysis calculated as percentage of dead cells in the sample corrected by that of the blank value underrated the biologic potency of muS110 (Figure 7F). This affected mostly the amplitude but also to a smaller extend the EC₅₀ values of specific lysis. The magnitude of this systemic error depended on the proliferative ability of the respective target cell, duration of the test and on the integrity of dead target cells. This could be circumvented by calculating specific lysis from the actual numbers of living PI negative target cells in the sample (n_{Sample}) and the blank value (n_{Blank}) as $100 * [1 - (n_{\text{Sample}} / n_{\text{Blank}})]$ (Figure 7E). First, it takes the assay dynamic in account and second, it resembles more closely the situation *in vivo*, in which the tumor growth of an untreated animal is compared to that of a treated animal. Assays relying on the release of apoptotic factors (caspase assay) or cellular enzymes (ToxiLight assay) suffer from a similar systemic error. The amount of all target cells present in the blank value was much higher than that in samples with high muS110 concentrations. The amount of effector cells rises with increasing muS110 concentrations. The resulting E:T ratio after 48 or 72 hours depends on the BiTE concentration (Figure 7E).

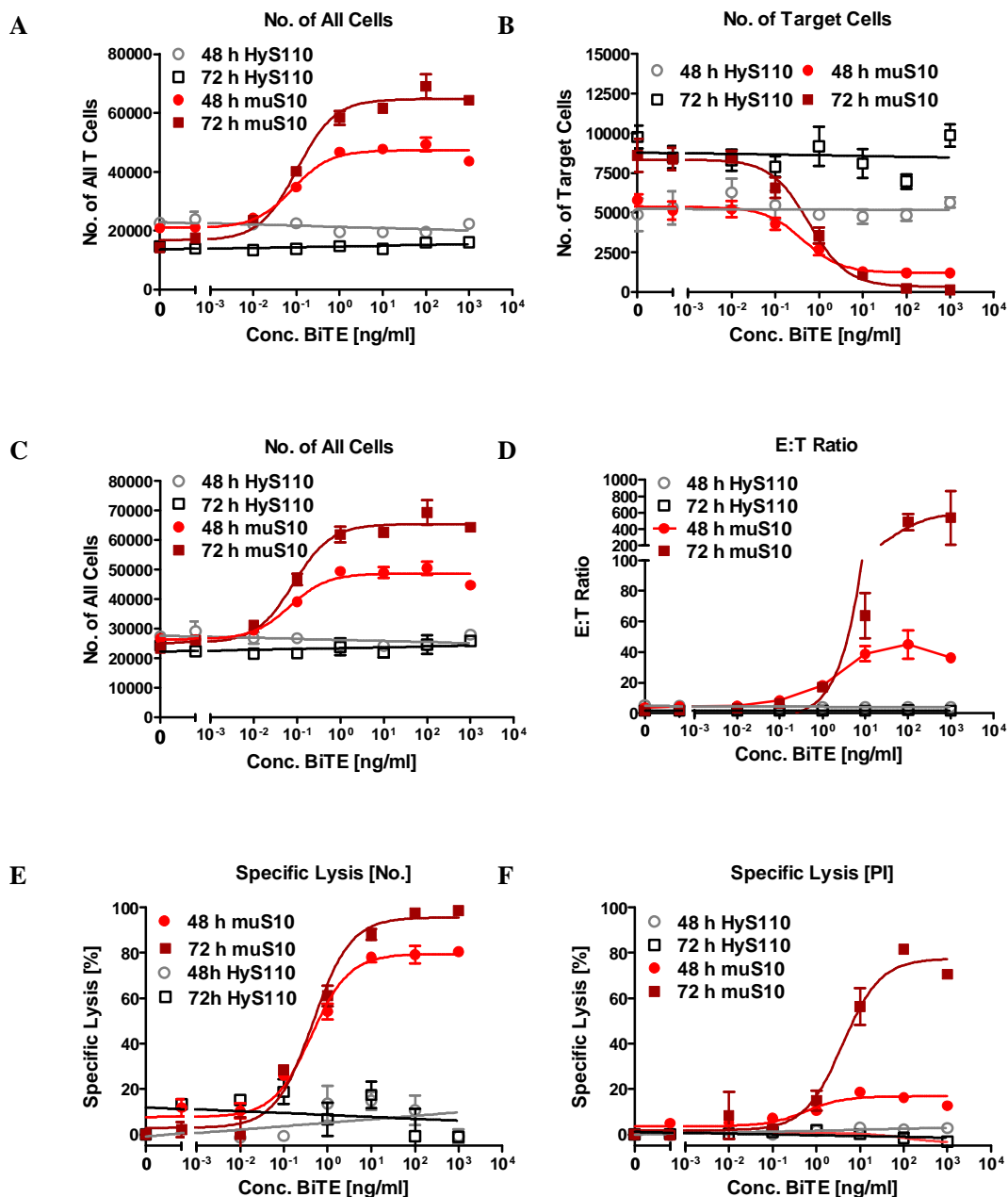


Figure 7: MuS110 mediated T cell proliferation and FACS analysis of redirected lysis

CHOMuEpCAM⁺ cells, labeled with PKH-26, were incubated for 48 or 72 hours with mouse splenocytes at an E:T ratio of 10:1 and increasing concentrations of muS110 or the control BiTE hyS110. T cells were stained for CD4 and CD8 and the vitality of cells was determined by PI exclusion. Cell number of (A) total T cells (of note, in some assays, the highest concentrations of muS110 reduced T cell vitality, therefore the number of all T cells is shown). (B) target cells and (C) all cells were determined with flow cytometry. (D) The E:T ratio was plotted against the increasing BiTE concentrations. Specific lysis was calculated (F) as percentage of living target cells in the sample corrected by that of the blank value or (E) with the number of living target cells in the sample and the blank value after following equation $100 * [1 - (n_{\text{Sample}} / n_{\text{Blank}})]$. Error bars indicate SEM of triplicates of one experiment. Each experiment was repeated four times.

Therefore, the source and the amount of measurable factors released by spontaneous or maximal lysis are different for each respective muS110 concentration. Normalization of muS110 induced lysis to spontaneous and maximal lysis of the blank value implies a systemic error. Unlike in the FACS based assay, the magnitude of this systemic error cannot be evaluated. There is no way to determine the fraction of soluble factors released by effector cell lysis, as it relies on BiTE-induced mitogenicity, which is depending on target cell presence. Hence, the cytotoxic bioactivity of muS110 was determined only by FACS based assays in the following sections.

5.1.3.2 Up-regulation of T cell activation marker induced by muS110

CD25 is the α - chain of the IL-2 receptor, which induces T cell proliferation and activation upon IL-2 ligation. Activation by the IL-2 receptor leads in a negative regulatory loop to its own down modulation and to the expression of inhibitory receptors like CD152 (92). CD69 is a glycoprotein acquired during lymphoid activation and functions as a signal-transmitting receptor. As both surface antigens are up-regulated upon normal T cell activation, their appearance was monitored during muS110-mediated redirected lysis of target cells. CHO-muEpCAM⁺ cells were incubated for 24, 48 or 72 hours with negatively isolated naive T cells at an E:T ratio of 10:1 in the presence of increasing concentrations of muS110 or the control BiTE muMec14. Like hyS110, muMEC14 shares the CD3 binding arm with muS110 but cannot bind to any other mouse protein, and was therefore alternatively used as second control BiTE. Cells were stained for CD4 and CD8 to identify T cells and for CD25 and CD69 to analyze T cell activation by flow cytometry (Figure 8).

MuS110 led to a dose dependent up-regulation of CD69 and CD25 on almost all CD4⁺ and CD8⁺ T cells. The EC₅₀ values for CD69 and CD25 up-regulation were 1.1 +/- 0.2 ng/ml after 24 hours, 0.5 +/- 0.2 ng/ml after 48 hours and 0.3 +/- 0.1 ng/ml after 72 hrs. Hence, a trend towards a time dependent reduction of EC₅₀ values was visible. The amplitude of CD69 up-regulation was most pronounced after 24 hours and decreased thereafter, whereas CD25 up-regulation was strongest after 72 hours. This is in concert with CD25 being an intermediate activation marker up-regulated 24 to 72 hours after T cell activation, whereas CD69 is known as one of the earliest inducible cell surface activation markers. Most probably it was already starting to be down regulated 24 hours after the initial T cell stimulus. Slight up-regulation of CD25 (20-40%) and CD69 (10-30%) was also observed at the highest concentration of control BiTE (1 μ g/ml) although no up-regulation of activation marker were seen at lower doses.

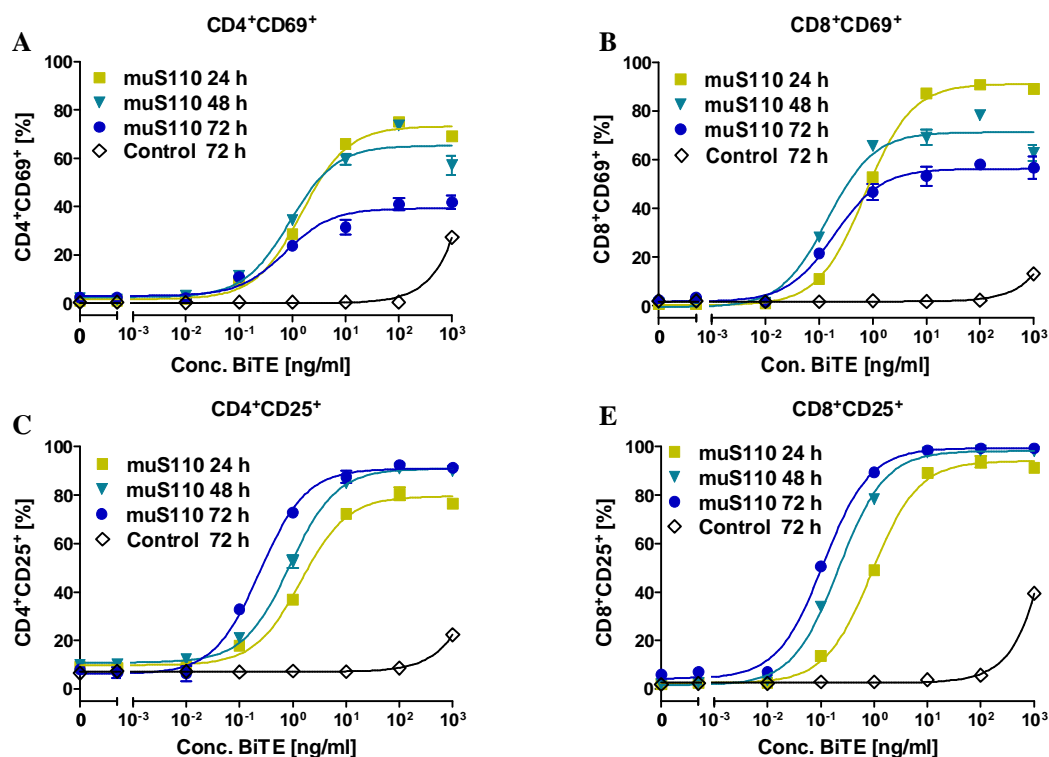


Figure 8: Up-regulation of the activation marker CD25 and CD69 induced by muS110

CHOMuEpCAM⁺ target cells were incubated for 24, 48 or 72 hours with negatively isolated mouse T cells (spleen) at an E:T ratio of 10:1 and increasing concentrations of muS110 or the control BiTE muMec14. Cells were stained with antibodies against CD4, CD8 and EpCAM to differentiate between target and T cells and with antibodies against CD25 and CD69 to monitor T cell activation. Cells were analyzed by flow cytometry to determine percentage of (A) CD69 and (C) CD25 CD4⁺ T cells and (B) CD69 and (D) CD25 CD8⁺ T cells. Error bars indicate SEM of triplicates. The experiment was repeated two times.

The stimulating potential of muS110 was also compared to a standard technique of *in vitro* T cell stimulation. Freshly isolated mouse splenocytes were activated with surface bound anti-CD3 and anti-CD28 antibodies (Dynabeads Mouse CD3/CD28 T cell expander) in the presence of IL-2 [100 U/ml] for 48 hours. Activated and naive mouse splenocytes were incubated with CHOMuEpCAM⁺ target cells (E:T = 10:1) for 48 hours in the presence of 100 ng/ml muS110. Naive splenocytes and activated splenocytes were analyzed for the activation markers CD134, CD62L and CD127, before and after the cytotoxic assay (after CT) by flow cytometry (Figure 9). An intracellular staining was performed to detect CD152, granzyme B and IFN- γ , which were also shown to be induced by MT110 (88).

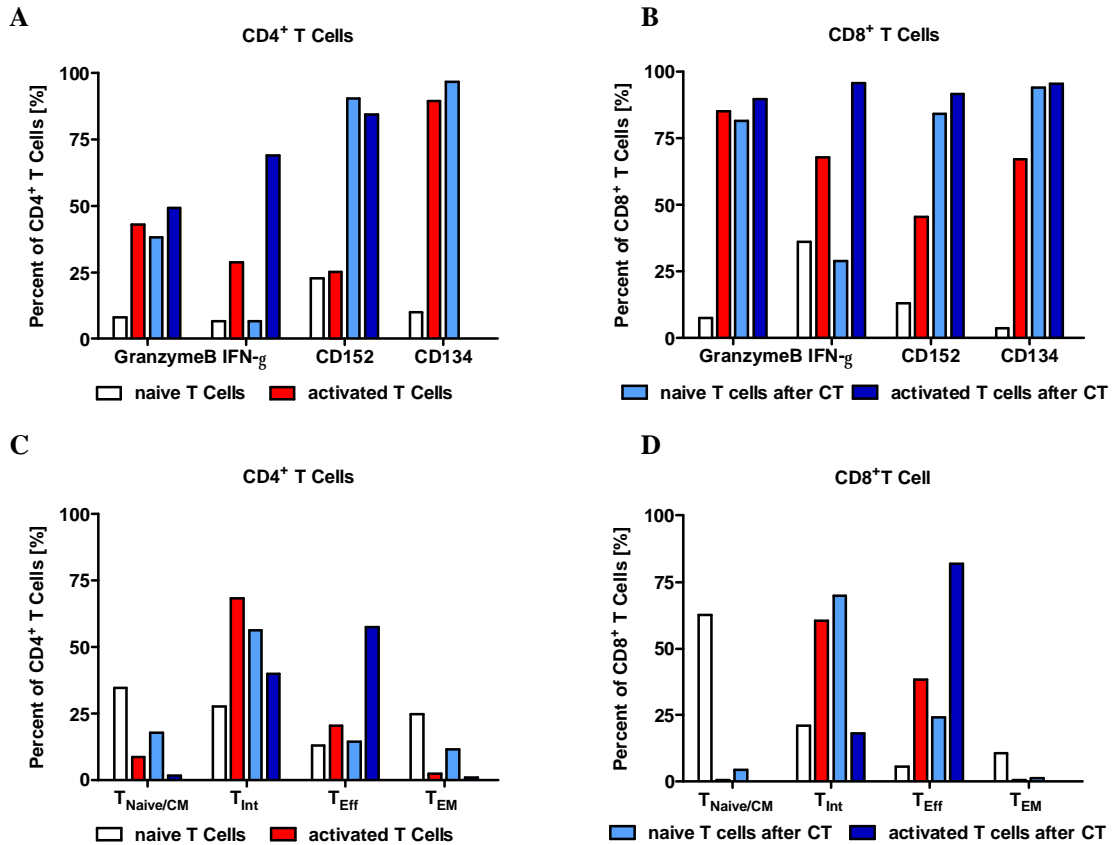


Figure 9: MuS110 induced T cell activation and transformation of naïve to effector T cells

To assess muS110 induced activation of T cells freshly isolated mouse splenocytes (naive T cells) or activated T cells were incubated with CHOMuEpCAM⁺ target cells (E:T = 10:1) for 48 hours in the presence of 100 ng/ml muS110. For T cell activation cells were stimulated for 48 hours with the Dynabeads Mouse CD3/CD28 T cell expander in the presence of 100 U/ml rhuIL-2. After muS110 stimulation (after CT) cells were stained with antibodies against CD4 and CD8 to identify T cells. A part of the cells were stained with antibodies against the surface marker CD127, CD62L and CD134. The rest was stimulated with PMA/ ionomycin in the presence of Brefeldin A for 4 hours and afterwards intracellular staining with antibodies against granzyme B, IFN- γ and CD152 was performed using the Cytotfix/ Cytoperm Kit. (A, B) Percentage of granzyme B, IFN- γ , CD152 and CD134 positive CD4 (A) and CD8 (B) cells. (C, D) Percentage of naive/ central memory T cells (T_{Naive/CM}, CD62L⁺ CD127⁺), intermediate T cells (T_{Int}, CD62L⁺ CD127⁻), effector T cells (T_{Eff}, CD62L⁻ CD127⁻), and effector memory T cells (T_{EM}, CD62L⁻ CD127⁺) in the CD4⁺ (C) and CD8⁺ (D) T cell compartment. The results are representative for four similar experiments.

Granzyme B is a serine protease released by cytoplasmic granules of cytotoxic effector T cells to induce apoptosis and cell destruction of target cells. IFN- γ is primarily secreted by activated T cells and natural killer cells and mediates a plethora of effects. It can promote macrophage activation, mediates antiviral and antibacterial immunity, enhances antigen presentation, orchestrates activation of the innate immune system, coordinates lymphocyte-

endothelium interaction, regulates the TH₁/TH₂ balance, and controls cellular proliferation and apoptosis (93). CD152, better known as CTLA-4, is up-regulated during TCR- and CD28-mediated T cell activation. It is an inhibitory receptor for B7 molecules and antagonizes the positive CD28 co-stimulus (94). CD134, also known as Ox40, is a member of the tumor necrosis factor (TNF) receptor superfamily and is expressed 24-72 hours following T cell activation. OX40 has a critical role in the maintenance of an immune response beyond the first few days onwards to a memory response due to its ability to enhance survival (95). Additionally the relative amount of naive or central memory T cells (T_{Naive/CM}, CD62L⁺ CD127⁺), intermediate T cells (T_{Int}, CD62L⁺ CD127), effector T cells with high lytic potential (T_{Eff} CD62L⁻ CD127) and effector memory T cells (T_{EM}, CD62L⁻ CD127⁺), known to produce huge amounts of IL-2 and proliferate strongly upon antigen stimuli, were determined (96).

The strength of muS110 induced T cell activation was comparable to that imposed by a full CD3/CD28 stimulation in the presence of IL-2. There was a similar up-regulation of granzyme B and CD134 and an even stronger up-regulation of CD152. Noticeable, approximately 50% of CD4⁺ and almost 80% of CD8⁺ T cells were granzyme B positive and therefore armed to destroy EpCAM⁺ target cells. In contrast to CD3/CD28/IL-2 stimulated splenocytes no rise of intracellular INF- γ was detected after muS110-induced activation of splenocytes (Figure 9A and B). However, subsequent muS110 activation of pre-activated T cells led to a strong increase of IFN- γ secreting T cells and almost 75% of CD4⁺ and more than 90% of CD8⁺ T cells were stained positively. CD3/CD28/IL-2 stimulation resulted in a comparable transition of T_{Naive/CM} and T_{EM} to T_{Eff} and T_{Int} cells as muS110 stimulation of naive splenocytes. The fraction of T_{Eff} cells was additionally increased by subsequent stimulation of pre-activated T cells with muS110 (Figure 9C and D). In this case more than 50% of CD4⁺ and ~80% of CD8⁺ T cells were armed effector cells, which correlated well with the percentage of granzyme B positive T cells.

Taken together in the presence of target cells muS110 induced potent cytotoxic effector T cells similar to that obtained by a full CD3/CD28 stimulation in the presence of IL-2. This was observed for naive T cells as well as already pre-activated T cells. The dose-dependent up-regulation of CD25 and CD69 might indicate the dose-dependency of this process. The high percentage of activated T cells (>80% CD25⁺ and CD69⁺ cells) after only 24 hours of stimulation and the almost complete absence of T_{Naive/CM} cells already after 48 hours might implicate that muS110 can fully activate all T cells and not only a small fraction of CD28 independent T_{EM}. Hence, muS110 would be depending only on a second binding partner but

not on any co-stimulatory signals provided by antigen presenting cells. For concentrations lower than 1 µg/ml, this activation was strictly dependent on the presence of appropriate target cells. No up-regulation of the most sensitive marker CD69 was observed for the control BiTE muMEC14. But in contrast to the human setting, higher doses were able to induce a less pronounced activation independently of a second binding partner.

5.1.3.3 Cytokine release induced by muS110

The *in vitro* potency of muS110 to induce cytokine secretion was additionally analyzed. Splenocytes or negatively isolated mouse T cells were incubated with or without CHOmuEp-CAM⁺ target cells (E:T= 10:1) in the presence of increasing concentrations of muS110 for 48 hours. The supernatant was analyzed for IL-2, IFN-γ, TNF-α, IL-6, IL-3, GM-CSF, IL-10 and IL-4 using the CBA flex set system (Figure 10).

MuS110 led to a dose dependent release of all cytokines tested, when target cells were present. In the absence of target cells only a slight increase in IFN-γ and TNF-α was observed for high doses of muS110. For IFN-γ the peak concentration was 5.4 ng/ml, for GM-CSF it was 3.4 ng/ml, for IL-2 it was 3 ng/ml, for IL-4 it was 2 ng/ml, for IL-10 it was 1.4 ng/ml, for TNF-α it was 0.2 ng/ml, for IL-3 it was 0.2 ng/ml, and for IL-6 it was 0.1 ng/ml. The EC₅₀ values of cytokine secretion were mostly between 0.5 and 5 ng/ml, namely 0.5 ng/ml for IL-6, 1.4 ng/ml for IFN-γ and TNF-α, 1.7 ng/ml for IL-2 and GM-CSF, 3.1 ng/ml for IL-4, 4.8 ng/ml for IL-10 and 14.5 ng/ml for IL-3.

Of note, some cytokines showed a comparable magnitude of secretion independently of the used effector cell preparation (IFN-γ, IL-2, TNF-α, IL-4 and GM-CSF) whereas others were weaker induced with naive negatively isolated T cells than with crude splenocytes as effector cells (IL-10 and IL-3). No secretion of IL-6 was measured with pure T cells as effector cells.

Taken together, in the presence of target cells muS110 led to proliferation of T cells, cytokine secretion, up-regulation of activation marker and a shift towards cytotoxic effector T cells resulting in the elimination of antigen positive target cells. The EC₅₀ values of its bioactivity ranged mostly between 0.5 and 5 ng/ml, and its effects were almost completely saturated at concentrations of 10-100 ng/ml. In terms of quality and quantity of their bioactivities muS110 can be considered as valid surrogate of MT110. However, in contrast to the human setting, muS110 lost its strict dependency on the presence of antigen positive target cells inducing a minor T cell activation at high doses by itself.

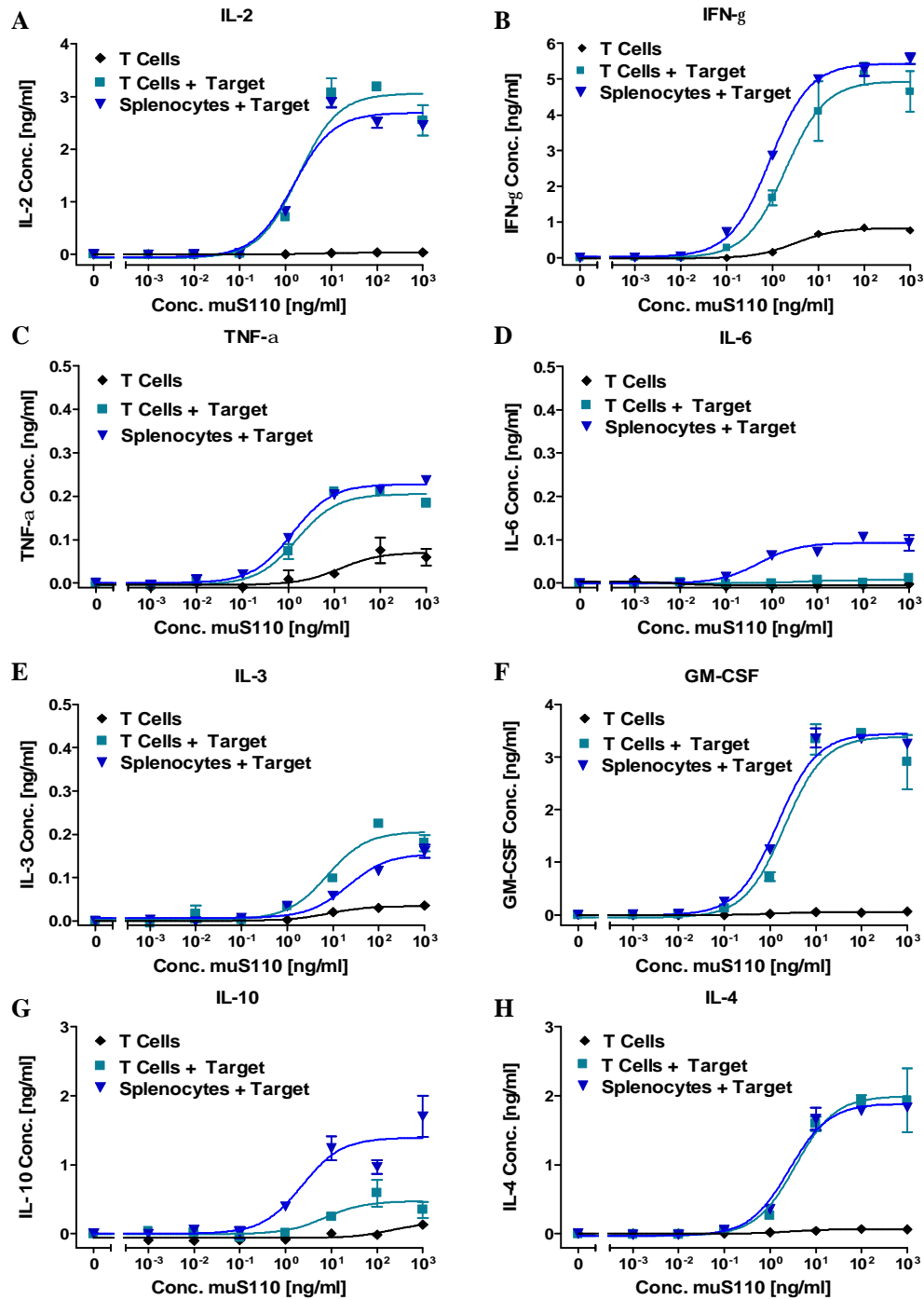


Figure 10: Cytokine secretion induced by muS110

To assess muS110 induced release of cytokines, splenocytes or negatively isolated mouse T cells (spleen) were incubated with or without CHOMuEpCAM⁺ target cells (E:T= 10:1) for 48 hours in the presence of increasing concentrations of muS110. The supernatant was analyzed for (A) IL-2, (B) IFN- γ , (C) TNF- α , (D) IL-6, (E) IL-3, (F) GM-CSF, (G) IL-10 and (H) IL-4 using the CBA flex set system. Error bars indicate SEM of duplicates. The experiment was repeated two times.

5.2 Pharmacotoxicological effects of muS110 *in vivo*

5.2.1 Characterization of single dose administration

5.2.1.1 Adverse effects induced by a single dose of muS110

The safety profile of muS110 was analyzed following i.v. injection of 5, 15 and 50 µg/kg muS110, and the control BiTE hyS110 (500 µg/kg) to 20 female BALB/c mice per treatment group. At the indicated time points serum concentrations of muS110 were determined to evaluate muS110 serum exposure. Overall, dose-dependent muS110 exposure could be demonstrated. Serum concentrations fell below the limit of quantification within 1 to 2 hours in animals, which had received 5 and 15 µg/kg muS110. Therefore, the terminal serum half-life of 4 hours could only be determined in the highest dose group receiving 50 µg/kg muS110 (Figure 11A).

A time- and dose-dependent onset of side effects was observed up to 24 hours after administration of muS110 (Figure 11; Table 4). The most prominent side effects were hypomotility, piloerection, body weight reduction, hypothermia and diarrhea. Administration of 5 µg/kg muS110 resulted in almost no side effects, whereas 15 µg/kg muS110 induced transient hypomotility, piloerection, diarrhea and a decrease in body temperature by approximately 3°C within the first 4 hours. Animals showed moderate to strong hunched posture, indicating discomfort but recovered quickly thereafter. Administration of 50 µg/kg muS110 induced more pronounced clinical signs, e.g., a pronounced drop in body temperature of 5.7°C persisting for at least 10 hours after treatment (Figure 11C). Bolus intravenous doses of ≥ 500 µg/kg were lethal in all animals within 24 hours. Animals treated with 500 µg/kg control BiTE hyS110 had only mild or no symptoms.

Table 4: Macroscopic side effects after single dose administration of muS110

MuS110 [µg/kg]	Hypomotility			Hunched posture			Diarrhea		
	0-2 hrs	2-10 hrs	10-24 hrs	0-2 hrs	2-10 hrs	10-24 hrs	0-2 hrs	2-10 hrs	10-24 hrs
5	+/-	-	-	+/-	+/-	-	-	-	-
15	+	-	-	+	+/-	-	+	-	-
50	+	+/-	-	+	+	+/-	+	+/-	-
				-	No effects				
				+/-	Weak effects				
				+	Moderate to strong effects				

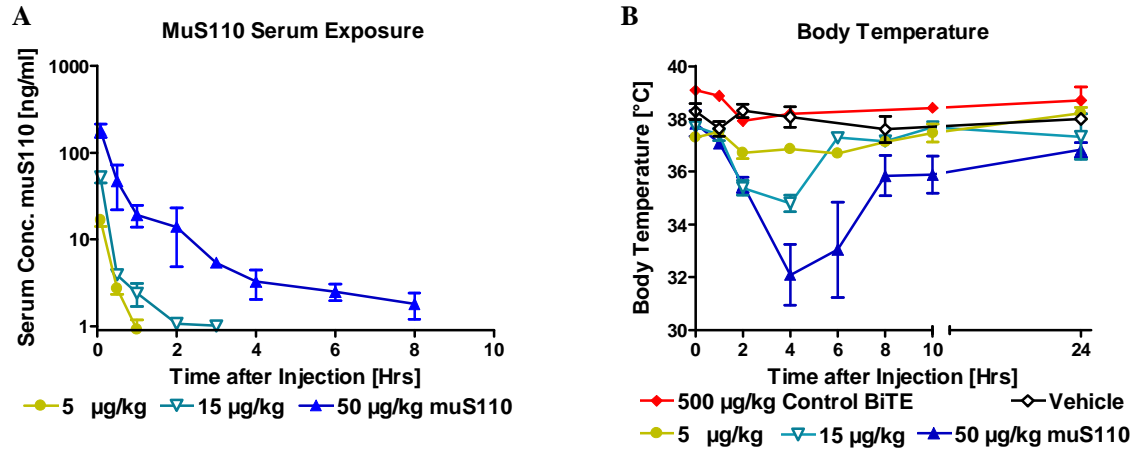


Figure 11: Serum exposure and body temperature after a single dose of muS110

Female BALB/c mice ($n = 20$) received i.v. injection of 5, 15 or 50 $\mu\text{g}/\text{kg}$ muS110 or 500 $\mu\text{g}/\text{kg}$ control BiTE antibody in a total volume of 200 μl . (A) Serum concentration of muS110 ($n = 4$); (B) body temperature ($n = 20$) as determined before and 0.5, 1, 2, 4, 6, 8, 10, and 24 hours after BiTE antibody injection. The red lines are results with the control BiTE antibody hyS110. Error bars indicate SEM. The experiment was conducted 3 times.

5.2.1.2 Systemic T cell activation induced by a single dose of muS110

Flow cytometric analysis for activated $\text{CD}25^+$ or $\text{CD}69^+$ T cells isolated from blood, spleen, and from mesenteric, *inguinalis superficialis* (data not shown) and cervical lymph nodes (data not shown) revealed a dose-dependent systemic T cell activation at the indicated time points after muS110 administration (Figure 12). The onset of T cell activation was slightly faster for $\text{CD}8^+$ than for $\text{CD}4^+$ cells. Time- and dose-dependent upregulation of CD69 and CD25 expression on T cells peaked 4 and 10 hours after intravenous injection of muS110, respectively, and sustained thereafter. Administration of 500 $\mu\text{g}/\text{kg}$ control BiTE antibody induced a less pronounced upregulation of the early activation marker CD69, while expression of CD25 was hardly affected. Binding of a BiTE antibody solely to CD3 was thus insufficient to induce strong and sustained T cell activation *in vivo* even at high doses.

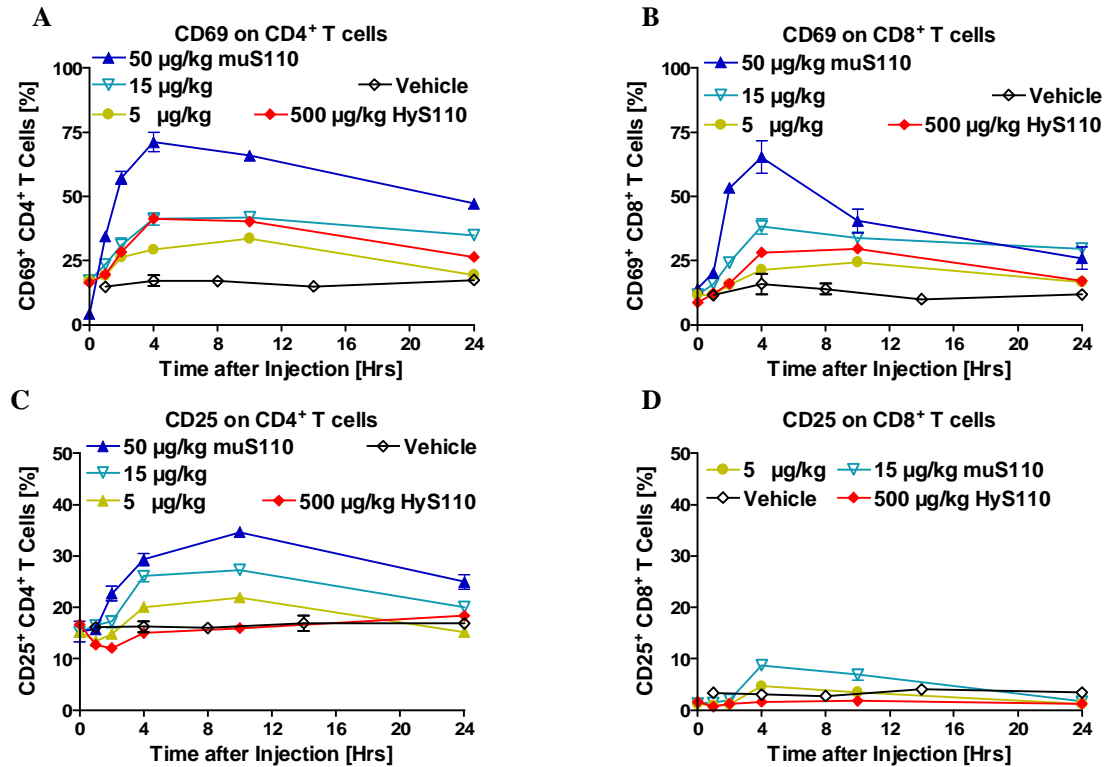


Figure 12: Up-regulation of CD69 and CD25 on T cells from mesenteric lymph nodes after a single dose of muS110

Female BALB/c mice (n= 20) received injection of 5, 15 or 50 µg/kg muS110 or 500 µg/kg control BiTE antibody in a total volume of 200 µl. Mesenteric lymph nodes were isolated before and 1, 2, 4, 10, and 24 hours after muS110 administration. (A and B) CD69 or (C and D) CD25 up-regulation was determined for CD4⁺ (right side) and CD8⁺ (left side) T cells using flow cytometry (n=4 animals). Of note, up-regulation of CD25 was not determined for CD8⁺ T cells at the highest muS110 dose due to experimental problems. Error bars indicate SEM. The experiment was conducted 2 times.

5.2.1.3 Transient systemic cytokine release induced by a single dose of muS110

MuS110 induced activation of T cell *in vitro* was accompanied by secretion of pro-inflammatory cytokines. High levels of systemic cytokines *in vivo* have been described to induce similar side effects as were observed after administration of muS110 (97-100). The serum of muS110-treated mice was analyzed for cytokine concentrations of IL-2, IFN-γ, TNF-α, IL-4, IL-6, IL-10 as well as IL-12/p70, IL-5, IL-3, MCP-1 and GM-CSF at various time points after BiTE antibody administration. MuS110 injection induced a dose-dependent and transient release of IL-2, IFN-γ, TNF-α, IL-4, IL-6, IL-10 (Figure 13) and IL-12/p70, MCP-1 and IL-5 (data not shown). Treatment with 5 µg/kg muS110 resulted in very low serum cytokine concentrations, whereas the 50 µg/kg induced a strong cytokine release.

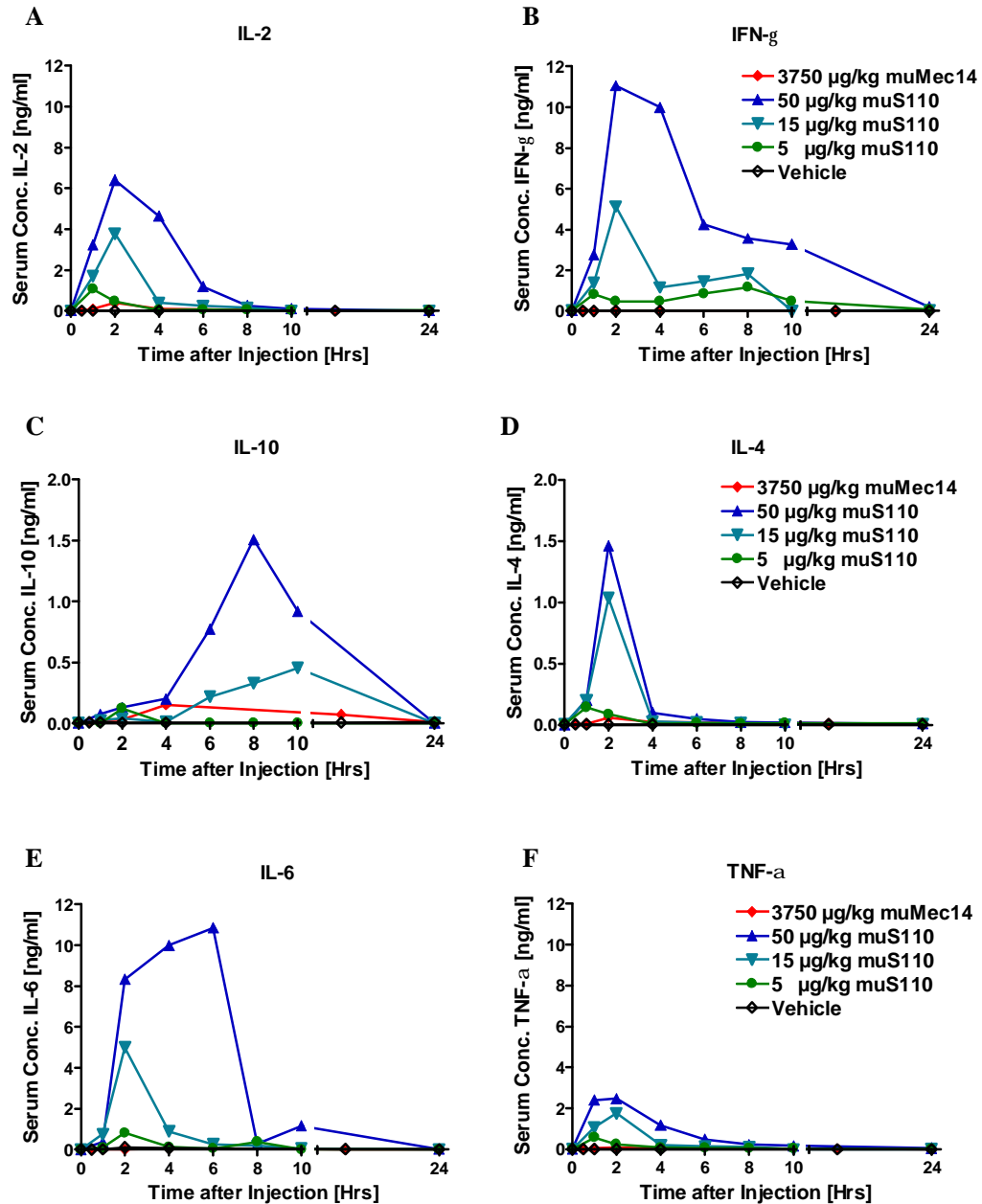


Figure 13: Serum cytokine profiles after intravenous administration of muS110.

Female BALB/c mice (n= 20) received intravenous bolus injection of 5, 15 or 50 µg/kg muS110 or 3750 µg/kg control BiTE antibody muMec14, respectively, in a total volume of 200 µl. Animals (n= 4) were bled before and 1, 2, 4, 6, 8, 10, 24 hours after BiTE antibody administration. Serum samples were pooled and analyzed for (A) IL-2, (B) IFN-γ, (C) IL-10, (D) IL-4, (E) IL-6 and (F) TNF-α using the mouse Th1/Th2 or inflammatory CBA Kit (BD Bioscience). The experiment was conducted three times.

For most cytokines, the onset of release was fast, and peak values were reached 2 hours after intravenous bolus injection of muS110. IL-5, IL-10 and IL-6 reached peak levels not before 6 to 8 hours. Most cytokine levels returned to baseline within 4-10 hours. Cytokine peak levels

seemed to coincide with the intensity and the course of clinical symptoms observed at different dose levels. Administration of the only CD3 binding control BiTE muMEC14 at a dose of 3750 $\mu\text{g}/\text{kg}$ did not result in elevated cytokine levels.

5.2.1.4 Peripheral lymphocytopenia induced by a single dose of muS110

Anti-CD3 mAbs are known to induce peripheral lymphocytopenia in mice (101). Early stages of lymphocytopenia are characterized by upregulation of adhesion molecules like CD44 on leukocytes and concomitant blood cell redistribution (102). In order to study effects of muS110 on blood cell redistribution, mice were treated by a single i.v. injection of 15 $\mu\text{g}/\text{kg}$ muS110 or the control BiTE antibody hyS110. Total numbers of leukocytes, myeloid derived cells (MDC, summarizes all bone marrow derived cells that are not lymphocytes), natural killer (NK) cells, T and B cell were determined at various time points after BiTE administration (Figure 14). The hematokrit was determined to investigate injection-related effects on blood volume.

Instead of an decrease caused by the injection of 100 μl liquid, a significant increase of the hematokrit was observed between 2 and 4 hours after muS110 injection, while only a minor increase was determined after injection of control BiTE antibody (Figure 14A). This is most likely a consequence of hemoconcentration, which can be caused by cytokine-induced vascular leakage (103), and may lead to an overestimation of blood cell numbers in animals receiving muS110. Treatment with 15 $\mu\text{g}/\text{kg}$ muS110 led to a rapid decrease in absolute leukocyte numbers, which was observed 2 hours after injection, lasted for more than 24 hours, and returned to baseline after 48 hours (Figure 14B). In response to muS110, the number of T cells decreased approximately 8-fold and that of B cells 5-fold (Figure 14C and D). The muS110 induced effect upon absolute numbers of NK cells or monocytes was variable and gave no clear result (Figure 14E and F), which might be due to the use of different animals for each time point. Administration of the control BiTE antibody had only a minor effect on absolute leukocyte or B cell numbers whereas absolute numbers of T cells decreased 2-fold and were back to normal levels after 48 hours.

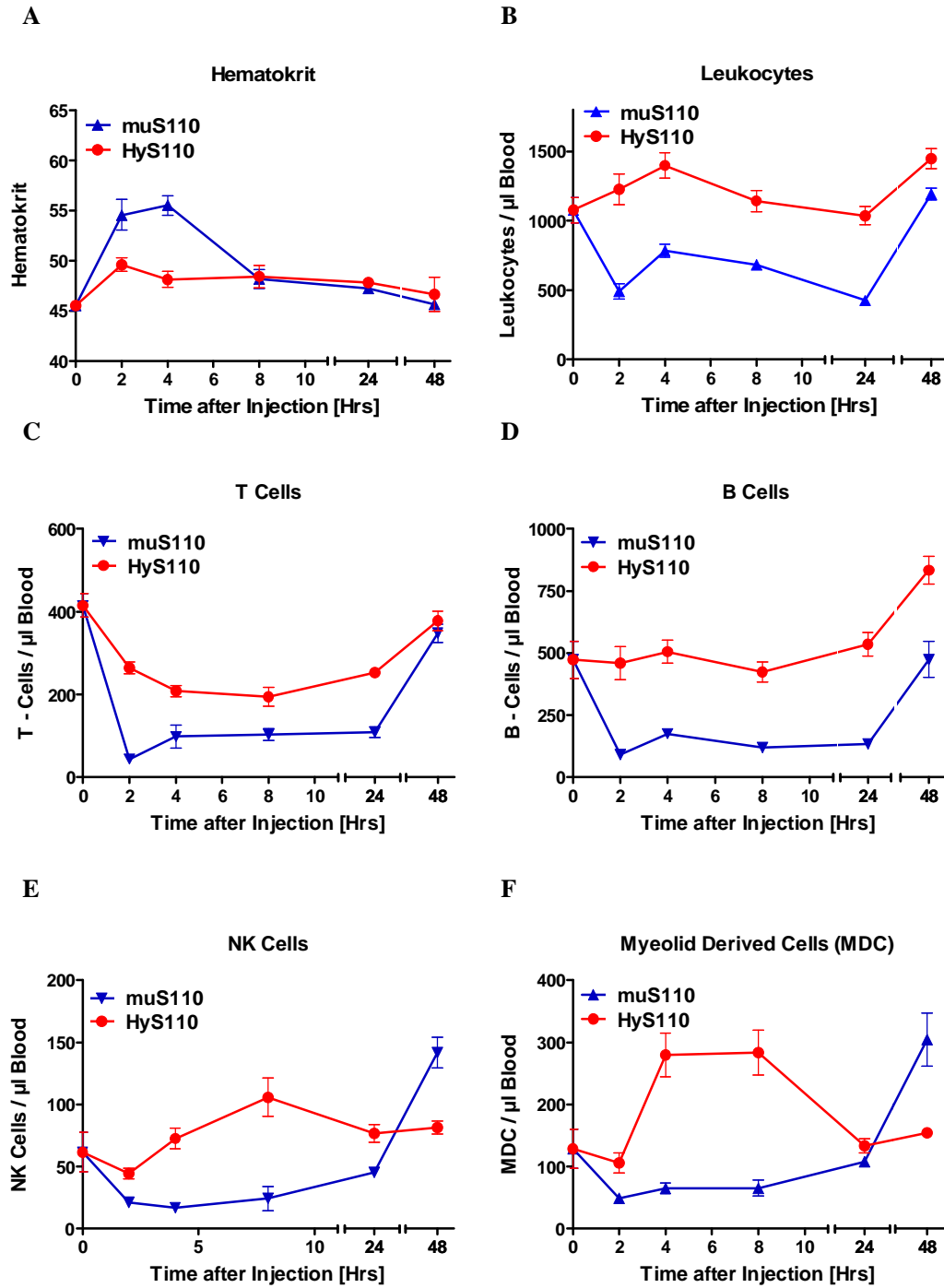


Figure 14: Peripheral lymphocytopenia induced by a single dose of muS110

Female C57BL/6 mice (n= 30) received i.v. injection of 15 $\mu\text{g}/\text{kg}$ muS110 or hyS110 control BiTE in a volume of 100 μl . (A) Hematokrit (B) total numbers of leukocytes (CD45), (C) T cells (CD45⁺CD3⁺), (D) B cells (CD45⁺CD19⁺), (E) NK cells (CD45⁺CD3⁺CD49b⁺) and (F) myeloid derived cells (CD45⁺CD49b⁺CD11c⁺) were determined at indicated time points after BiTE antibody administration (n=5, each time point different animals) with antibodies directed against mouse CD45, CD3, CD49b, CD11c and CD19 with TruCount Tubes. Error bars indicate SEM. Data is representative for 2 different experiments.

5.2.1.5 Comparison of pharmaco-toxicological effects of muS110, KT3 and 145-2C11

Administration of the conventional anti-CD3 mAbs 145-2C11 and KT3 to mice leads to the cytokine release syndrome. Rising systemic levels of pro-inflammatory cytokines, like TNF- α , IFN- γ , IL-2, IL-6 and IL-3 lead to acute but transient systemic symptoms like hypothermia, hypoglycemia, hypomotility, piloerection, diarrhea and hypotension resembling a septic shock. Doses exceeding 2.5-5 mg/kg are associated with high mortality (101).

The pharmaco-toxicological effects of the anti-CD3 mAb 145-2C11 and KT3 were directly compared to that of the BiTE antibody muS110. 10 female BALB/c mice per group received i.v. injection of 5 mg/kg 145-2C11, KT3 or 50 μ g/kg muS110. Onset of adverse side effects (Table 5, Figure 15A), systemic T cell activation (Figure 15B-D) and systemic cytokine levels (Figure 16) were evaluated at indicated time points for all three compounds.

A similar time- and dose-dependent onset of side effects was observed up to 24 hours after administration of all three anti-CD3 antibodies (Figure 15A, Table 5). The magnitude and course of macroscopic side effects like hypomotility, piloerection, body weight loss, hypothermia and diarrhea were comparable for all three compounds. However, the onset was faster and the duration of side effects shorter after muS110 injection than after administration of the complete anti-CD3 antibodies. The faster reversibility of muS110 induced side effects might be a direct consequence of the shorter serum half life of a BiTE compared to a mAb. The faster onset of clinical symptoms coincided with the faster kinetic of systemic T cell activation and the faster rise of cytokine serum concentrations observed after muS110 administration in contrast to the application of KT3 and 145-2C11 (Figure 15C and D, Figure 16).

The course of cytokine secretion was comparable but seemed to be delayed by 2 hours. This might reflect the dependence of anti-CD3 mAbs on the interaction of the Fc part with Fc receptors on accessory cells to evolve full activating potential (104-108). The expression of these receptors is up-regulated by T cell secreted cytokines (mainly IFN- γ), and is therefore self energizing but needs time to evolve. MuS110 in contrast needs only the presence of antigen positive target cells to develop its full activating potential.

Administration of anti-CD3 mAbs results in immunosuppression, which is, at least in part, a result of activation induced down-regulation of the CD3 – TCR surface complex impairing alloantigen induced T cell activation by antigen presenting cells (109, 110). Unlike bivalent anti-CD3 mAbs (111), muS110 treatment did not significantly down-modulate the TCR on T cells (Figure 15B).

Table 5: Comparison of macroscopic side effects after single dose administration of muS110, KT3 and 145-2C11

Drug	[mg/kg]	Hypomotility			Piloerection			Diarrhea		
		0-2	2-10	10-24	0-2	2-10	10-24	0-2	2-10	10-24
muS110	0.05	+	+/-	-	+	+	-	+	+/-	-
145-2C11	5	+/-	+	+/-	+/-	+	+/-	+/-	+	+/-
KT3	5	+/-	+	-	+/-	+	-	+/-	+	-

- No effect +/- Weak effects + Moderate to strong

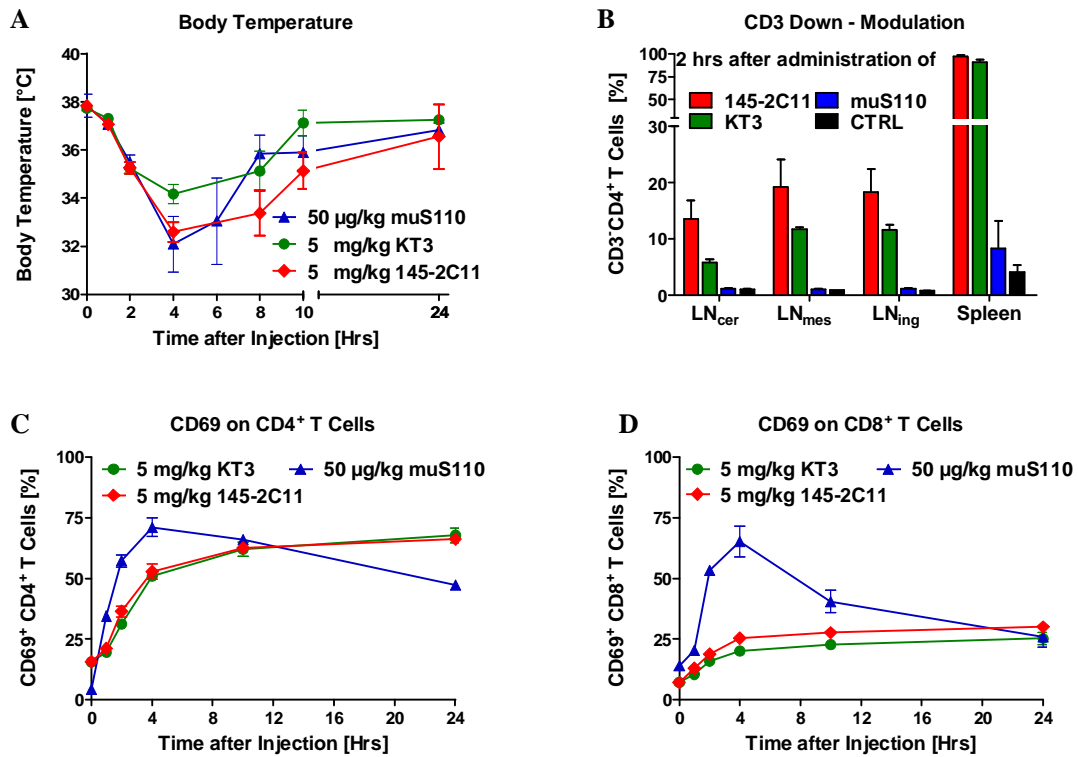


Figure 15: Hypothermia, systemic T cell activation and CD3 down-modulation induced by administration of muS110, KT3 and 145-2C11

Female BALB/c mice (n= 10) received i.v. injection of the complete anti-CD3 mAb 145-2C11 or KT3 [both 5 mg/kg] or muS110 [50 µg/kg] in a volume of 200µl. (A) Body temperature (n= 4) as determined before and 1, 2, 4, 6, 8, 10, and 24 hours after antibody injection. (B) Leukocytes of lymph nodes *mesenteriales*, *cervicales* and *inguinalis superficialis* (LN_{mes}, LN_{cer}, LN_{ing}) and the spleen (n= 2) were isolated 2 hours after antibody injection and were stained with antibodies against CD3, CD4 and CD8. Percentage of CD3⁺ CD4⁺ cells was determined to evaluate antigen binding-induced CD3 down-modulation. (C, D) Mesenteric lymph nodes (n=2) were isolated before and 1, 2, 4, 10, and 24 hours after muS110 administration and up-regulation of CD69 was determined for (C) CD4⁺ and (D) CD8⁺ T cells by flow cytometry. Error bars indicate SEM. The experiment was performed twice.

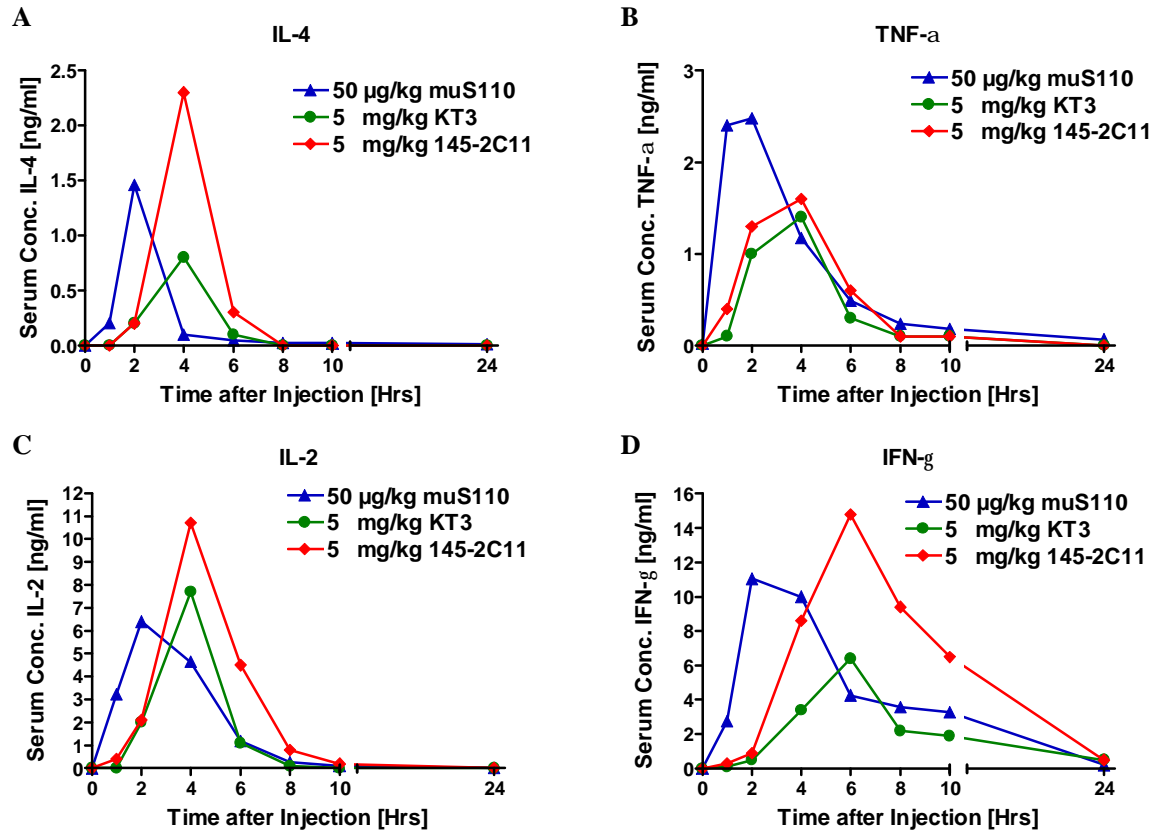


Figure 16: Serum cytokine concentrations after administration of muS110, KT3 and 145-2C11

Female BALB/c mice (n= 10) received i.v. injection of 5 mg/kg anti-CD3 mAb 145-2C11, KT3 or 50 μg/kg muS110 in a volume of 200 μl. Animals were bled at 1, 2, 4, 6, 8, 10, and 24 hours after injection of the respective antibodies. Serum samples of 2 mice per time point were pooled and analyzed for (A) IL-4, (B) TNF-α, (C) IL-2, (D) IFN-γ using the mouse Th1/Th2 CBA Kit (BD Bioscience). The experiment was performed twice.

The adverse effects observed after muS110 administration were comparable to those observed after administration of anti-CD3 mAbs. Their progression overlapped with the kinetic of systemic T cell activation and cytokine release. Thus, most likely the T cell activating potential of muS110 was responsible for its toxicity. The administration of control BiTEs sharing the CD3 moiety but being unable to bind to second binding partners did hardly induce adverse symptoms or cytokine release. This confirmed again the similar *in vitro* findings and the dependency on the presence of a second binding partner to induce profound T cell activation. Therefore, we performed histo-pathological analysis to identify an easily and fast accessible EpCAM⁺ target tissue, which could have provided the second binding partner for the immediate systemic T cell activation observed.

5.2.2 Histopathological analysis of mice repeatedly treated with muS110

Apart from cytokine release by activated T cells, another conceivable adverse reaction for an EpCAMxCD3-bispecific BiTE antibody is damage to EpCAM-expressing normal epithelial tissues by redirected cytotoxic T cells. Many tissues of mice show expression of EpCAM at various intensities, as determined by immunohistochemical staining of tissue with muS110 (Table 2). In a vehicle-controlled study, sixteen male and female BALB/c mice per group received daily intravenous injections of 10 µg/kg/day muS110 for seven days followed by 100 µg/kg/day muS110 for 28 days. Histopathological analysis of various tissues was performed by a certified pathologist. Despite expression of EpCAM on organs such as kidney (score = 1), lung (= 1), pancreas (= 3), pituitary (= 2-3), parathyroid (= 3-4), colon (= 4), or prostate (= 3), daily dosing of mice with muS110 for 35 days revealed no evidence for histo-pathological detectable lesions in normal tissues expressing the EpCAM target antigen (Table 6). This was also true for evaluation of other cohorts after 7 and 14 day treatment (data not shown). No lesions were found aiming at the accessible EpCAM⁺ target cells, necessary as second binding partner for muS110 to induce the fast, adverse symptoms seen *in vivo*.

Table 6: Histo-pathological examination of EpCAM⁺ tissues from mice treated with muS110.

The EpCAM expression score is described in Amann et al. (85) as follows: 1 = light staining 2 = moderate staining 3 = medium-strong staining 4 = intense staining; 'GI tract other' includes duodenum, ileum and jejunum. All slides were evaluated by a certified pathologist to ensure the quality of interpretation.

EpCAM Positive Tissue	Score of EpCAM Expression	Number of Analyzed Animals Vehicle	Number of Analyzed Animals MuS110	MuS110 Specific Histopathological Findings
Caecum	2	32	30	None
Colon	4	32	30	None
Eyes	2	32	30	None
GI tract other	2-4	32	30	None
Kidneys	1	32	30	None
Liver	1	32	30	None
Lung and bronchi	1	32	30	None
Lymph nodes mandibular	1	32	30	None
Lymph nodes mesenteric	1	32	30	None
Oesophagus	2-4	32	30	None
Pancreas	3	32	30	None
Pituitary	2-3	32	30	None
Salivary glands	2-4	32	30	None
Thymus	1	32	30	None
Parathyroids	3-4	23	22	None
Ureters	2	32	30	None
Urinary Bladder	2	32	30	None
Male Reproductive System				
Prostata	3	16	16	None
Testes	1	16	16	None
Female Reproductive System				
Mammary area (caudal)	2	16	14	None
Uterus	2-4	16	14	None
Uterine cervix	2	16	14	None
Vagina	2	16	14	None

5.2.3 EpCAM⁺ mouse lymphocytes

5.2.3.1 Presence of EpCAM⁺ cells in mouse but not in human lymphocytes

MT110 induced T cell activation was only found in the presence of huEpCAM⁺ target cells. However, in the mouse system T cell activation by muS110 was observed in the absence of added EpCAM⁺ target cells. This was more prominent with crude splenocyte preparations but almost absent with naive, negatively isolated T cells as effector cells. Therefore, mouse lymphocytes were analyzed for the presence of EpCAM⁺ target cells. Mouse PBMC and lymphocytes isolated from spleen, mesenteric and cervical lymph nodes were analyzed for EpCAM expression by FACS. About 3.1% of CD19⁺ B cells were found to express EpCAM in the

mouse leukocyte population (Figure 17A, right panel). No EpCAM⁺ cells were found above the background of the isotype control antibody in human PBMC, freshly isolated from human blood (Figure 17A, left panel (30)). EpCAM expression by murine lymphocytes (CD45, CD3, and CD19), NK cells (CD49b) and MDCs (Ly6G) was analyzed in more detail using cell-type specific antibodies for FACS analysis. The majority of EpCAM⁺ cells in mouse blood co-expressed CD19 or CD45/RB220, showing their B cell origin (Figure 17C).

EpCAM⁺ B cells made up for 2-3% of leukocytes found in various lymphoid organs and blood. To rule out mouse strain specificity, PBMC from strains CD-1, C57BL/6N, C3H/HEN and BALB/c were analyzed for EpCAM⁺/CD19⁺ double-positive B cells. As shown in Figure 17B, the percentage of EpCAM⁺ B cells did not significantly differ between mouse strains and gender, and had a mean incidence of 1-3%.

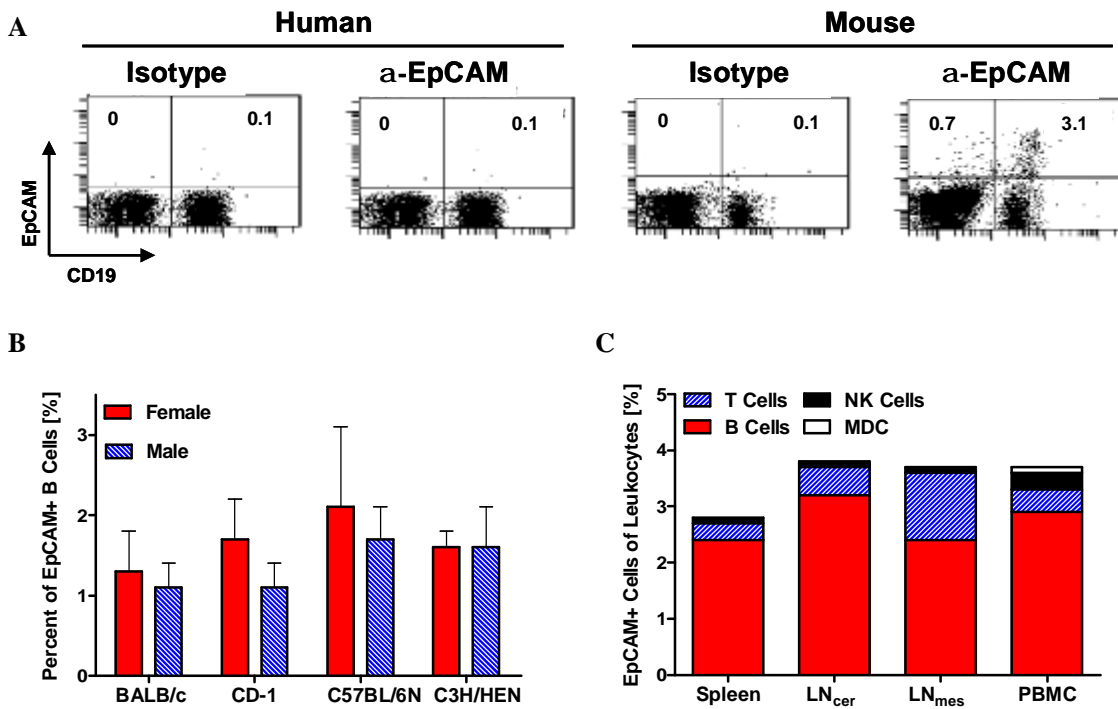


Figure 17: Existence of EpCAM⁺ lymphocytes in mice.

Human PBMC (left panel) and mouse splenocytes (right panel) were double-stained for CD19 and EpCAM, or with the corresponding isotype control antibodies. (B) PBMC of six female and male BALB/c, C57BL/6N, C3H/HEN and CD-1 mice were stained for CD19 and EpCAM and analyzed by flow cytometry. (C) Cells isolated from spleen, LN_{cer}, LN_{mes} and from PBMC (n=2) were stained for CD3 (T cells), CD19 (B cells), CD49b (NK cells) and Ly6G (MDC) in combination with an anti-mouse EpCAM mAb, or the corresponding isotype control. Percentage of cells positive for EpCAM and the respective markers are shown. Error bars indicate SEM. All experiments were at least repeated three times.

5.2.3.2 Dependence of muS110-induced T cell activation on EpCAM⁺ lymphocytes

The capacity of small numbers of EpCAM⁺ cells to induce BiTE -mediated T cell activation and cytokine release was evaluated *in vitro*. A complete depletion of EpCAM⁺ cells from mouse PBMC could not be achieved, even when magnetic bead- and FACS-based approaches were combined. However, reduction of EpCAM⁺ cells in mouse splenocytes from 2.2 to 0.4% was found to substantially reduce up-regulation of the activation marker CD25 by muS110 for both, CD8⁺ and CD4⁺ T cells (Figure 18A and C). Release of cytokines IFN- γ , IL-2, TNF- α , and IL-4 was almost completely abrogated by reduction of EpCAM⁺ cells from 2.2 to 0.4%, with cytokine levels coming close to those seen with the control BiTE antibody (Figure 18E).

Complementing, the effect of addition of human EpCAM⁺ cells to human PBMC was also analyzed for MT110 (Figure 18B and D). Human PBMC, which are essentially devoid of EpCAM⁺ cells, were co-cultivated for 48 hours with different amounts of EpCAM⁺ human carcinoma Kato III cells. No activation of CD8⁺ or CD4⁺ T cell could be detected in the absence of EpCAM⁺ target cells (79). However, addition of 2% EpCAM⁺ cells to human PBMC led to activation of approximately 50% of CD8⁺ and 25% of CD4⁺ T cells in a MT110 dose-dependent manner. The upregulation of CD25 was accompanied by release of IFN- γ , TNF- α and IL-10 from human PBMC (Figure 18 F). Addition of only 0.2% EpCAM⁺ cells to human PBMC no longer strongly induced CD25 expression on CD4⁺ and CD8⁺ human T cells by MT110. However, the presence of 0.2% EpCAM⁺ cells still caused a release of TNF- α and a small response of IFN- γ in response to MT110.

These data suggest that EpCAM⁺ B cells in the mouse leukocyte compartment could be responsible for the profound and fast T cell activation, robust cytokine release and, ultimately, for the acute dose limiting side effects of muS110 injection in mice. In Figure 19 the sum of all induced cytokines after 48 hours in an *in vitro* cytotoxicity assay is plotted against the respective muS110 concentrations for naive, negatively CD3 enriched T cells (0.3% EpCAM⁺ lymphocytes) and crude splenocytes (2.3% EpCAM⁺ lymphocytes) with or without the addition of 10% EpCAM⁺ target cells. This figure shows the magnitude of cytokine secretion solely induced by only 2.3 % EpCAM⁺ lymphocytes.

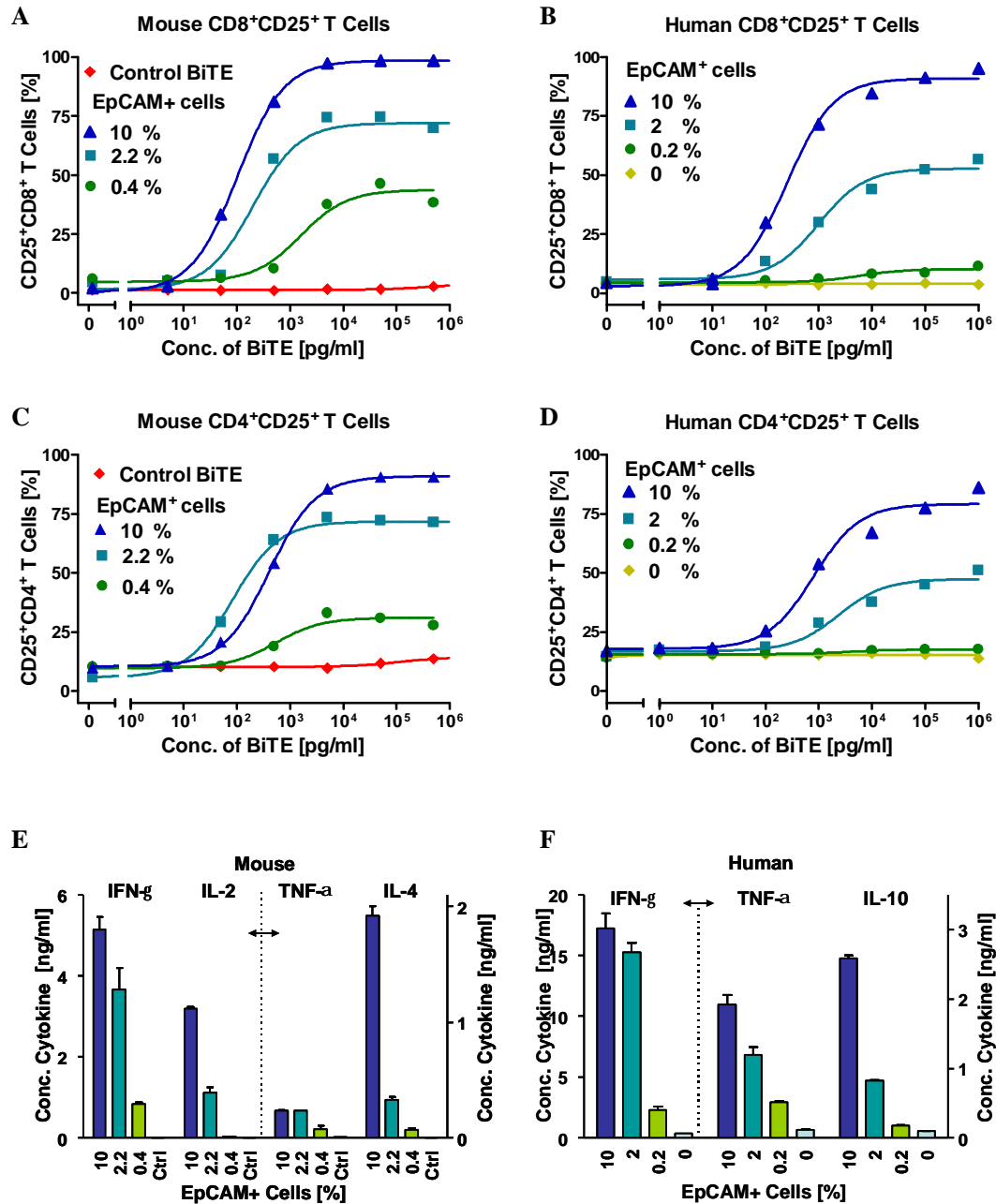


Figure 18: Dependence of muS110 and MT110 induced T cell activation on EpCAM⁺ target cells

(A, C, E) Mouse splenocytes (2.2% EpCAM⁺ cells) or splenocytes partially depleted of EpCAM⁺ cells (0.4% EpCAM⁺ cells) were incubated for 48 hours with the indicated concentrations of muS110, or with control BiTE antibody in the absence or presence of 10% CHOmuEpCAM⁺ cells. (B, D, F) Human PBMC were incubated for 40 hours in the absence or presence of 0.2%, 2% or 10% KatoIII cells with the indicated concentrations of MT110. Thereafter CD8⁺ and CD4⁺ lymphocytes were analyzed for CD25 expression by flow cytometry. (A and B) Percentage of CD8⁺CD25⁺ and (C and D) percentage of CD4⁺CD25⁺ cell are shown. Representative results of three independent experiments are shown. Error bars indicating SEM are present! (E) Mouse splenocytes (2.2% EpCAM⁺ cells) or splenocytes partially depleted of EpCAM⁺ cells

(0.4% EpCAM⁺ cells) were incubated for 48 hours with 100 ng/ml muS110 or control BiTE hyS110 with or without 10% CHOMuEpCAM⁺ cells. (F) Human PBMC were incubated for 40 hours in the absence or presence of 0.2%, 2% or 10% KatoIII cells with 100 ng/ml MT110. Supernatants were analyzed for cytokine levels using the (E) mouse CBA Th1/Th2 detection kit (BD Bioscience) or the (F) human CBA Flex set (BD Bioscience). Error bars indicate SEM. The dashed lines separate measurements shown at different scale. The experiment was repeated three times

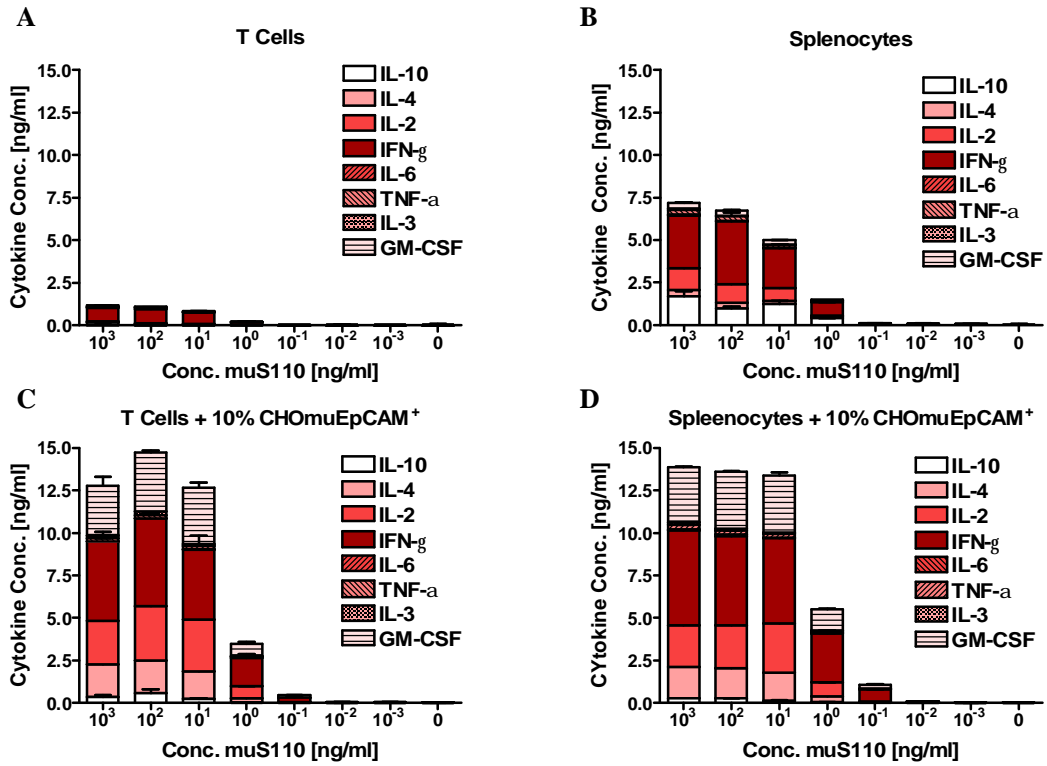


Figure 19: Dose dependent cytokine release after muS110 induced target cell lysis

To access muS110 induced release of cytokines negatively isolated mouse T cells (0.3% EpCAM⁺ cells) or freshly isolated splenocytes containing 2.3 % EpCAM⁺ lymphocytes were incubated with or without 10% CHOMuEpCAM⁺ target cells (E:T= 10:1) 48 hours in the presence of various concentrations of muS110. The supernatant was analyzed for the presence of IL-2, IFN- γ , TNF- α , IL-6, IL-3, GM-CSF, IL-10 and IL-4 using the CBA flex set system. The total amount of cytokines present after 48 hours of incubation is plotted against the muS110 concentrations for (A) T cells with 0.3% EpCAM⁺ cells, (B) splenocytes containing 2.3% EpCAM⁺ cells, (C) T cells with 0.3% EpCAM⁺ cells + 10% CHOMuEpCAM⁺ target cells, or (D) splenocytes containing 2.3% EpCAM⁺ cells + 10% CHOMuEpCAM⁺ target cells. Error bars indicate SEM of duplicates. The experiment was repeated twice.

5.2.4 Characterization of multiple dose administrations

5.2.4.1 Adverse effects induced by repetitive doses of muS110

The safety profile of muS110 was analyzed following i.v. bolus injections for seven consecutive days of 2, 10, and 50 $\mu\text{g}/\text{kg}/\text{day}$ muS110 or vehicle, to 10 male BALB/c mice per treatment group. At the indicated time points, serum concentrations of muS110 were determined in order to evaluate muS110 exposure (Figure 20A). The kinetic profiles averaged over 7 days showed that dose-linear muS110 exposure was obtained.

Daily i.v. administrations of vehicle or the two lower doses of muS110 (2 and 10 $\mu\text{g}/\text{kg}/\text{day}$) were generally well tolerated and none of the animals showed severe clinical signs or died during the course of the study. Repeated daily treatment with the 50 $\mu\text{g}/\text{kg}/\text{day}$ dose of muS110, however, induced pronounced but mostly reversible clinical signs. Side effects occurred within 8 hours after each muS110 administration. Thirty percent of animals died or were euthanized for well-fare reasons after the third or fourth injection (Figure 20B).

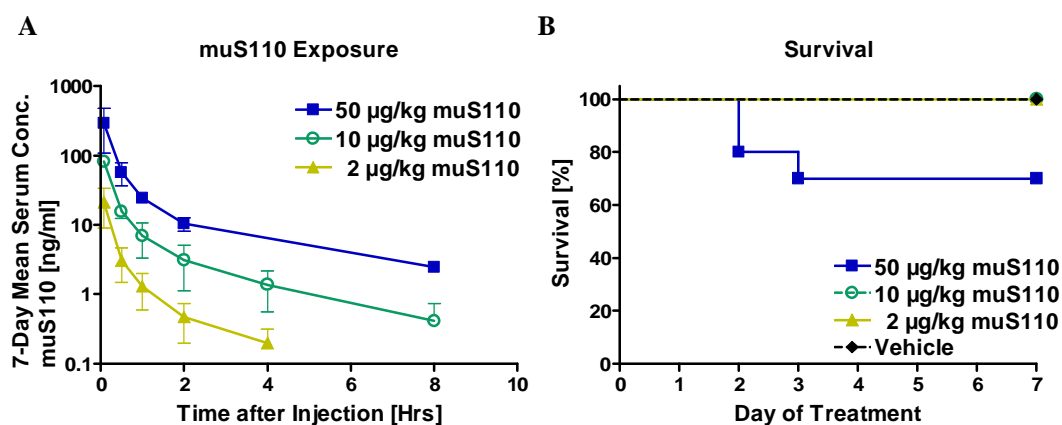


Figure 20: MuS110 exposure and survival after repeated administration of muS110

BALB/c mice ($n = 10$) received daily intravenous bolus injections of vehicle, 2, 10, or 50 $\mu\text{g}/\text{kg}/\text{day}$ muS110 for 7 days in a volume of 200 μl . (A) Serum concentration of muS110 ($n = 2$) were daily determined 15 min, 1, 2, 4, 8, and 24 hours after each injection. Data shown was averaged for 5 consecutive injections. (B) Survival was followed for seven days. Error bars indicate SEM. The experiment was repeated twice.

Dose dependent side effects, such as hypothermia (Figure 21B), weight loss (Figure 21A), piloerection and diarrhea were similar to those observed after single-dose i.v. injection of muS110 (5.2.1.1) (112). The highest dose group lost up to 15% body weight after the first three injections. Thereafter all mice gained body weight despite ongoing daily muS110 treatment. Animals treated with vehicle, 2 $\mu\text{g}/\text{kg}/\text{day}$ and 10 $\mu\text{g}/\text{kg}/\text{day}$ muS110 did not show sig-

nificant body weight changes. Relative to the control animals the highest dose group showed a drop in body temperature of almost 10% after the first three injections. The hypothermia worsened after the second and third injection as the onset was faster and the duration prolonged. Temperature was not completely recovered 24 hours after each injection. Animals receiving 10 $\mu\text{g}/\text{kg}/\text{day}$ muS110 showed a less severe drop of only 2.5-5 % and the animals recovered completely after 8 hours. Animals receiving 2 $\mu\text{g}/\text{kg}/\text{day}$ muS110 showed no significant alterations of body temperature compared to control animals. After the fourth injection all side effects declined despite continued muS110 treatment. No treatment related side effects were seen after the fifth to seventh injection for all animals. This indicated that dose-dependent side effects seemed to be self-limiting and animals could adapt to repetitive treatment with muS110.

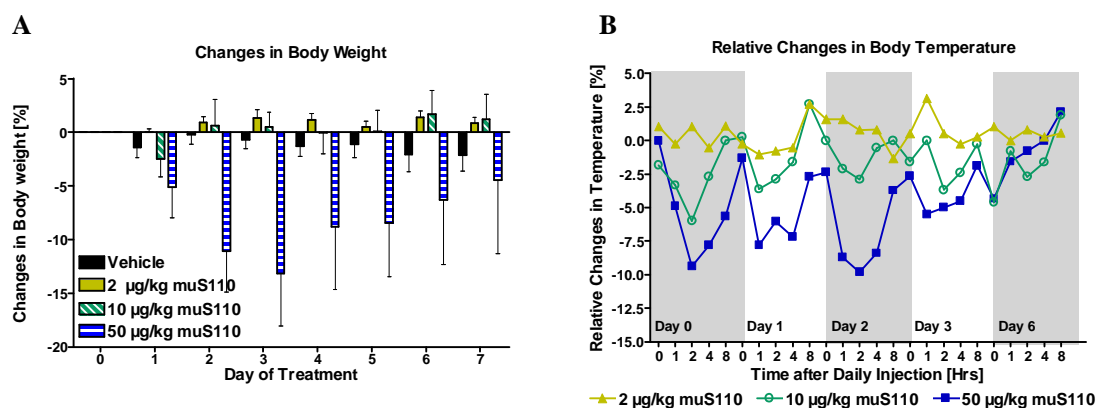


Figure 21: Weight loss and hypothermia caused by repeated administration of muS110

Repeated dosing of muS110 led to hypothermia and body weight loss. However, animals adapted to repeated treatment and recovered after the fourth injection despite ongoing muS110 medication. BALB/c mice ($n=10$) received daily i.v. injections of vehicle, 2, 10, or 50 $\mu\text{g}/\text{kg}/\text{day}$ muS110 for 7 days in a volume of 200 μl . (A) Body weight of all animals was determined daily prior to injection. Percentage of body weight change in comparison to beginning of the experiment is shown. (B) Body temperature was determined before and 2, 4 and 8 hours after each injection on day 0-3 and 6 of experiment. Percentage of body temperature changes normalized to vehicle treated animals is shown. Error bars indicate SEM. The experiment was repeated twice.

5.2.4.2 Cytokine release induced by repetitive muS110 treatment

Daily dosing of muS110 induced a systemic and transient release of inflammatory cytokines, including IL-2, IFN- γ , TNF- α , IL-6, IL-10, and IL-4 (Figure 23). No active TGF- β was found at any time point after muS110 injection. In general, serum concentrations of all cytokines returned to baseline levels by approximately 8 hours after each injection.

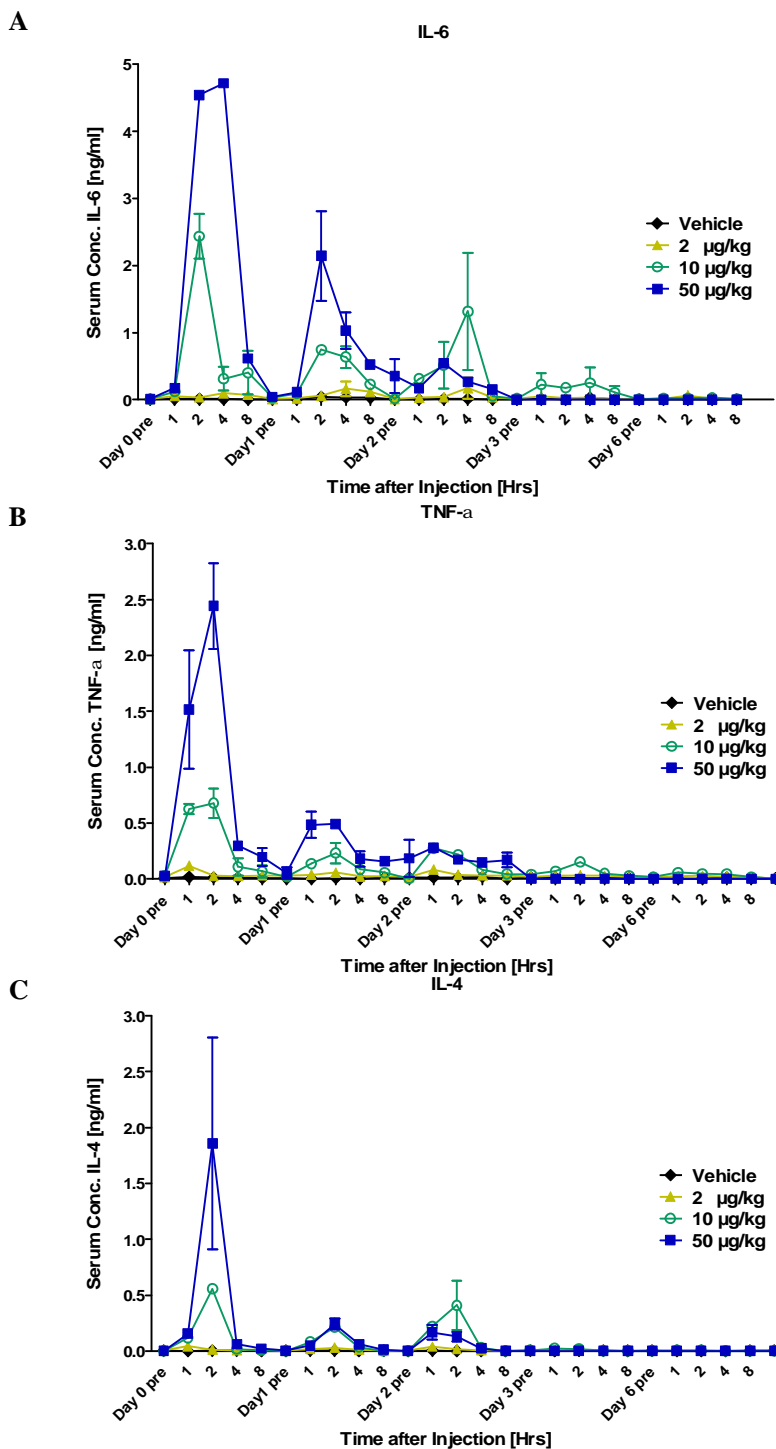


Figure 24: Cytokine release induced by repetitive muS110 treatment

Male BALB/c mice (n= 10) received daily i.v. injections of 50 μg/kg/day muS110 for 7 days in a volume of 200 μl. Animals (n= 2) were bled prior, 15 min, 1, 2, 4, 8, and 24 hours after each muS110 administration on day 0, 1, 2, 3 and 6 of the experiment. Serum samples were analyzed for (A) IL-6, (B) TNF-α, (C) IL-4, (D) IFN-γ, (E) IL-2, (F) IL-10 using the CBA Flex set (BD Bioscience). Error bars indicate SEM. The experiment was repeated twice.

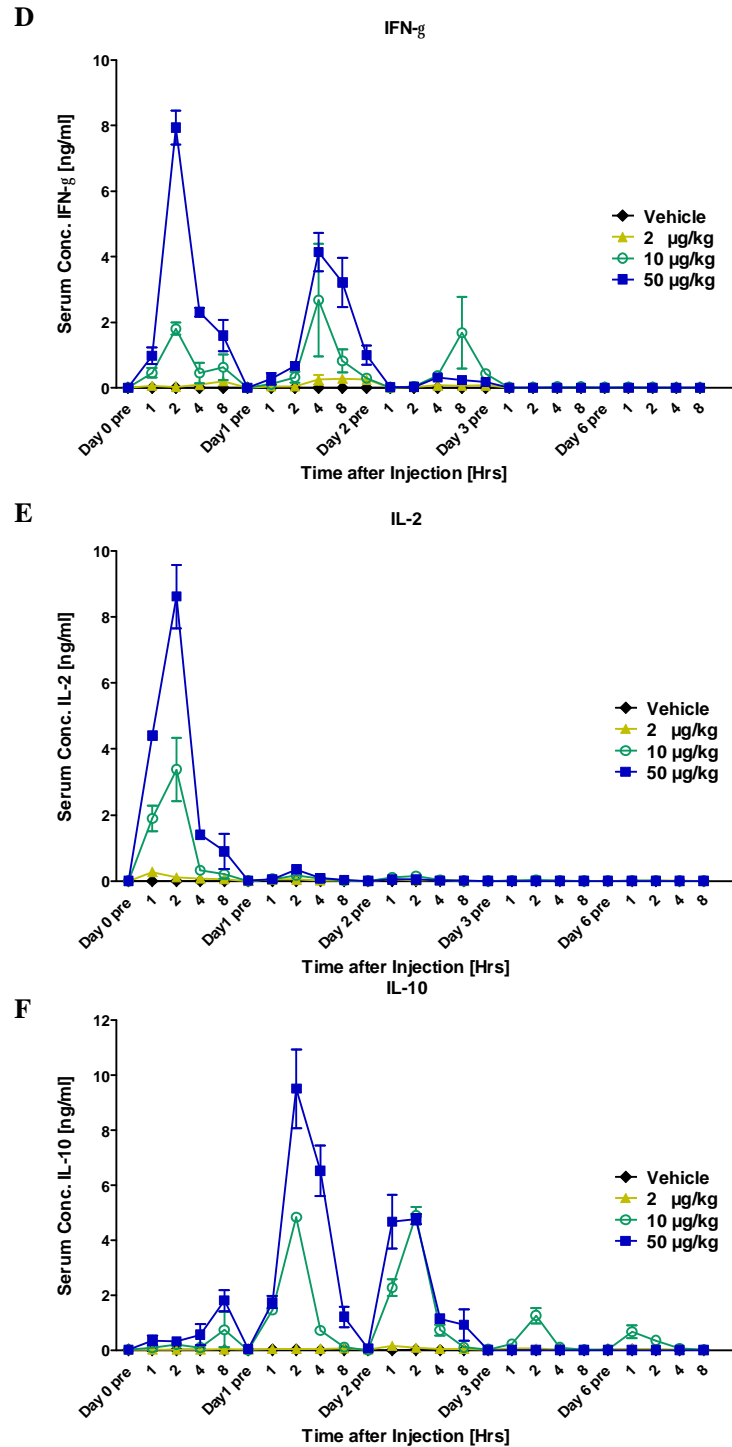


Figure 22 Cytokine release induced by repetitive muS110 treatment

Male BALB/c mice (n= 10) received daily i.v. injections of 50 µg/kg/day muS110 for 7 days in a volume of 200 µl. Animals (n= 2) were bled prior, 15 min, 1, 2, 4, 8, and 24 hours after each muS110 administration on day 0, 1, 2, 3 and 6 of the experiment. Serum samples were analyzed for (A) IL-6, (B) TNF-α, (C) IL-4, (D) IFN-γ, (E) IL-2, (F) IL-10 using the CBA Flex set (BD Bioscience). Error bars indicate SEM. The experiment was repeated twice.

These kinetics were similar to those observed after single-dose administration of muS110 (Figure 13)(112). The cytokine release was for each cytokine self-limiting and, with the exception of IL-10, much reduced after the second and third injection of muS110. No further cytokine release was detectable after the fourth to seventh injection. Especially the absence of IFN- γ , TNF- α and IL-6 after the fourth muS110 injection may explain the observed slowing down of side effects. These cytokines are known to be central figures of the cytokine release syndrome observed after administration of conventional anti-CD3 antibodies.

IL-10 had an exceptional time-course of secretion and showed only a slight increase of serum concentration 8 hours after the first muS110 injection but was highest after the second and third muS110 administration (Figure 22F).

5.2.4.3 Cytotoxic T cells induced by repetitive doses of muS110

The appearance of cytotoxic T cells *in vivo* after repeated muS110 injection was analyzed. Four female BALB/c mice per group received daily intravenous bolus injections of vehicle or 25 $\mu\text{g}/\text{kg}/\text{day}$ muS110 for 3 days. Splenocytes, PBMC and lymphocytes from mesenteric lymph nodes were isolated and stained with antibodies against CD127 and CD62L to determine distribution of naive or central memory T cells ($T_{\text{Naive/CM}}$, $\text{CD62L}^+ \text{CD127}^+$), intermediate T cells (T_{Int} , $\text{CD62L}^+ \text{CD127}$), effector T cells with high lytic potential (T_{Eff} $\text{CD62L}^- \text{CD127}$) and effector memory T cells (T_{EM} , $\text{CD62L}^- \text{CD127}^+$) (96). Additionally intracellular staining with antibodies against granzyme B, IFN- γ and CD152 was performed.

Daily treatment with muS110 led to the systemic induction of effector T cells in all analyzed compartments. This was most prominent for CD8^+ T cells where 50 to 75% of T cells were effector T cells in comparison to only 10% in the control animals. Additionally, 25% of CD8^+ splenocytes and up to 75% of blood CD8^+ T cells were also positive for granzyme B, which identified them as cytotoxic T cells. Peripheral CD4^+ T cells showed magnified granzyme B secretion in comparison to control animals (50% versus 10%) and a noticeable gain of effector T cells (35% versus 25%) whereas CD4^+ T cells from spleen and lymph nodes were mainly in an intermediate state. Only a minor difference of IFN- γ secretion to control animals was found for CD4^+ and CD8^+ splenocytes but was well established in peripheral T lymphocytes. The suppressive receptor CD152 was up-regulated, again more prominent for CD8^+ than for CD4^+ T cells. Taken together repetitive treatment with muS110 induces predominantly cytotoxic CD8^+ T cells, which were distributed systemically. Additionally an increase of peripheral CD4^+ effector T cells positive for granzyme B was noted.

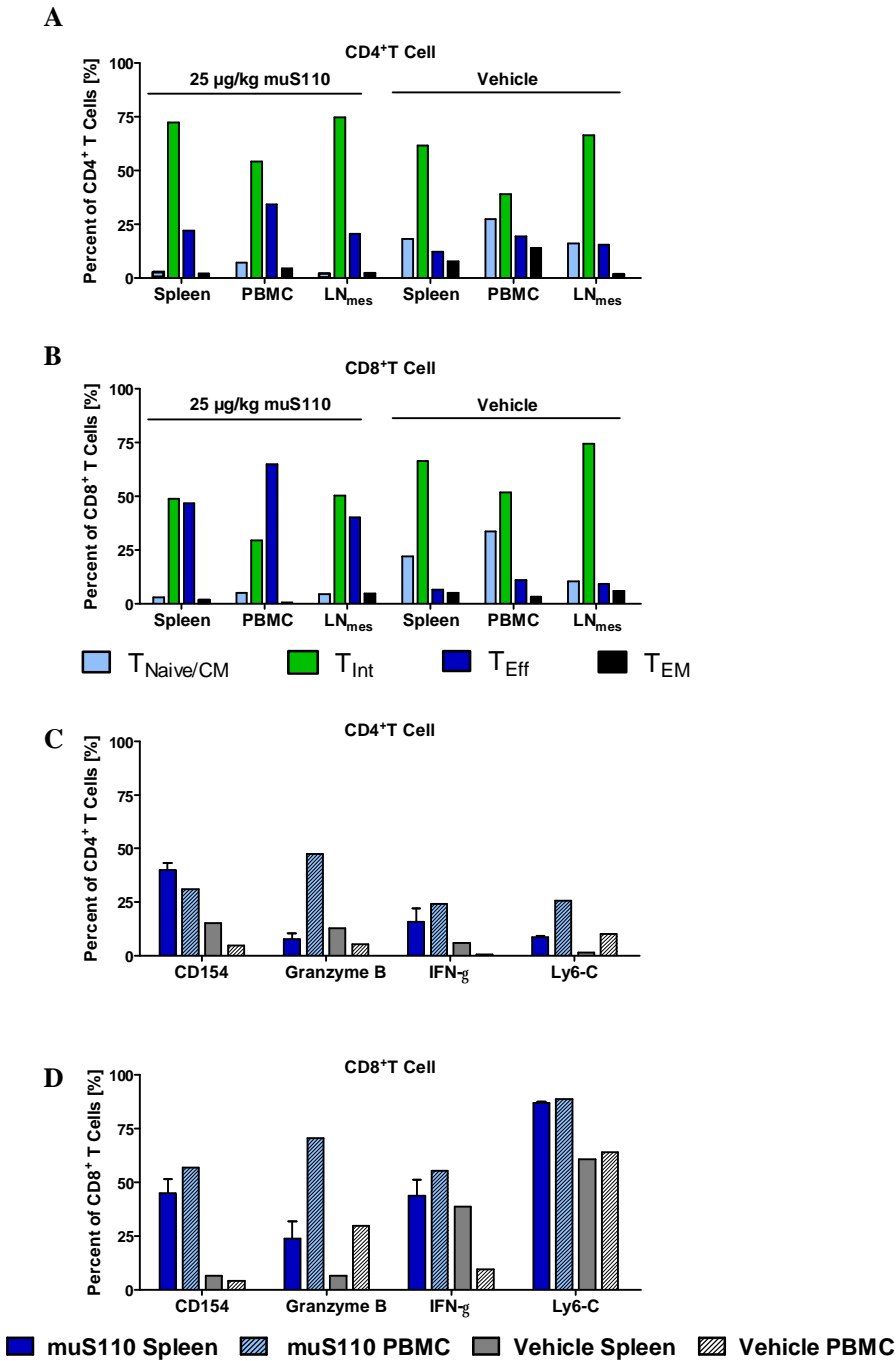


Figure 23: Cytotoxic T cells induced by repeated muS110 injections

BALB/c mice (n= 4) received daily i.v. injections of vehicle or 25 µg/kg/day muS110 for 3 days in 200 µl. Splenocytes and PBMC were isolated and stained with antibodies against (A, C) CD4 and (B, D) CD8 to identify T cells. (A, B) A part of the cells were stained with antibodies against the surface marker CD127 and CD62L. Percentage of naive/ central memory T cells (T_{Naive/CM}, CD62L⁺ CD127⁺), intermediate T cells (T_{Int}, CD62L⁺ CD127⁻), effector T cells (T_{Eff}, CD62L⁻ CD127⁻) and effector memory T cells (T_{EM}, CD62L⁻ CD127⁺). (C, D) Intracellular staining with antibodies against Ly6-C, granzyme B, IFN- γ , and CD152 was performed after PMA/Ionomycin/ BrefeldinA stimulation. Error bars show SEM. The experiment was repeated twice.

5.2.5 Increased muS110 tolerability and immune modulation

5.2.5.1 Tolerability increase of muS110 after *in vivo* depletion of EpCAM⁺ lymphocytes

Due to its mode of action EpCAM⁺ lymphocytes should be eliminated by muS110 induced target cell lysis over time. A high percentage of CD8⁺ T cells were granzyme B positive and therefore ready to lyse target cells. A reduced number of EpCAM⁺ target cells should lead to reduced systemic cytokine secretion, as the magnitude of cytokine release correlated with the amount of target cells present (Figure 18, Figure 19). A decrease of cytokine levels should in turn reduce the appearance of side effects, which might be one explanation for the increased tolerability of muS110 after repeated administration. For *in vivo* tumor treatment it was desirable to find a way to increase the maximal tolerated dose. Thus, it was tested if an eradication of the easily accessible EpCAM⁺ lymphocytes by low doses of muS110 might increase tolerability to high doses.

A low-dose pre-treatment for 7 days with a daily i.v. dose of 10 µg/kg muS110 was suitable for substantial redirected lysis of EpCAM⁺ B and T cells in mice (Figure 24A). This low-dose regimen caused only mild and reversible side effects (5.2.4.1). EpCAM⁺ B cells were reduced from 3.1 to 0.3%, EpCAM⁺ T cells from 0.8 to 0.2%, still leaving a total of 0.5% EpCAM⁺ lymphocytes in the periphery. Control animals treated with either daily i.v. doses of 10 µg/kg control BiTE antibody or PBS vehicle showed no alterations in the number of EpCAM⁺ lymphocytes (data not shown).

Mice with substantially reduced EpCAM⁺ lymphocytes and control animals were challenged with daily i.v. doses of 100, 300 and 500 µg/kg/day muS110 for a total of 10 days. Animals receiving 10 µg/kg/day of the control BiTE antibody (data not shown) showed severe side effects and hypothermia, upon high-dose muS110 challenge such that all had to be euthanized within 48 hours due to ethical considerations. In contrast, all animals pre-treated with a low-dose of muS110 survived doses of 100, 300 and 500 µg/kg of muS110 given daily i.v. for 10 days. Only mild and reversible side effects were noted in these animals such as a modest and transient reduction of body temperature (Figure 24B) and body weight (data not shown). These side effects could be due to a limited T cell activation triggered by the remaining 0.5% EpCAM⁺ lymphocytes, consistent with the *in vitro* data obtained with EpCAM depleted T cells (Figure 18).

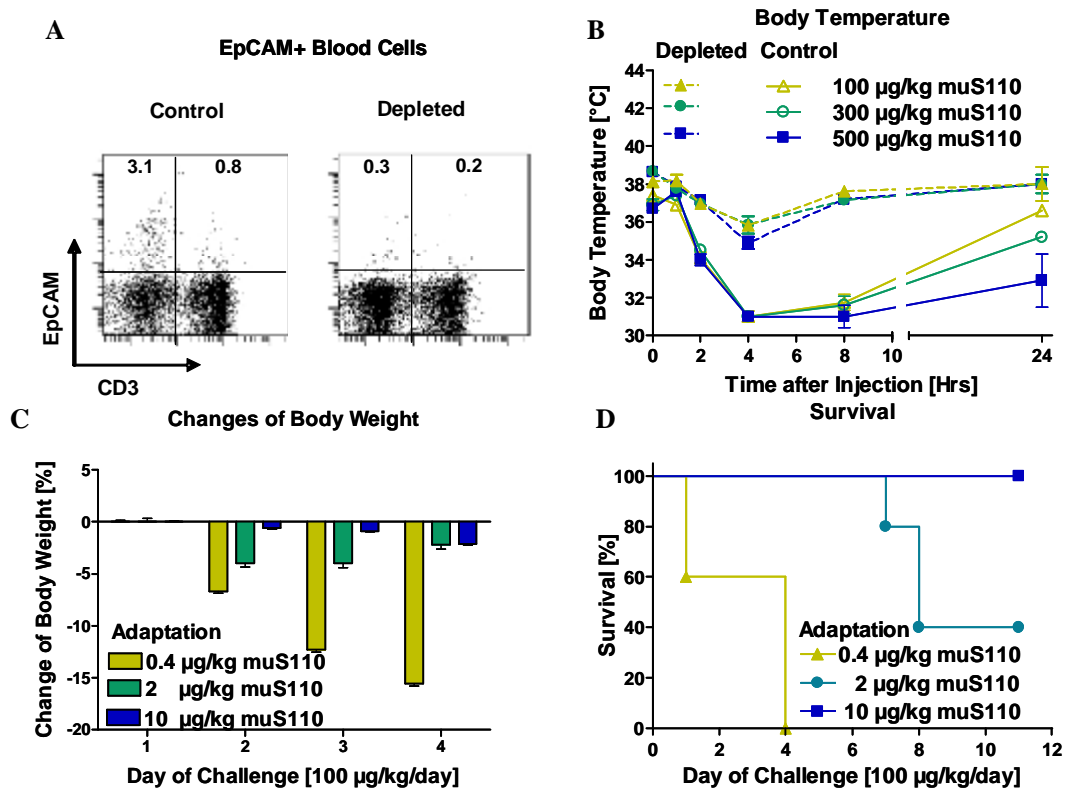


Figure 24: Increase of tolerability to muS110 by low-dose pre-treatment

(A and B) Female BALB/c mice ($n=5$) received daily i.v. injections of vehicle or 10 µg/kg/day muS110 for 7 days (adaptation). Thereafter, animals were challenged with i.v. injections of 100, 300 and 500 µg/kg/day muS110 (challenge). (A) Splenocytes isolated from PBS control and low-dose muS110 pre-treated mice were stained for CD3 and EpCAM by specific mAbs. The percentage of EpCAM⁺ cells in the respective gates is given relative to the total number of lymphocytes analyzed by FACS. (B) Body temperature ($n=5$) profiles were determined for low-dose muS110 adapted and control mice following 1, 2, 4, 8, and 24 hours after high-dose BiTE antibody challenge. (C and D) Female BALB/c mice ($n=5$) received daily intravenous bolus injections of 0.4, 2, or 10 µg/kg/day muS110 for 7 days (adaptation). Thereafter, animals were challenged with daily i.v. injections of 100 µg/kg/day muS110 (challenge). (C) Body weight of all animals was determined before each injection on day 1, 2, 3, and 4 of challenge. Percentage of body weight changes in comparison to the beginning of the challenge is shown. (D) Survival was monitored daily. Error bars indicate SEM. Experiments are performed twice. The injection volume was always 200 µl.

To proof the correlation between lower numbers of EpCAM⁺ lymphocytes, reduced systemic T cell activation and resulting enhanced tolerability the pattern of cytokine release to a muS110 challenge was analyzed after low-dose pre-treatment. Female BALB/c mice were treated by i.v. injection with low doses of muS110 (0.4, 2, or 10 µg/kg/day), or BiTE control antibody (at 10 µg/kg/day), for seven days ('adaptation' phase). This was followed by daily treatment with otherwise lethal doses of 100 µg/kg/day muS110 for 18 days ('challenge' pe-

riod). During this long-term study, survival (Figure 24D), body weight (Figure 24C), clinical condition, and body temperature (data not shown) were monitored.

Again all animals adapted with 10 $\mu\text{g}/\text{kg}/\text{day}$ muS110 were protected from mortality by subsequent challenges with 100 $\mu\text{g}/\text{kg}/\text{day}$ muS110. Animals adapted with 2 $\mu\text{g}/\text{kg}/\text{day}$ muS110 followed by 100 $\mu\text{g}/\text{kg}/\text{day}$ doses survived at least the first seven days of high-dose treatment. Pre-treatment of animals with 0.4 $\mu\text{g}/\text{kg}/\text{day}$ had no protective effect and 40% of animals died within the first two days of high-dose treatment, the remaining animals on the fourth day of challenge. Pre-treatment of animals with low doses of muS110 also ameliorated in a dose-dependent fashion the occurrence of side effects, such as reduction of body weight and of body temperature (data not shown).

The increase in tolerability to muS110 by a low-dose adaptation with muS110 coincided with a reduction of cytokine release (Figure 25).

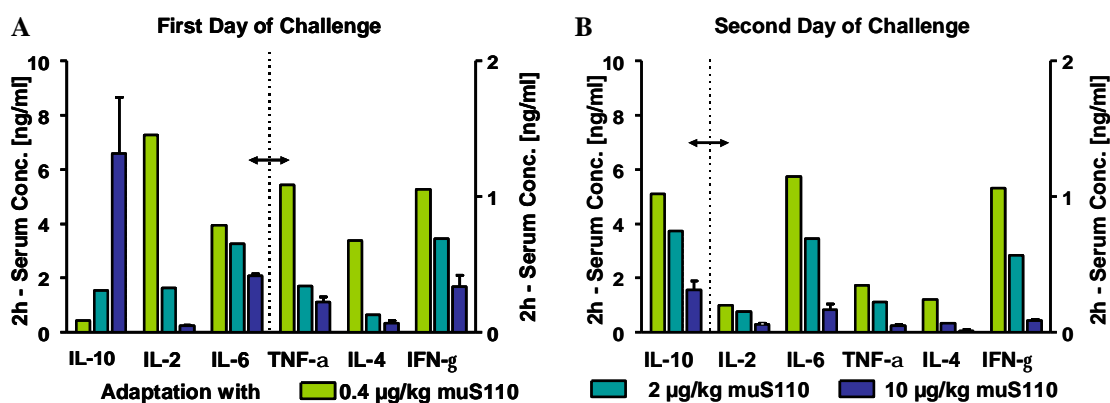


Figure 25: Protection from cytokine surge after muS110 low dose pre-treatment followed by high dose challenge

Animals adapted with a 7 day low dose treatment with muS110 were protected against a cytokine surge upon a subsequent high dose challenge. This protection correlated with the serum levels of IL-10 present at the first day of challenge. Female BALB/c mice ($n=5$) received daily i.v. injections of 0.4, 2, or 10 $\mu\text{g}/\text{kg}/\text{day}$ muS110 for 7 days (adaptation) in avolume of 200 μl . Thereafter, animals were challenged with daily i.v. injections of 100 $\mu\text{g}/\text{kg}/\text{day}$ muS110 (challenge). Animals ($n=2$) were bled 2 hours after muS110 administration on (A) day 1 and (B) day 2 of challenge. Serum samples were analyzed for IFN- γ , IL-2, TNF- α , IL-6, IL-10, and IL-4. Dotted lines and arrows relate to different scales. Error bars indicate SEM. Experiments was performed twice.

Blood was taken 2 hours after muS110 administration during the first five days of the 100 $\mu\text{g}/\text{kg}/\text{day}$ challenge, and serum levels of IL-2, IFN- γ , TNF- α , IL-6, IL-3, GM-CSF, IL-4, and IL-10 were determined. Low-dose pre-treatment with 0.4 $\mu\text{g}/\text{kg}/\text{day}$ muS110 per day resulted in high serum concentrations of IL-2, IFN- γ , TNF- α , IL-6, and IL-4 after the first and second

day of high-dose challenge. Pre-treatment with 2 µg/kg/day resulted in intermediate cytokine levels, and pre-treatment with 10 µg/kg/day muS110 resulted in the lowest serum concentrations of cytokines after the first and second day of challenge. Blunting of cytokine responses was thus dependent on the adaptation dose of muS110 and most effective after a one-week adaptation of mice at 10 µg/kg/day muS110.

However, the kinetic of IL-10 release was different from that of all other cytokines in response to a first and second high-dose challenge with muS110. IL-10 serum concentrations were not decreased but strongly elevated 2 hours after the first high-dose challenge of animals pre-treated with 10 µg/kg/day muS110. Induction of IL-10 was not as pronounced in animals pretreated with 2 and 0.4 µg/kg/day muS110.

After the second high-dose challenge, IL-10 expression was reduced in animals pretreated with 10 µg/kg/day muS110 while it was strongly elevated in animals, which had received lower muS110 doses for pre-treatment. The contra wise time-course of IL-10 ruled against a mere depletion of EpCAM⁺ target cells as solemn cause for increased tolerability after repeated muS110 administration. In this case, all cytokines should have been reduced in a similar way.

IL-10, also described as a “cytokine synthesis inhibitory factor” (113), is an anti-inflammatory cytokine and has pleiotropic effects in immune regulation and inflammation. It down-regulates the expression of TH₁ cytokines IL-2, IFN-γ, that of IL-3, TNF-α and GM-CSF. It reduces the surface expression of MHC class II antigens and costimulatory molecules on macrophages. It is mainly expressed in monocytes and TH₂ cells, CD4⁺CD25⁺FoxP3⁺ regulatory T cells but also in a certain subset of activated T cells and B cells. It was shown that short term treatment with anti-CD3 specific antibodies, like kOKt3yl (Ala-Ala), can elicit operational tolerance in transplantation and autoimmunity (114). Patients treated with the humanized, FcR non-binding kOKt3yl (Ala-Ala) induced a sub-population of CD4⁺ T cells, which secreted IL-10 and expressed high levels of surface TGF-β. These cells resembled Tr1 regulatory T cells and might have an important role as immune modulators in using this antibody. The prominent appearance of IL-10 might indicate a similar immune regulatory mechanism in the adaptation of animals to repeated muS110 administration although no evidence for TGF-β involvement was found after muS110 treatment.

The mAb KoKt3yl (Ala-Ala) induced *in vivo* a mild cytokine release syndrome with stronger IL-10 release in ratio to IFN-γ levels, increased the CD4⁺CD25⁺FoxP3⁺ regulatory T cells

numbers and the CD8⁺/CD4⁺ ratio (115). Therefore, animals adapted for one week with 10 µg/kg/day muS110 were monitored for the presence of CD4⁺CD25⁺FoxP3⁺ regulatory T cells and the ratio of CD8⁺ to CD4⁺ T cells. Significantly elevated levels of CD4⁺CD25⁺FoxP3⁺ regulatory T cells (10% compared to normally 6% of CD4⁺ cells) were found in the spleen but not in the blood. Additionally a significantly higher CD8⁺/CD4⁺ ratio was found in the blood of adapted mice in comparison to vehicle treated control mice (Figure 26).

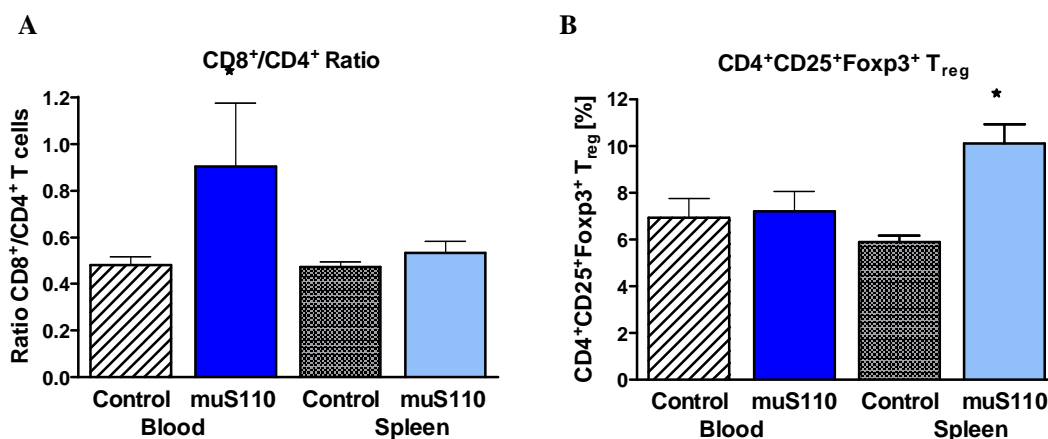


Figure 26: Induction of CD4⁺CD25⁺FoxP3⁺ regulatory T cells and changes in the CD8⁺/CD4⁺ ratio upon low dose muS110 adaptation

Female BALB/c mice (n= 6) received daily i.v. injections of vehicle (control) or 10 µg/kg/day muS110 for 7 days in a volume of 200 µl. (A) 24 hours after the last injection splenocytes and PBMCs were stained with antibodies against CD4 and CD8 and analyzed for the CD8⁺/CD4⁺ T cell ratio by flow cytometry. (B) Additionally cells were stained intracellularly with antibodies against CD25 and FoxP3 for the presence of CD4⁺CD25⁺FoxP3⁺ T cells. Error bars indicate the SEM. Asterisk indicate P values < 0.02 obtained with student's T test. The experiment is representative for two individual experiments

5.2.5.2 *Ex vivo* T cell activation after repeated administration of muS110

Stimulation of T cells via the TCR in the absence of co-stimulatory signals can lead to T cell anergy, which is characterized by down regulation of effector functions in re-stimulated T cells (116). Redirected lysis by muS110 *in vivo* involved repeated TCR signaling in the absence of co-stimuli. Almost complete elimination of EpCAM⁺ lymphocytes abrogated the second binding partner in healthy mice and T cell activation took place in the presence of high IL-10 concentrations. Hence, reduction of systemic cytokine levels after repeated administration of muS110 could have also been a consequence of T cells anergy, possibly imposed by regulatory T cells. Thus, T cells isolated from low dose muS110 adapted animals were tested for signs of anergy, e.g. impairment of the proliferative potential. Female BALB/c mice received i.v. injections of 10 µg/kg/day muS110, or vehicle, for 7 consecutive days. One day

after the 7th administration, half of the animals were sacrificed ('acute phase'). The remaining animals were killed after a 'recovery phase' of 7 days. Splenocytes were isolated from each animal and labeled with CFSE, a dye visualizing cell cycling by FACS analysis. The CFSE-labeled splenocytes were restimulated *in vitro* in the presence of recombinant human IL-2 using the Dynabeads CD3/CD28 T Cell Expander, or were left untreated to obtain background values. The capacity to enter the cell cycle and proliferate in response to an exogenous stimulus was monitored by the dilution of the CFSE signal in T cells.

No significant difference in the proliferation between re-stimulated T cells from muS110 or vehicle treated animals could be observed after treatment or a 1-week recovery period (Figure 27A). T cells had not lost their proliferative potential during repetitive treatment of mice with muS110. Analysis of the FACS histograms of CFSE-labeled cells revealed a difference with respect to the synchronicity of cell division (Figure 27B). T cells isolated from muS110 treated animals divided synchronously by showing just one major species of labeled cells, while T cells isolated from vehicle control animals divided asynchronously, showing discrete cell populations of various cell generations. Upon *in vitro* re-stimulation the cytokine release of cells from muS110-treated animals was significantly lower than that from vehicle treated ones ($p < 0.02$ using the student's t test) (Figure 27C). Recovery for one week normalized the cytokine secretion levels upon re-stimulation (Figure 27D).

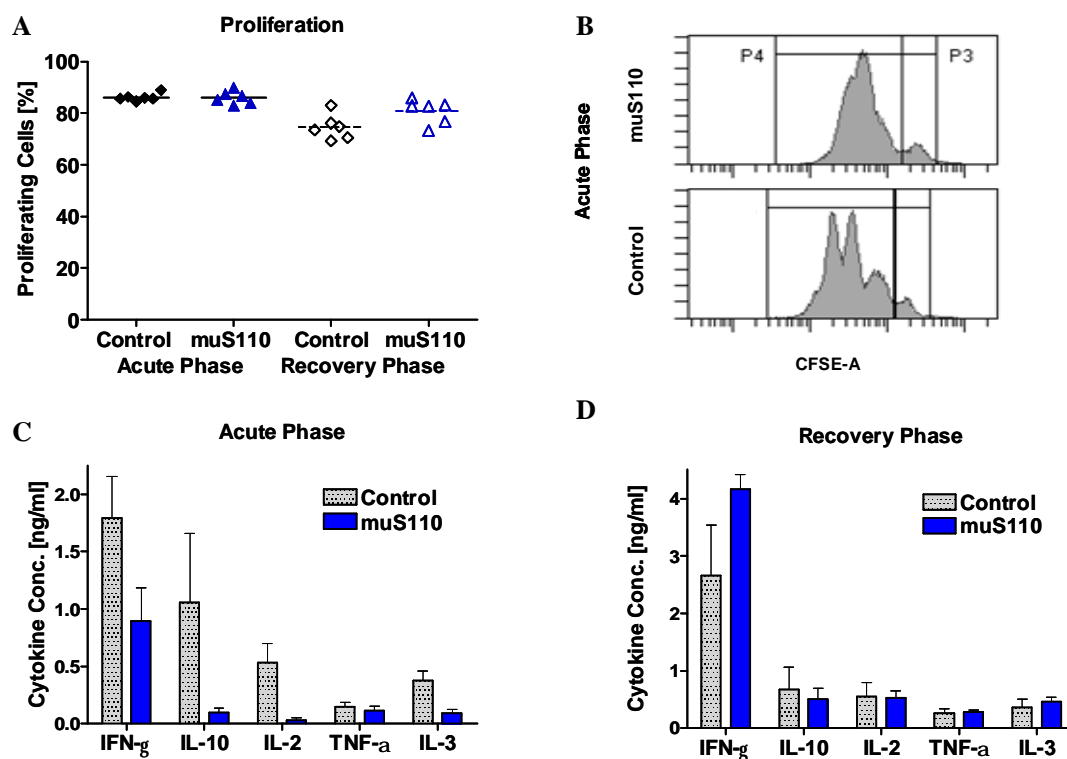


Figure 27: Repeated administration of muS110 does not impair restimulation of T cells.

Female BALB/c mice ($n = 12$) received daily intravenous bolus injections of vehicle (control) or $10 \mu\text{g/kg/day}$ muS110 for 7 days in a volume of $200 \mu\text{l}$. Six animals were killed 24 hours after the 7th injection (Acute Phase) whereas 6 animals were allowed to recover for additional seven days (Recovery Phase). Splenocytes were isolated 24 hours after 7th injection, labeled with CFSE, and stimulated with Dynabeads CD3/CD28 T Cell expander in the presence of 10 U/ml rhIL-2. (A) After 72 hours, proliferation was monitored by FACS analysis of CFSE distribution. (B) Mean fluorescence intensity is shown. (C, D) Supernatant of samples with splenocytes obtained after (C) acute phase or (D) recovery phase were analyzed for concentrations of TNF- α , IL-2, IL-10, IFN- γ , IL-6, and IL-3. Error bar indicated the SEM. Experiment was performed twice.

5.2.5.3 Cytotoxic and proliferative capacity of T cells after repeated administration of muS110

To rule out a relieve of a potential muS110-induced T cell anergy by addition of IL-2, which could have explained the observed synchronous cell proliferation, T cells were tested for redirected lysis after acute and recovery phase in the absence of recombinant human IL-2. As shown in Figure 28A, T cells from vehicle and muS110 treated animals showed a similar potency to induce lysis of CHOMuEpCAM⁺ cells with almost identical EC₅₀ values for half maximal lysis. ($0.24 \pm 0.03 \text{ ng/ml}$ versus $0.28 \pm 0.05 \text{ ng/ml}$).

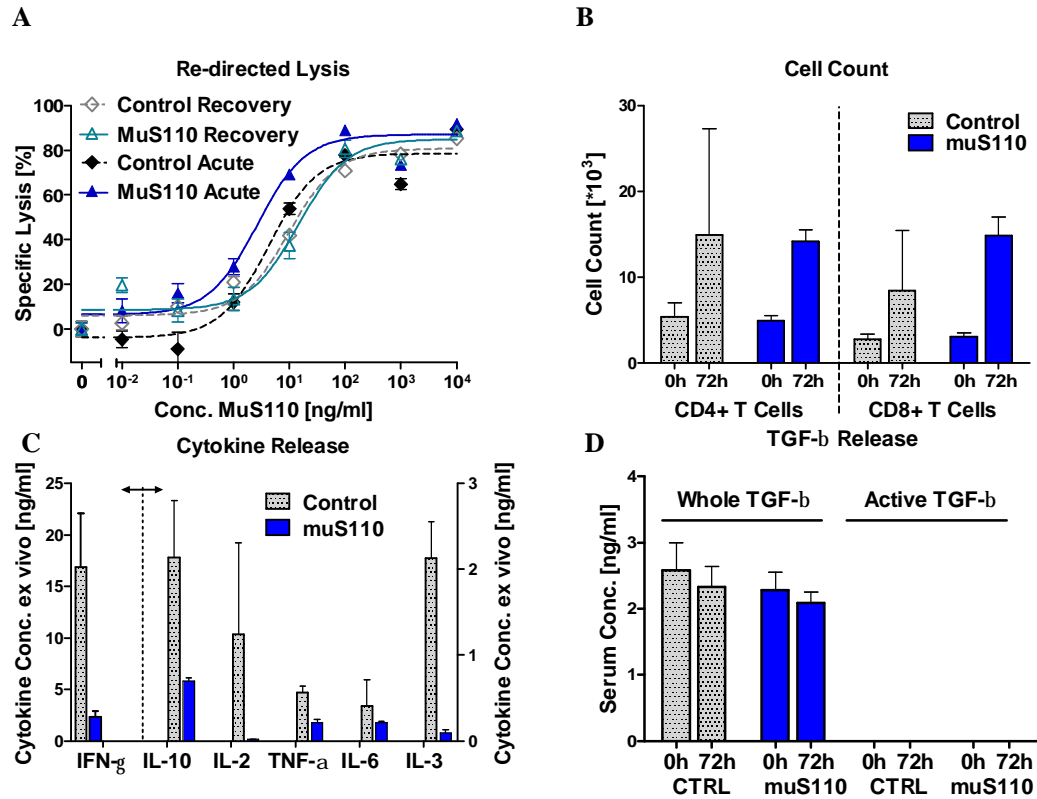


Figure 28: Cytotoxic and proliferative capacity of T cells after repeated administration of muS110

Female BALB/c mice ($n = 12$) received daily intravenous bolus injections of vehicle (control) or $10 \mu\text{g}/\text{kg}/\text{day}$ muS110 for 7 days in a volume of $200 \mu\text{l}$. Six animals were killed 24 hours after the 7th injection (Acute Phase) whereas 6 animals were allowed to recover for additional seven days (Recovery Phase). (A) Splenocytes were isolated after acute or recovery period and were used as effector cells for redirected target cell lysis of CHO/muEpCAM⁺ target cells. Cell lysis was determined by FACS analysis of nuclear PI uptake. The assay was performed in triplicates. Data represents global fit for 6 animals. (B) Absolute cell number/ well of CD4⁺ and CD8⁺ T cells were analyzed pre and 72 hours after redirected lysis in samples containing 100 ng/ml muS110 (C, D) Supernatants of samples containing 100 ng/ml muS110 were analyzed for (C) TNF- α , IL-2, IL-10, IFN- γ , IL-6, IL-3 and (D) TGF- β content. Error bars indicate SEM. Experiments were repeated twice.

This suggests that muS110 treatment does not impair the cytotoxic capacity of T cells. The BiTE control antibody muMEC14 did not mediate lysis of CHOmuEpCAM⁺ cells (data not shown). To evaluate the ability of T cells to proliferate the absolute count of living CD4⁺ and CD8⁺ T cells was measured before and after redirected lysis using flow cytometry. Absolute cell counts after redirected lysis were amplified 3-4 fold for CD8⁺ T cells and 2-3 fold for CD4⁺ T cells independently of prior *in vivo* treatment with or without muS110 and of exogenous addition of IL-2 (Figure 28B). In fact, IL-2 was not detectable in culture supernatants after *in vitro* re-stimulation of muS110-pretreated T cells with muS110 (Figure 28C).

As observed in the proliferation experiment, cytokine release upon *in vitro* re-stimulation with muS110 was much reduced in muS110-treated animals compared to vehicle controls (Figure 28C). As *in vivo* no latent or active TGF- β was found in the cell culture supernatant (Figure 28D). The ratio of CD8⁺ to CD4⁺ cells slightly shifted toward CD8⁺ T cells after muS110 *in vivo* stimulation, which became even more prominent 72 hours after *in vitro* re-stimulation of T cells with muS110 (data not shown). As in the control group a dose dependent up-regulation of CD69 and CD25 on CD4⁺ and CD8⁺ T cells was observed after the acute as well as after the recovery phase (Figure 29). Of note, again CD8⁺ cells seem to be more activated by muS110 *in vivo* treatment than CD4⁺ cells.

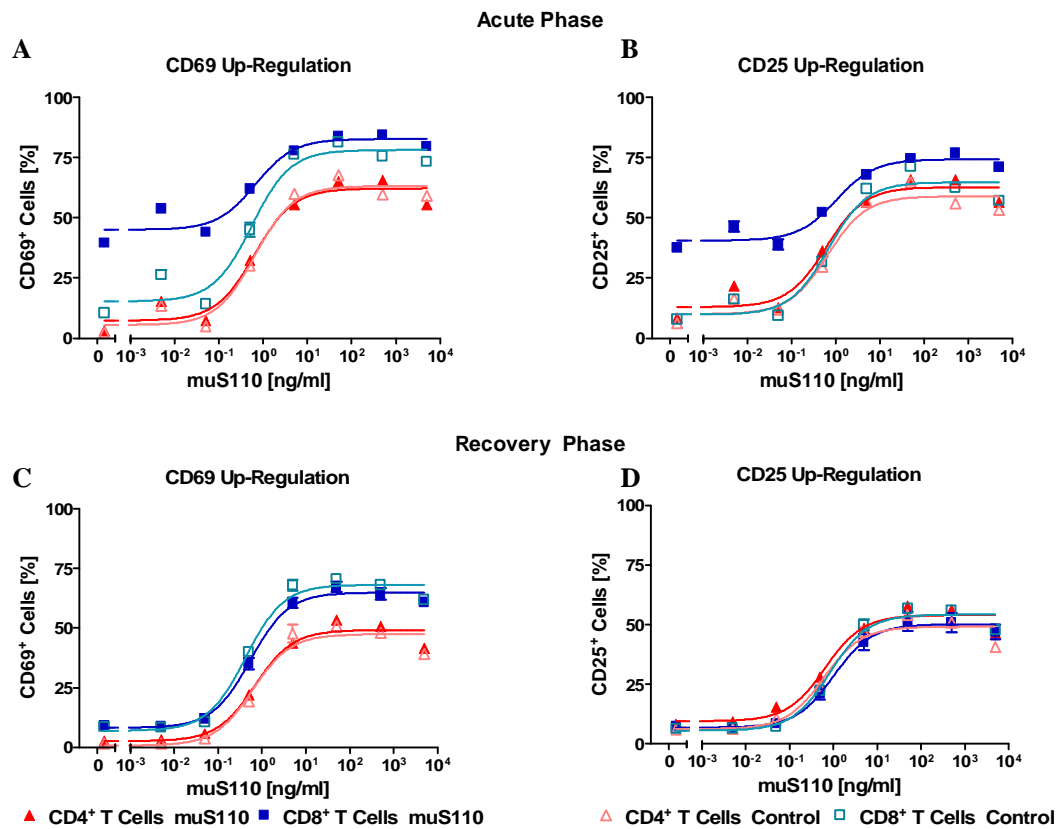


Figure 29: MuS110 induced *ex vivo* T cell activation after low dose adaptation

T cells of low dose muS110 adapted animals activated upon *ex vivo* re-stimulation with muS110 and did not show signs of anergy. Female BALB/c mice (n= 10) received daily intravenous bolus injections of vehicle (control) or 10 μ g/kg/day muS110 for 7 days in a volume of 200 μ l. Six animals were sacrificed 24 hours after the 7th injection. Splenocytes were isolated after (A, B) acute period or (C, D) recovery period and were used as effector cells for redirected target cell lysis of CHO/muEpCAM⁺ target cells for 72 hours. Afterwards cells were stained with antibodies against CD4, CD8, CD25 and CD69 and analyzed with flowcytometry. Up-regulation of CD69 (left side) and CD25 (right side) is shown as function of muS110 concentration. Error bars indicate the SEM for triplicates of six animals. Experiment was repeated twice.

Conclusively no signs of anergy were found for lymphocytes isolated from muS110 adapted animals. However, these T cells had impaired ability for cytokine secretion after *in vitro* re-stimulation via an anti-CD3 stimulus, which was normalized after one week free of muS110 injections. Even in the face of a full T cell activating stimulus T cells from adapted animals did hardly produce cytokines in comparison to those of untreated animals, although they were not hampered in their ability to proliferate, up-regulate activation markers and lyse target cells. This indicated again that mere loss of EpCAM⁺ target cells upon repeated treatment with muS110 was not the only cause of adaptation to muS110.

5.2.6 Impact of glucocorticoids on muS110 tolerability *in vivo*

Glucocorticoids, like methylprednisolone (mPDS) and dexamethasone, repress the expression of a wide variety of cytokines including IL-2, IL-3, IL-4, IL-6, IL-8, and IFN- γ (117). They are used for treatment of a variety of allergic, inflammatory, and autoimmune disorders (118). Cytokine-related side effects of anti-CD3 antibodies have been shown to be significantly reduced by glucocorticoid pre-treatment (99, 119). Hence, the impact of dexamethasone and mPDS on the tolerability of single dose and repeated administrations of muS110 was tested.

The safety profile of muS110 was analyzed in 20 female BALB/c mice following i.v. injection of 50 $\mu\text{g}/\text{kg}$ muS110 with or without pre-treatment with 10 mg/kg dexamethasone one hour before muS110 administration. At the indicated time points serum concentrations of muS110 were determined in order to evaluate muS110 exposure. Overall, dose-dependent muS110 exposure was similar for both treatment groups (Figure 30A).

In both groups a time- and dose-dependent onset of side effects was observed for up to 24 hours after administration of muS110 (Figure 30B). Most prominent side effects were hypomotility, piloerection, hypothermia and diarrhea (Table 7). Hypomotility and piloerection were significantly reduced in animals treated with dexamethasone. The onset of diarrhea was completely prevented in dexamethasone treated animals and the observed hypothermia was less pronounced (2°C versus 5.7°C) and reversible already after 4 hours.

In general, tolerability of 50 $\mu\text{g}/\text{kg}$ muS110 with dexamethasone pre-treatment was comparable to that of single muS110 doses between 5 and 15 $\mu\text{g}/\text{kg}$. Dexamethasone slightly decreased the overall systemic T cell activation as indicated in Figure 30C, where CD25⁺ and CD69⁺ expression of T cells isolated from mesenterial lymph nodes is shown. Dexamethasone was also able to significantly reduce the following cytokine release (Figure 30D). With excep-

tion of IL-10, the peak levels of all cytokines analyzed were reduced by 50 to 90% after dexamethasone pre-treatment and were comparable to serum concentrations obtained after administration of 5 – 15 µg/kg muS110.

Table 7 : The effect of glucocorticoid pre-treatment on the tolerability of muS110

MuS110 [µg/kg]	Pretreatment Dexamethasone	Hypomotility			Piloerection			Diarrhea		
		0-4 hrs	4-10 hrs	10-24 hrs	0-4 hrs	4-10 hrs	10-24 hrs	0-4 hrs	4-10 hrs	10-24 hrs
50	-	+	+/-	-	+	+	+/-	+	+/-	-
50	10 mg/kg	+/-	+/-	-	+/-	+/-	+/-	-	-	-

- No effects
+/- Minimal to weak effects
+ Moderate effects

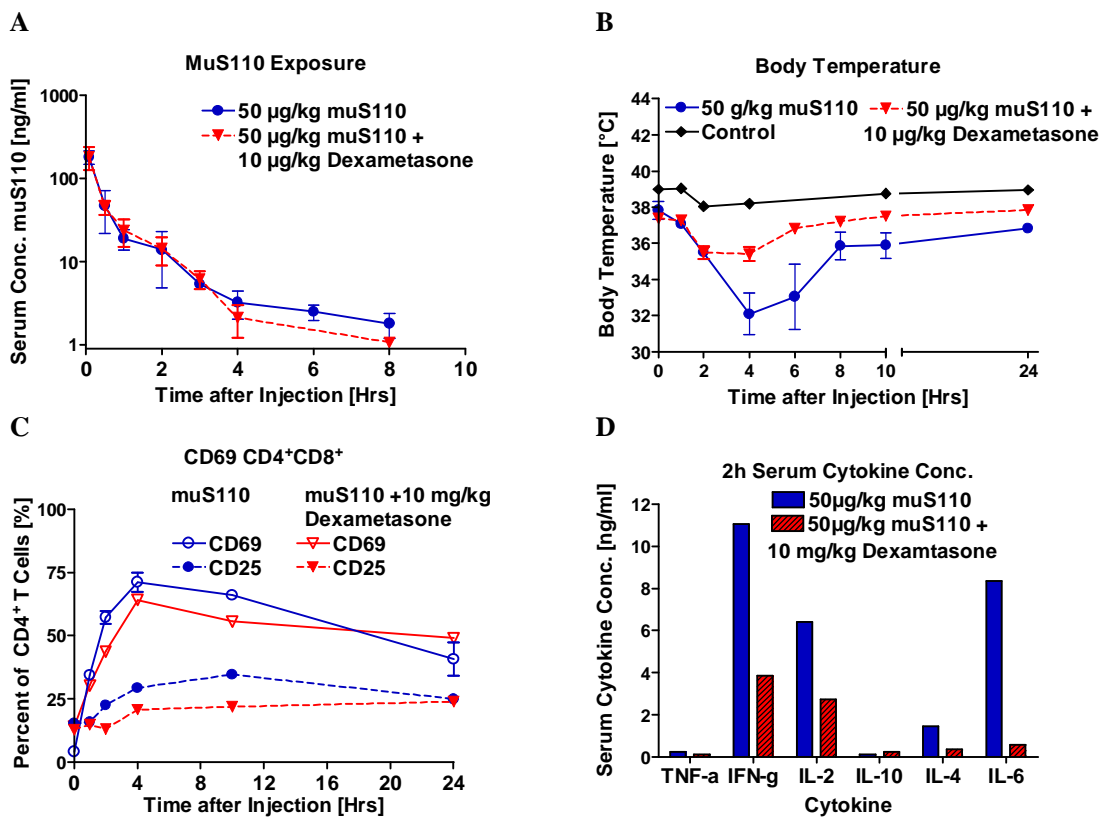


Figure 30: Effects of glucocorticoid pre-treatment on the tolerability of muS110

Female BALB/c mice (n= 20) received i.v. injection of 50 µg/kg muS110 with or without pre-treatment with 10 mg/kg dexamethasone one hour before muS110 administration. (A) Serum concentrations of muS110 (n=4) were determined 5 min, 1, 2, 4, 6, 8, 10, and 24 hours after muS110 injection. (B) Body temperature was determined at the indicated time points after muS110 administration. (C) Mesenteric lymph nodes (n=2) were isolated before and 1, 2, 4, 10, and 24 hours after muS110 administration. CD25 and CD69 surface expression were determined for CD4⁺ T cells by flow cytometry. Error bars indicate SEM. (D) Animals (n=4) were bled 2 hours after muS110 injection and pooled serum samples were analyzed for IL-2, IFN-γ, TNF-α, IL-6, IL-4 and IL-10 concentrations. The experiment was performed twice.

Glucocorticoid treatment was clearly able to increase tolerability to single dose muS110 injection; therefore, it was analyzed whether this could also be observed for repetitive muS110 administration. 30 mg/kg mPDS was administered one hour before and after the first injection of muS110. Thus, the capability of mPDS to prevent or decrease the first dose effect and the impact of mPDS on muS110 dose adaptation was analyzed.

BALB/c mice received i.v. bolus injections of 10 $\mu\text{g}/\text{kg}/\text{day}$ muS110 for 7 days with or without intra-peritoneal injection of 30 mg/kg mPDS one hour before and after the first injection of muS110. Administration of muS110 resulted in an average loss of body weight by 4% and a mild but reversible reduction of motility for up to 4 hours after the first and second injection. Both adverse effects were completely prevented by pre-administration of mPDS. Serum cytokine levels of IL-2, TNF- α , IL-6, and IL-10 were found to be increased 2 hours after injection of muS110 with a significant adaptation after the third injection. Co-administration of mPDS efficiently inhibited cytokine release after the first injection of muS110 but, with the exception of IL-10, was no longer effective after the second injection of muS110. As observed before, IL-10 concentration was stronger elevated upon the second administration of muS110, but decreased in total by pre-treatment with mPDS (Figure 31A and B). Although mPDS treatment effectively curbed the release of IL-10 in response to muS110, this did not prevent the adaptation effect on cytokine release later on.

Splenocytes isolated 24 hours after the 7th muS110 injection were stained with antibodies against CD127 and CD62L to determine distribution of naive, intermediate, effector, central and effector memory T cells. Additionally intracellular staining with antibodies against granzyme B, IFN- γ and CD152 was performed. The shift from $T_{\text{Naive/CM}}$ and T_{EM} towards T_{Eff} and T_{Int} compartment was smaller after repeated treatment with 10 $\mu\text{g}/\text{kg}/\text{day}$ than after 25 $\mu\text{g}/\text{kg}/\text{day}$ muS110 (compare Figure 31 and Figure 23). Treatment with mPDS did not prevent induction of T_{Eff} cells (Figure 31C). CD8^+ T cells were to a similar extent positive for granzyme B, IFN- γ and CD152 whereas these effects were even more pronounced for CD4^+ T cells after combined glucocorticoid/ muS110 treatment than after muS110 treatment alone (Figure 31D).

It has been shown that treatment with anti-CD3 antibodies induced CD8^+ regulatory T cells, which down-regulate activation of CD4^+ T cells (120). Figure 23 shows that muS110 induced slightly more CD8^+ than CD4^+ cytotoxic effector cells and that CD8^+ T cell numbers increased stronger than that of CD4^+ T cells (Figure 26). Therefore, regulation of CD4^+ T cells

might play a role in BiTE induced adaptation as well, however, no regulatory CD8⁺ T cells were found so far. It was speculated that glucocorticoids might hamper this adaptation process (121). This could be an explanation for the slightly more activated appearance of CD4⁺ T cells after glucocorticoid co-treatment.

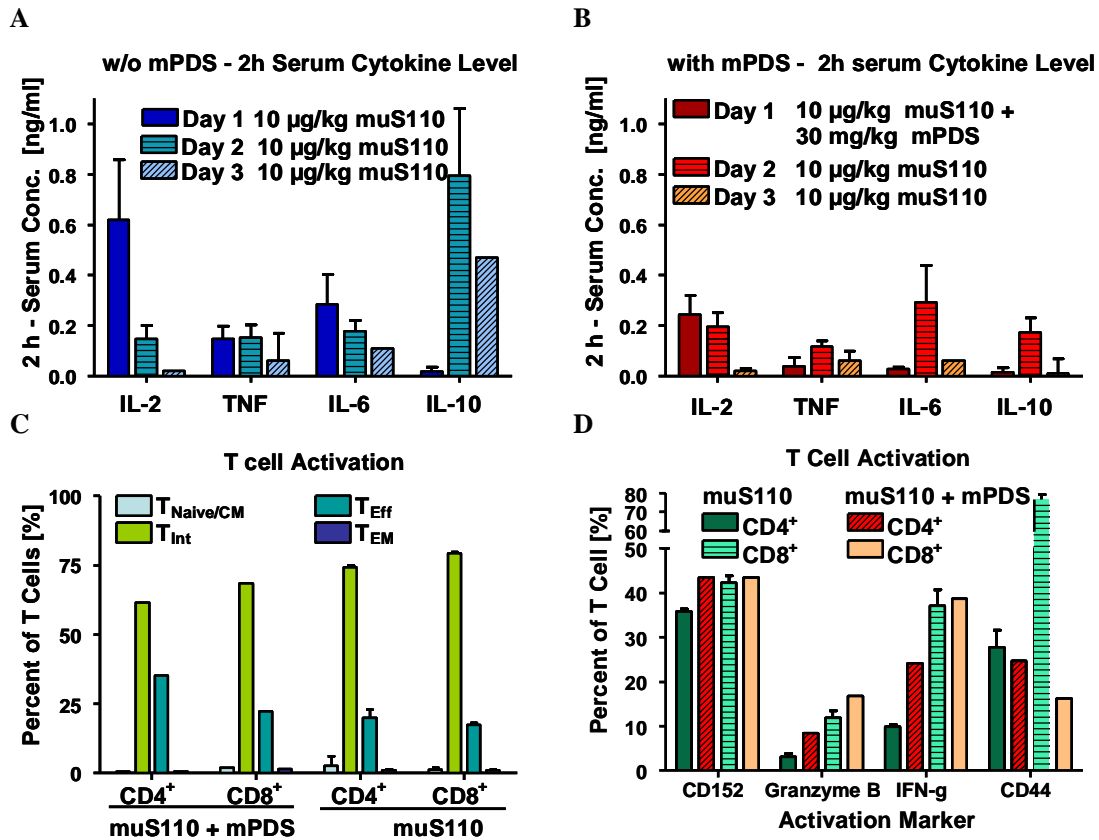


Figure 31: Impact of mPDS on muS110 induced T cell activation and systemic cytokine levels

Female BALB/c mice (n= 12) received intravenous bolus injections of 10 µg/kg/day muS110 for 7 days with or w/o intraperitoneal injection of 30 mg/kg mPDS one hour prior and one hour after the first muS110 injection. (A, B) Animals (n= 6) were bled 2 hours after first muS110 administration and serum samples were analyzed for IL-10, TNF-α, IL-4, IL-6 IL-2, and IFN-γ of animals treated (B) with mPDS or (A) w/o mPDS. (C, D) Splenocytes were isolated 24 hours after 7th muS110 injection. A part of the cells were stained with antibodies against the surface marker CD127, CD62L. (C) Percentage of naive/ central memory T cells (T_{Naive/CM}, CD62L⁺ CD127⁺), intermediate T cells (T_{Int}, CD62L⁺ CD127⁻), effector T cells (T_{Eff}, CD62L⁻ CD127⁻) and effector memory T cells (T_{EM}, CD62L⁻ CD127⁺) are shown. (D) Intracellular staining with antibodies against CD44, granzyme B, IFN-γ, and CD152 was performed after PMA/ Ionomycin/ Brefeldin A stimulation. Error bars indicate SEM. Cytokine determination was performed in two different experiments, flow cytometry analysis of T cells only once.

The glucocorticoid mPDS did not impair cytotoxic T cell effector functions. Splenocytes from animals receiving muS110 or a combination of muS110 and mPDS were isolated after the 7th muS110 injection. The cytotoxic capacity of these cells was evaluated by muS110 induced redirected lysis of CHOmuEpCAM⁺ target cells (Figure 32A). Similar EC₅₀ values for redirected lysis were obtained with T cells from animals treated with or without mPDS. Cells from animals treated with muS110 revealed EC₅₀ values of 0.28 +/- 0.06 ng/ml, those from muS110 plus mPDS-treated animals EC₅₀ values of 0.35 +/- 0.04 ng/ml. Likewise, their potential to proliferate in response to an exogenous stimulus was unchanged for the two groups (Figure 32B).

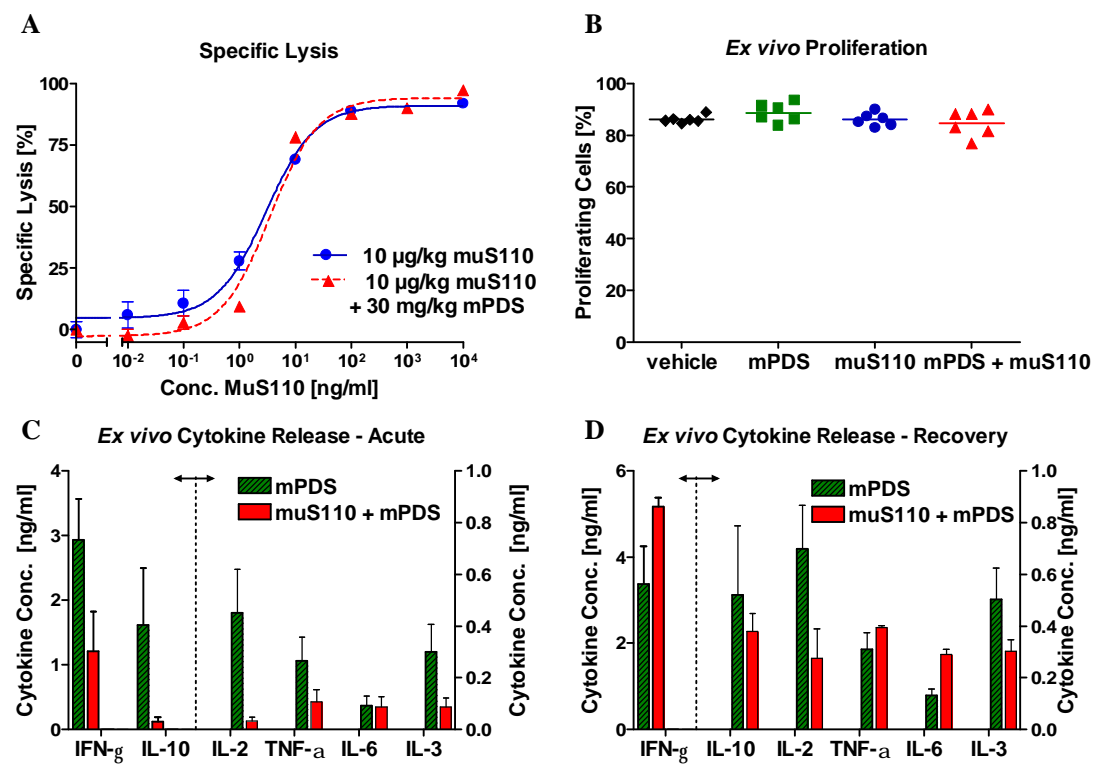


Figure 32: Impact of mPDS co-administration during muS110 low dose adaptation on T cell effector functions

Female BALB/c mice (n= 12) received i.v. injections of 10 µg/kg/day muS110 for 7 days with or without i.p administration of 30 mg/kg mPDS one hour prior and one hour after the first muS110 treatment. Six animals were sacrificed 24 hours after 7th injection (acute) whereas 6 animals were allowed to recover for additional seven days (recovery). (A) Splenocytes were isolated and used as effector cells for redirected target cell lysis of CHOmuEpCAM⁺ cells. Cell lysis was determined by FACS analysis of PI incorporation. Data represents global fit of 6 animals. (B, D) Splenocytes were labeled with CFSE and stimulated with Dynabeads CD3/CD28 T cell expander in the presence of 10 U/ml rhIL-2. After 72 hours, (B) proliferation was monitored by FACS analysis of CFSE distribution. (C, D) Supernatants of tests using splenocytes obtained after (C) acute phase or (D) recovery phase were analyzed for concentrations of TNF- α , IL-2, IL-10, IFN- γ , IL-6, and IL-3. Error bar indicated the SEM of six animals.

After the acute phase, the cytokine release by cells from muS110/ mPDS-treated animals was significantly lower upon *in vitro* re-stimulation for most cytokines compared to cells from only mPDS treated animals ($p < 0.05$) (Figure 32C). After recovery for one week, comparable cytokine levels were induced upon re-stimulation in cells from both groups (Figure 32D).

Hence, mPDS was able to increase the tolerability of muS110 by improving the first dose response and simultaneously allowing muS110 induced self-adaptation. This suggests that glucocorticoid hormones are suited to further improve the tolerability of muS110 in combination with a muS110 low-dose adaptation regimen.

5.3 *In vivo* efficacy

5.3.1 MuS110 efficacy and toxicity in mouse pulmonary metastasis models

The *in vivo* anti-tumor efficacy of muS110 was tested in syngenic B16F10muEpCAM⁺ and CT-26muEpCAM⁺ mouse pulmonary metastasis models. Therefore, either 1×10^5 CT-26muEpCAM⁺ or 1×10^5 B16F10muEpCAM⁺ tumor cells were i.v. injected into the lateral tail vein of BALB/c (8-12 per group) and C57BL/6 mice (6 mice per group), respectively. The tumor cells were trapped in the small pulmonary venules around the alveoles of the lung where they formed small tumor colonies on the lung surface. In the B16F10muEpCAM⁺ tumor model treatment started one hour after tumor cell inoculation. Until day 17 after tumor cell inoculation animals were i.v. injected five times a week with PBS control buffer or different doses of muS110 (0.5, 2, 5 and 12.5 $\mu\text{g}/\text{kg}/\text{day}$ or increasing doses from 12.5-200 $\mu\text{g}/\text{kg}/\text{day}$, in which the starting dose was doubled every second injection after the fourth treatment day). In the CT-26muEpCAM⁺ tumor model muS110 administration was initiated three days after tumor inoculation to allow formation of lung colonies. Until day 17 after tumor cell inoculation animals were treated daily i.v. with PBS control buffer or different doses of muS110 (0.5, 2, 5 and 12.5 $\mu\text{g}/\text{kg}/\text{day}$ or increasing doses from 12.5-400 $\mu\text{g}/\text{kg}/\text{day}$, in which the starting dose of 12.5 $\mu\text{g}/\text{kg}$ was doubled every second day after the fourth injection). The growth kinetic of lung colony formation was monitored with PBS treated sentinel animals. All animals were killed on day 17 of the study due to a strong lung tumor burden and number of tumor cell colonies on the lung surface was determined macroscopically.

In both cases daily i.v. treatment with muS110 led to a significant and dose dependent inhibition of lung tumor colony formation (Figure 33).

In the B16F10muEpCAM⁺ tumor model treatment with 0.5 $\mu\text{g}/\text{kg}$ did only show a reduction of lung tumor colonies by 24%, which was not significant. Treatment with 2 or 5 $\mu\text{g}/\text{kg}$ re-

sulted in a significant reduction by 40% and 60%, respectively. Treatment with 12.5 $\mu\text{g}/\text{kg}$ muS110 reduced the number of lung tumor colonies by 75%. The strongest effect was seen in the intra-animal dose escalation group (12.5-200 $\mu\text{g}/\text{kg}$ muS110) in which tumor growth was prevented in 1/6 animal totally and the number of tumor colonies was reduced in the remaining animals by 87% (Figure 33B and D).

The *in vivo* efficacy of muS110 was less pronounced in the delayed treatment of CT26muEpCAM⁺ lung metastases. Treatment with 0.5 $\mu\text{g}/\text{kg}$ had a non-significant effect on the number of lung tumor colonies (reduction by 6.7%), whereas treatment with 2 $\mu\text{g}/\text{kg}$, 5 $\mu\text{g}/\text{kg}$ and 12.5 $\mu\text{g}/\text{kg}$ resulted in a significant reduction by 38.9%, 50.6% and 56% of tumor burden, respectively. With a reduction by 63% the strongest effect was seen again in the intra-animal dose escalation group (12.5-400 $\mu\text{g}/\text{kg}$ muS110). All animals developed lung metastases (Figure 33A and C).

Side effects in the highest dose groups such as loss of body weight, diarrhea, and mild sedation/excitation were only transient. The loss of body weight was approximately 5-7.5% with a rapid recovery thereafter. However, total recovery of the body weight to pre-experimental values was delayed in the intra-animal dose escalation group. In the lower dose groups, no such treatment related side effects were observed (Figure 33).

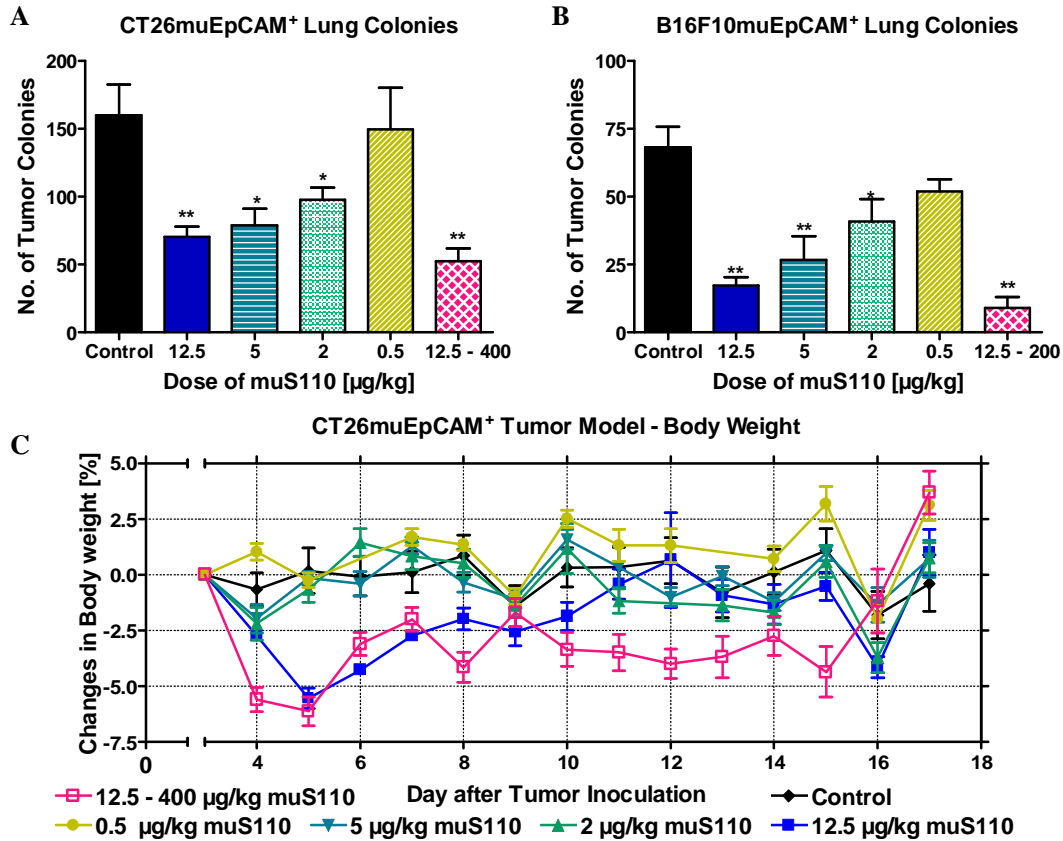


Figure 33: MuS110 efficacy and toxicity in mouse pulmonary metastasis models

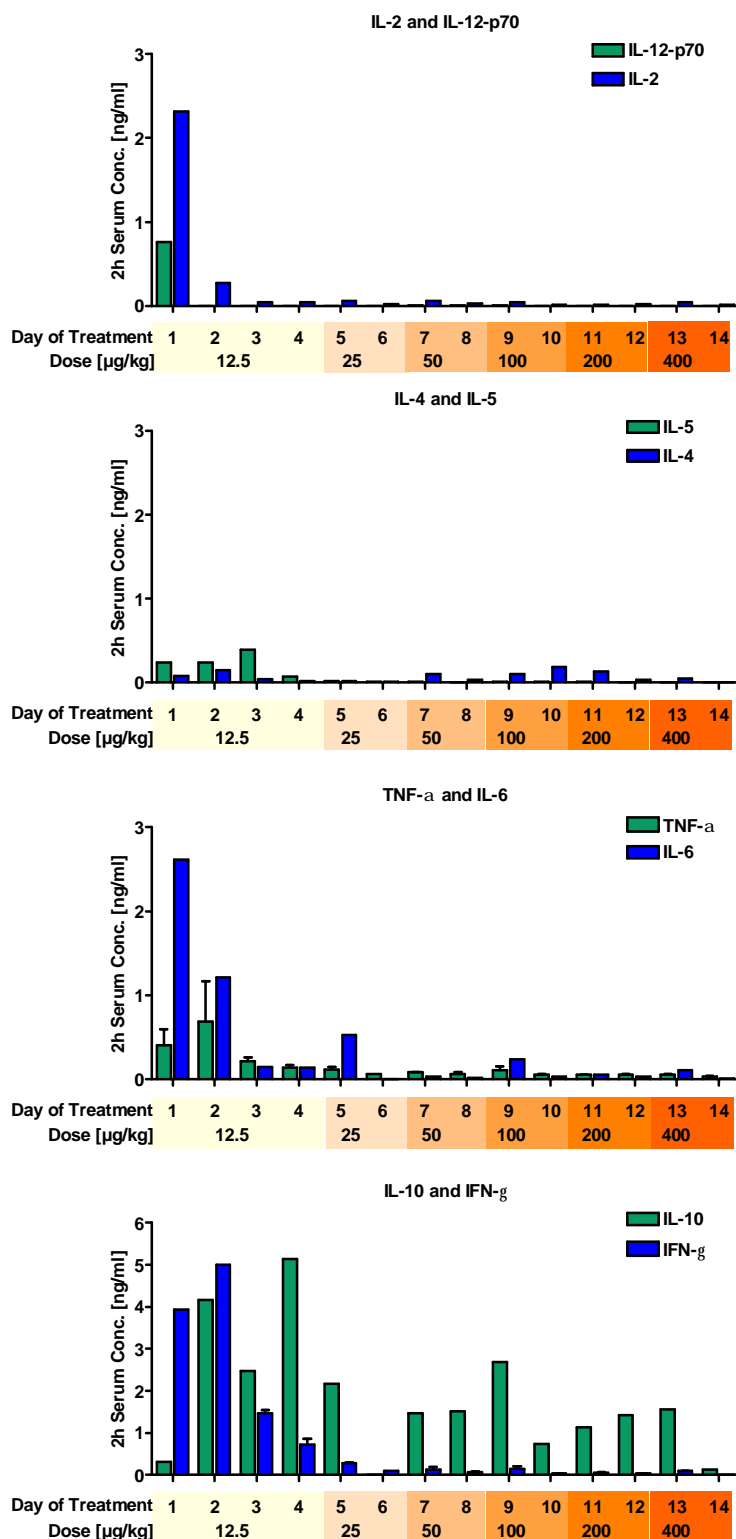
(A, C) Eight to twelve mice per group i.v. inoculated with 1×10^5 CT26muEpCAM⁺ tumor cells on day 0. Mice were treated from day 3 after tumor cell inoculation with the indicated dose of muS110 by daily i.v. injections (200 μl). (B) Six mice per group were i.v. inoculated with 1×10^5 B16F10muEpCAM⁺ tumor cells on day 0. Mice were treated i.v. daily starting 1 hour after tumor cell inoculation with the indicated doses of muS110 (B) Mice were killed on day 17 of experiment and lungs examined macroscopically for the presence of tumor nodules. (C) Body weight was determined 3 times a week. SEM is shown. Asterisks indicate significant differences between the treatment and the control group as calculated with the Student's T Test (*P<0.05; ** P< 0.01). Experiments with B16F10muEpCAM⁺ tumor cells were repeated twice, that with CT26muEpCAM⁺ tumor cells three times.

Serum cytokine level of IL-2, IL-12p70, IFN-γ, TNF-α, IL-6, IL-4, IL-5 and IL-10 were determined two hours after each muS110 administration for 2 animals of the intra-animal dose escalation group (12.5-400 μg/kg muS110) using the mouse TH₁/TH₂ CBA Kit and the mouse inflammation CBA kit (both BD Bioscience). Coincident with the induction of clinical signs, daily dosing of 12.5 μg/kg muS110 induced a systemic and transient release of inflammatory cytokines, including IL-2, IL-12p70, IFN-γ, TNF-α, IL-6, IL-4, IL-5 and IL-10 (Figure 34).

The cytokine release was self-limiting and, with the exception of IL-10, much reduced after the fourth injection of muS110. Although the dose of muS110 was doubled every second day

after the fourth injection only small amounts of cytokines were detectable in the serum after each following injection. This is most probably due to muS110 induced suppression of cytokine release by activated T cells, which was already shown in section 5.2.5. An exception was IL-10, which showed only a slight increase after the first muS110 injection but a strong elevation after each following muS110 administration. This is in accordance with the strong IL-10 release upon high dose muS110 challenges after low dose adaptation (Figure 25) and might be another proof for the immune-suppressive effects of this cytokine. The superiority of the dose escalation schedule over administration of a constant muS110 shows that muS110 induced immune modulation suppresses the systemic release of cytokines and limits related adverse effects but does not comprise the cytotoxic potential of effector T cells.

Figure 34: Serum cytokine level during dose escalation of muS110 in a CT26muEpCAM⁺ pulmonary metastasis model



Eight to twelve mice per group were intravenously inoculated with 1×10^5 CT26muEpCAM⁺ tumor cells on day 0. Mice were treated from day 3 after tumor cell inoculation with the indicated doses of muS110 (12.5-400 µg/kg muS110) by daily intravenous injections (200 µl). Serum cytokine level of IL-2, IL-12p70, IFN-γ, TNF-α, IL-6, IL-4, IL-5 and IL-10 were determined 2 hrs after each daily muS110 administration for 2 animals using the Mouse TH₁/TH₂ CBA Kit and the mouse inflammation CBA kit (both BD Bioscience). Serum of 2 animals was prior to measurement. Error bars show SEM and are representative for deviations of results between the two different CBA kits for one cytokine.

5.3.2 MuS110 efficacy and toxicity in an orthotopic 4T1 breast cancer model

The *in vivo* anti-tumor efficacy of muS110 against solid tumors was tested in a syngenic, orthotopic 4T1 mouse breast carcinoma model. A mixture of 5×10^3 mouse T cells and 2×10^4 4T1 tumor cells was inoculated into the mammary fat pad of 6 BALB/c mice per group and animals were s.c. treated daily with either PBS or muS110 (0.5, 1, 5, or 15 $\mu\text{g}/\text{kg}/\text{day}$). The tumor volumes were measured on the indicated days with a caliper, and the tumor weight of dissected tumor at the end of the experiment (Figure 35A and E).

Daily s.c. treatment with 5 or 15 $\mu\text{g}/\text{kg}/\text{day}$ muS110 starting at day 0 induced a significant reduction of tumor growth while 0.5 and 1.5 $\mu\text{g}/\text{kg}/\text{day}$ muS110 were not effective, but all animals developed a tumor until the end of the study. However, treatment with 5 $\mu\text{g}/\text{kg}/\text{day}$ muS110 was with 82% reduction of tumor volume at day 30 after tumor inoculation slightly more effective than the 15 $\mu\text{g}/\text{kg}/\text{day}$ dose resulting only in 68% reduction.

S.c. treatment with muS110 induced mild dose dependent side effects. Only the highest dose group (15 $\mu\text{g}/\text{kg}/\text{day}$) showed a transient loss of body weight after the first two injections, which normalized on the third day (Figure 35B). Repeated s.c. administration seemed to be better tolerated than similar i.v. doses of muS110 (compare Figure 33E and Figure 35 B). Skin irritations occurred at the area of injection at all dose levels and scar tissue developed at about 7 days after start of treatment. After the third week of treatment all side effects had vanished. The escalating dose schedule was also tested in the solid 4T1 breast carcinoma model. A mixture of 2×10^4 4T1 tumor cells and 5×10^3 (E:T = 1:5), 1×10^4 (E:T = 1:1) and 5×10^4 (E:T = 5:1) mouse T cells, respectively, was inoculated into the mammary fat pad of 6 BALB/c mice per group. Until day 18 after tumor cell inoculation animals were s.c. injected five times a week with PBS control buffer or escalating doses of muS110 (12.5-200 $\mu\text{g}/\text{kg}/\text{day}$, in which the starting dose was doubled every second injection after the fourth treatment day). The tumor volumes were determined on the indicated days with a caliper. After the end of treatment the tumor growth was monitored for additional 17 days without further treatment. Thereafter animals were killed and dissected tumors were weight (Figure 35C and F).

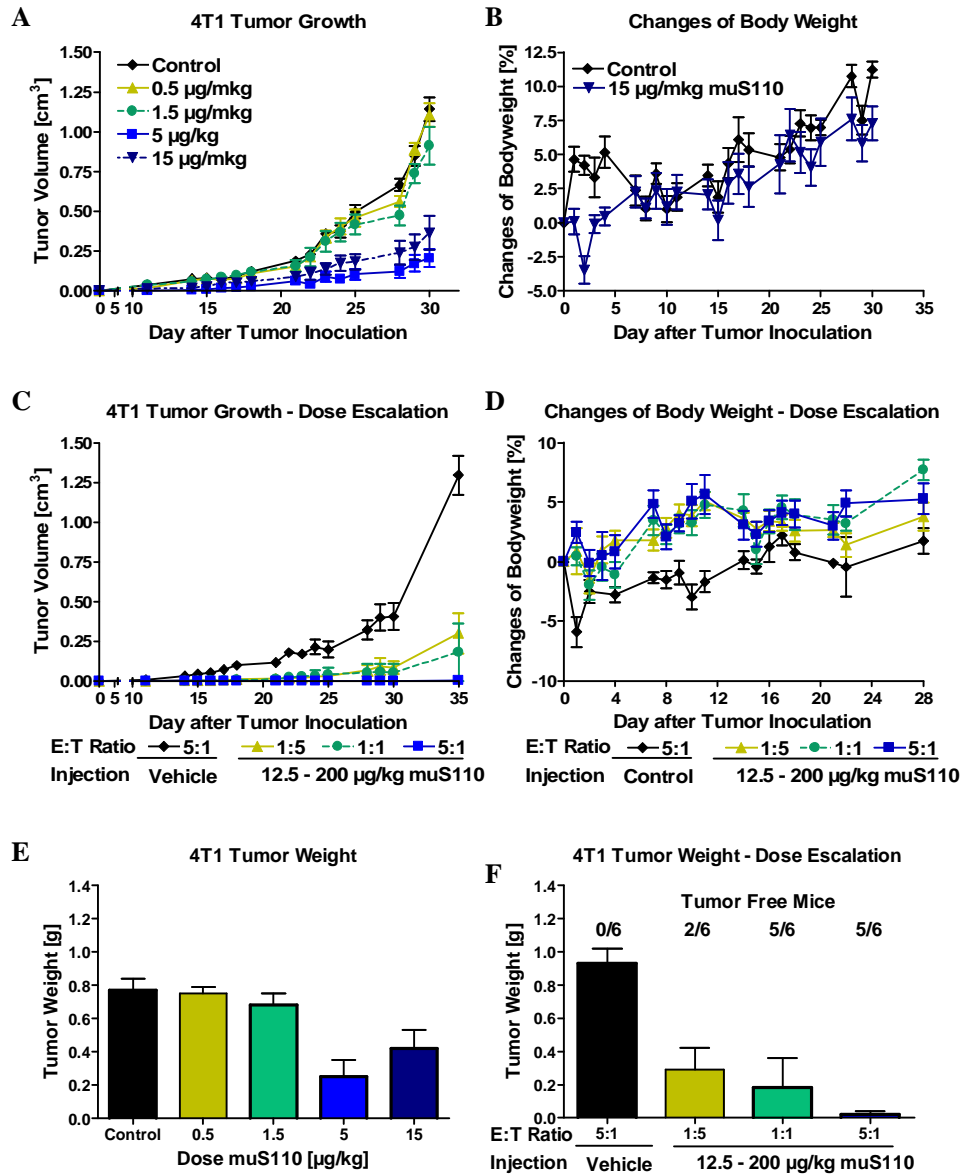


Figure 35: MuS110 efficacy and toxicity in an orthotopic, syngenic 4T1 breast cancer model

(A, B and E) Mixtures of 5×10^3 mouse T cells and 2×10^4 4T1 tumor cells were orthotopically injected into the mammary fat pad of six BALB/c mice per group and tumor size measured daily. Mice were treated daily by s.c. injection (50 μ l) with 0.5, 1, 5, or 15 μ g/kg/day muS110 or PBS control vehicle starting one hour after tumor inoculation. (C, D and E) Mixtures of 2×10^4 4T1 tumor cells and 5×10^3 (E:T = 1:5), 1×10^4 (E:T = 1:1) and 5×10^4 (E:T = 5:1) mouse T cells, respectively, were inoculated into the mammary fat pad of 6 BALB/c mice per group. Until day 18 after tumor cell inoculation animals were s.c. injected (50 μ l) five times a week with PBS or escalating doses of muS110 (12.5-200 μ g/kg/day). After the end of treatment the tumor growth was monitored for additional 17 days. (A and C) Tumor volume and (B and D) body weight of muS110-treated BALB/c mice was determined during treatment. (E and F) Weight of dissected tumors was determined at the end of the study. Error bars show SEM. Experiments were conducted twice.

The escalating dose regimen had clearly enhanced anti-tumor efficacy in comparison to treatment with constant muS110 doses. The overall tumor reduction was higher than 76% at day 35 after tumor inoculation for all muS110 treated animals in comparison to the control group and correlated with the E:T ratio at the day of tumor inoculation. The smallest effect of 76% reduction was observed at an E:T ratio of 1:5. Equal amount of T cells and tumor cells (E:T=1:1) resulted in a reduction of 90% tumor volume. The best result with a reduction by 99% of tumor volume was obtained at an E:T ratio of 5:1. Of note, 17 days after treatment stop, 2 out of 6 animals with an E : T ratio of 1:5 and 5 out of 6 animals with an higher E:T ratio were still tumor free.

Only mild muS110 induced dose dependent side effects occurred and were similar to those observed after constant muS110 dosage in the highest dose group (15 µg/kg/day). All animals showed initially a transient loss of body weight by ~2.5% after the first two injections, which normalized on the third day (Figure 35D). However, as already observed in the CT26muEpCAM⁺ tumor model (Figure 33) the increase of body weight was slower after repeated escalated than after constant muS110 doses. Again skin irritations occurred at the site of injection in all muS110 treated animals independently from the E:T ratio and scar tissue developed at about 7 days after start of treatment. After the third week of treatment all side effects had vanished.

6 DISCUSSION

6.1 The bioactivity of muS110

MuS110 is a BiTE designed to lyse mouse EpCAM positive tumor cells utilizing mouse T cells. In the presence of EpCAM⁺ target cells muS110 induced dose-dependent proliferation of T cells, cytokine secretion and up-regulation of activation marker CD69 and CD25. A transformation of resting to cytotoxic effector T cells correlated with lysis of all analyzed EpCAM⁺ target cell lines. The effects of muS110 *in vitro* were almost completely saturated at concentrations from 10 - 100 ng/ml and the EC₅₀ values of its bioactivity ranged between 0.3 and 5 ng/ml.

MuS110 mediated T cell activation was similar to that obtained by CD3/CD28 stimulation in the presence of IL-2 and independent from any physiological co-stimulation. Although the expression of CD134 (Ox40) is normally delayed and of fourfold lower level upon stimulation solemnly via the CD3 antigen, even this marker showed a comparable up-regulation after muS110 and after CD3/CD28/IL-2 stimulation (95). MuS110 might fully activate all T cells, and not only a small fraction of CD28 independent memory T cells. This is indicated by a high percentage of activated T cells (>80 % CD25⁺ and CD69⁺ cells) already after 24 hours of stimulation, the generation of over 80% granzyme B positive CD8⁺ CTLs and the almost complete absence of T_{Naive/CM} cells after 48 hours. This rapid and sound answer of almost all T cells argues against a mere expansion of only a small pool of co-stimulation independent cells. However, it cannot be ruled out that CD28 independent memory T cells might be activated first and facilitate thereafter muS110 induced activation of naive T cells, for example by providing co-stimuli like IL-2. It was published for MT103, a human CD19 specific BiTE, that CD8⁺ memory CTLs were most potent with MT103, whereas sorted naive T cells, positive for CD45RA, were not able to mediate redirected lysis (64). Carefully performed analysis of activation kinetics can finally address this question for muS110.

For concentrations below 1 µg/ml muS110-induced T cell activation was strictly dependent on the presence of EpCAM⁺ target cells. Additionally, no up-regulation of the most sensitive marker CD69 was observed in the absence of appropriate target cells for the control BiTE muMEC14. However, in contrast to the human system, higher doses of muS110 or muMEC14 were able to induce a slight T cell activation independent of a second binding partner (79). This loss of strict target cell dependency might be a direct consequence of higher affinity of mouse BiTEs to CD3ε, resulting in a higher receptor occupancy at used concentrations. The

potency of CD3-mediated activation is defined by receptor cross-linking, assembly of an immunological synapse and frequency of receptor occupation over time (122). At the highest BiTE concentration used in cytotoxicity assays roughly 90% of mouse CD3 receptors but only 15% of human CD3 receptors were occupied by the respective BiTEs (Figure 36)

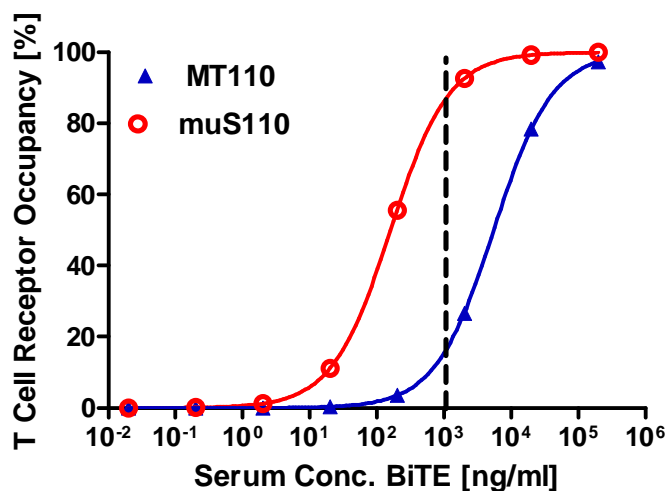


Figure 36: Comparison of CD3 occupation for muS110 and MT110.

At the highest concentration used in cytotoxicity assays roughly 90% of mouse CD3 receptors but only 15% of human CD3 receptors were occupied. Based on the equation $F = \frac{[mAb]}{[mAb] + KD}$, the fraction (F) of all receptor molecules that are bound to the respective ligand was calculated for both, MT110 and the human CD3 ϵ target and muS110 and the mouse CD3 ϵ target. The T cell receptor occupancy was plotted against the various BiTE concentrations. The dashed line indicates the highest concentration used in cytotoxic assays.

Triggering of almost all CD3 receptors of a T cell at once might induce a signal sufficient to overcome the need for a second binding partner, which is observed analogous with high doses of anti-CD3 antibodies in the absence of co-stimulatory signals (123, 124). *In vivo*, target cell independent activation might be of minor importance. T cell activation induced by the control BiTE was of minor strength and only a small fraction of T cells was affected. Additionally, the c_{max} of the highest applied single dose, ~ 200 ng/ml, was not enough to saturate the CD3 antigen.

6.2 MuS110 as murine surrogate of MT110

MT110 uses a systemic immunotherapeutic approach against EpCAM⁺ tumor cells. Acute pancreas toxicity was induced by two other EpCAM-specific, monoclonal antibodies tested in clinical phase I studies, suggesting accessibility of EpCAM on normal pancreas tissue to these antibodies (50, 125). Two other anti-EpCAM antibodies showed good tolerability in man, suggesting differences in EpCAM antigen recognition by the various antibodies (126, 127).

Thus, it was mandatory to evaluate potential damage to EpCAM positive tissue by MT110. However, cross-reactivity was only found with chimpanzee. Consequently, the mouse specific surrogate muS110 was developed, to establish a pre-clinical model in an immune-competent host with a similar EpCAM distribution as in human.

Two premises were analyzed to validate the surrogate approach. First, similar EpCAM expression in mouse and man, as significant differences in target expression would have limited the use of mice as a toxicological test species; second, comparability of *in vitro* properties of MT110 and muS110.

Prior to this work the tissue distribution of EpCAM in mouse and human was analyzed in a histo-pathological study. In both species, EpCAM staining patterns were largely confined to the cell surface, showed no difference with respect to polarized expression on epithelial cells, and stained a similar proportion of cells in tissues. In particular pancreas, a critical organ for toxicity of anti-EpCAM antibodies, showed comparable EpCAM expression in man and mouse. Differences in EpCAM expression between man and mouse were noted for adrenal gland and testis tissues, which were positive in human but not in mouse tissue samples. However, a key difference was EpCAM expression on 2-4% of mouse lymphocytes, which was not seen on human lymphocytes. As reported for the B cell-specific BiTE antibody MT103 in chimpanzee, the immediate encounter of T cells and B target cells in blood can cause transient cytokine release by MT103 (128). The toxicity of a BiTE targeting only localized EpCAM antigen in tumor tissue might be less pronounced. Thus, the presence of easily accessible EpCAM⁺ lymphocytes in mice may rather enhance the toxicity profile of muS110 in relation to MT110. However, only a careful dose escalation clinical phase I study will ultimately determine the tolerability of MT110 in humans.

MuS110 was constructed to yield structural, biochemical and biological characteristics similar to those of MT110. But after all, distinct antibodies had to be used for generation of muS110 and MT110, and the comparison of the two BiTE antibodies was hampered by the use of different effector and target cells, and species differences.

The binding affinity to EpCAM was comparable for muS110 and MT110 (21 +/- 2.6 nM to 13 +/- 0.25 nM). Epitope mapping showed that MT110 bound to the same sub-domain of human EpCAM as muS110 in mouse EpCAM. Most probably only a glycine residue in position 44 and a leucine residue in position 40 of mouse EpCAM, which are absent in the human protein, prevent cross-reactivity of MT110 to the mouse protein (Amann et al., in press). How-

ever, the binding affinity to the CD3 antigen was about 35 times stronger for muS110 than for MT110 (2.9 +/- 0.4 nM to 100 +/-15 nM; (85)). Thus, MT110 binds preferably to the tumor antigen, turning the cell surface into a T cell activating matrix before it recruits T cells. MuS110 binds more likely first to T cells and enables these cells to specifically bind to antigen positive tumor cells.

Activation of their respective effector cells was highly comparable for both BiTEs. MT110 and muS110 induced proliferation of T cells, up-regulation of activation markers like CD69 and CD25, induction of granzyme B positive cytotoxic T cells, release of the same cytokines, and finally elimination of antigen positive target cells *in vitro* (79). For both BiTEs the half maximal kill of CHO cells transfected with the respective target antigen was comparable, namely for MT110 in the human system 0.65 +/- 0.5 ng/ml (n=5) and for muS110 in the mouse system 2.51 +/- 1.2 ng/ml (n=10) (85). The amplitude of specific lysis was less pronounced in the mouse than in the human setting. Both BiTEs were restricted to the presence of target cells expressing the respective EpCAM, to elicit full T cell activation, although high doses of mouse control BiTEs mediated weak activation of T cells in the absence of appropriate target cells as well. Human specific BiTEs never showed unspecific T cell activation (79).

While higher CD3 affinity may have increased the risk of non-conditional T cell activation by muS110, it apparently did not positively affect the potency of redirected lysis by muS110. If anything, MT110 was more potent with human T cells than muS110 with mouse splenocytes in redirected lysis of human or mouse EpCAM-expressing CHO target cells, respectively (79, 85).

Taken together, the surrogate approach might lead to an overestimation of MT110 toxicity and an underestimation of its potency. Therefore, it was considered to be safely applicable despite differences between host species and drug candidates.

6.3 The therapeutic window of muS110

6.3.1 First dose response to muS110

MuS110 induced a dose dependent onset of side effects including hemoconcentration, hypomotility, piloerection, body weight reduction, hypothermia, gastrointestinal symptoms and diarrhea up to 24 hours after injection. Most probably these adverse side effects of muS110 were caused by a transient release of inflammatory cytokines through systemically activated T cells.

T cells in blood, spleen and various lymph nodes were found to newly express activation markers CD69 and CD25 in response to muS110 injections. Simultaneously, the serum levels of several inflammatory cytokines, e.g. IL-2, IFN- γ , TNF- α , IL-4, IL-6 and IL-10, increased shortly after injection of muS110. Most cytokine concentrations peaked after 2 hours and were back to baseline level after 24 hours. Serum cytokine peak levels as well as kinetics seemed to coincide with the intensity and the course of clinical symptoms observed at different dose levels. Glucocorticoids reduced T cell activation and cytokine release, which in turn considerably increased the tolerability of muS110 for mice.

The systemic T cell activation was accompanied by a fast and profound peripheral lymphocytopenia for up to 48 hours. This might have been due to activation induced upregulation of adhesion molecules like CD44. Anti-CD3 mAbs are known to induce peripheral lymphocytopenia in mice as well (102). The release of certain cytokines, like IL-2 and TNF- α , may foster lymphocyte adhesion and migration further (129, 130).

All observed clinical signs were described previously in mice in response to agonistic anti-CD3 monoclonal antibodies or direct administration of inflammatory cytokines (97, 98, 101, 131-135). The anti-CD3-induced acute syndrome is likewise caused by polyclonal activated T cells, releasing cytokines in the circulation. Activation of the complement system and Fc receptor-bearing accessory cells plays here an additional role. The increasing systemic levels of pro-inflammatory cytokines like TNF- α , IFN- γ , IL-2, IL-6 and IL-3 resulted in similar acute but transient systemic symptoms like hypothermia, hypoglycemia, hypomotility, piloerection, diarrhea and hypotension, neutrophil activation, activation of coagulation and fibrinolysis, which resembles altogether a septic shock (136-138). A pneumonia-like picture, including inflammatory cell infiltration, diffuse vascular congestion and even thrombosis was observed in the lung. Cell vacuolization, cell necrosis and vascular congestion were the rule in the liver. Doses exceeding 2.5 mg/kg were associated with high mortality (101).

The effects induced by 50 μ g/kg muS110 and 5 mg/kg of the anti-CD3 antibodies clone 145-2C11 or KT3 were comparable. The onset of side effects, T cell activation and cytokine release was delayed for two hours using conventional antibodies but all symptoms were otherwise of similar quality. The delay might reflect the dependence of anti-CD3 mAbs on the interaction of Fc-part with Fc-receptors on accessory cells to fully evolve their activating potential (104-108). The expression of these receptors is up-regulated by T cell-released cyto-

kines, is therefore self energizing but needs time to evolve. MuS110 in contrast needs only the presence of EpCAM positive target cells to develop its full activating potential.

These evidences suggest that the high T cell activating potential of muS110 might also be the reason for its dose limiting toxicity in mice. Doses higher than 100 µg/kg muS110 were lethal within 24 hours. The maximum tolerated dose (MTD) of muS110 in mice was 50 µg/kg muS110. Doses of 10 µg/kg muS110 were determined as no observed adverse effect level (NOAEL).

Clinically, glucocorticoids are used to reduce the adverse effects of the anti-CD3-induced acute syndrome (99). Glucocorticoids hamper cell-mediated immunity by reduction of T cell proliferation and activation, down-regulation of adhesion molecules and induction of glucocorticoid induced apoptosis (139). This class of anti-inflammatory and immune-suppressive steroid hormones is characterized by the ability to bind to the cytosolic glucocorticoid receptor and is used to suppress various allergic, inflammatory and autoimmune disorders. The formed receptor-ligand complex translocates in the cell nucleus. There it can either trigger transactivation of target genes containing glucocorticoid response elements, or interact with specific transcription factors like AP-1, NF-AT or NF-κB resulting in transrepression of their targeted genes. Additionally corticosteroids act at a posttranscriptional level by suppressing the cytokine protein synthesis (140). Suppressed genes are that coding for various cytokines like IL-1, IL-2, IL-3, IL-4, IL-5, IL-6, IL-8, IL-12, TNF-α, GM-CSF and IFN-γ (141).

High doses mPDS (50 mg/kg) given 1-3 hours before injection of the anti-mouse CD3 mAb 145-2C11 decreased the systemic release of IFN-γ, TNF-α, IL-2 and IL-6 and significantly reduced mortality, hypothermia, diarrhea, nephrotoxicity and other lesions induced to lymph nodes and kidneys (99). Likewise, co-administration of dexamethasone and mPDS, respectively, enhanced tolerability of muS110 by a similar mechanism. However, BiTE mediated target cell lysis was not decreased. Therefore glucocorticoids can be used in clinical settings to prevent putative BiTE induced adverse effects.

Mouse EpCAM positive target cells as second binding partner were mandatory to elicit a profound T cell activation with muS110 *in vitro*. Administration of the control BiTEs hyS110 or muMEC14, which share the anti-CD3 binding moiety of muS110 but lack specificity for a second mouse specific protein, were well tolerated. Thus, side effects of muS110 related to systemic T cell activation had to rely on a bispecific binding of the BiTE antibody to both, CD3 on T cells and to EpCAM on an easy accessible binding partner. Appearance of CD8⁺

CTLs after muS110 treatment *in vivo* indicated that target cells most probably would be eliminated over time by redirected lysis. One possible target could have been epithelial cells, which frequently and highly express EpCAM in mice. However, histo-pathological analysis of mice daily dosed with muS110 doses up to 100 µg/kg/day for 35 days revealed no evidence for lesions in normal tissues expressing the EpCAM target antigen. Essentially, all histo-pathological findings noted with EpCAM⁺ tissues in 30 muS110-treated animals were observed at a similar frequency in the 32 vehicle control animals. Absence of any significant damage of normal EpCAM-expressing epithelia suggests that EpCAM on normal epithelial tissues was not accessible to muS110-redirectioned T cells.

A number of recent studies have shown that EpCAM on normal epithelial cells is in complex with other proteins in the plasma membrane within so-called tetraspanin webs. Protein partners of EpCAM include tetraspanins CD9 and 14.1, claudin 7 and CD44 (12, 44, 142). These protein-protein interactions may reduce the accessibility of EpCAM on the surface of normal tissue and leave only a few epitopes for recognition by antibodies. Upon neoplastic transformation, EpCAM can be over-expressed on certain tumor cells, which may overcome sequestration by certain protein partners. Likewise, free EpCAM may arise from loss of protein partners or *de novo* expression during transformation, as has been reported for CD9 (143). Accessibility of EpCAM-expressing cells to both, antibodies and immune effector cells may further increase upon degradation of extracellular matrix by tumor cell-derived proteases, and by loss of tight junctions in tumor tissue. In support for a sequestration of EpCAM in normal epithelia, immunohistochemical studies showed that EpCAM is concentrated within intercellular boundaries, while it is evenly distributed on the surface of tumor cells (144).

There may in fact be three levels contributing to a differential recognition of EpCAM. First, a molecular level, where accessibility of certain EpCAM epitopes is controlled by protein partners, second, a cellular level, where EpCAM is sequestered at least in part by its sub-cellular distribution within highly structured normal epithelium, and third, a tissue level, where access of immune effector cells to epithelium is diminished by intact extracellular matrix. Future research is required to investigate these various possibilities and determine their contribution to a therapeutic window as seen with some, but not all EpCAM-directed therapeutic approaches.

It is thus conceivable that EpCAM on cells of structurally sound epithelia was either not bound by BiTE antibody, or that cell-bound BiTE antibody had no reach to local T cells because a close contact to them was hampered by extracellular matrix, basal membranes, tight

junctions, and other mechanical barriers. On the other hand, the proteolytic environment and disorder of cancer cells in tumor tissue may give both, BiTE antibodies and T cells, much improved access to EpCAM⁺ target cells. The observation that even high doses of muS110 apparently did not elicit detectable damage to normal epithelia in a mouse model, may indicate that certain EpCAM-specific BiTE antibodies can have a robust therapeutic window for treatment of cancer (112). The finding that muS110 and MT110 bound their respective EpCAM proteins with the same affinity and in the same sub-domain suggests that the safety data obtained with muS110 in mice regarding the EpCAM target toxicity may have predictive value for MT110 in humans (Amann et al. in press).

However, a low percentage of mouse lymphocytes were found that express EpCAM. These were mostly peripheral B cells and to a lesser extent T cells. EpCAM expression on mouse lymphoid cells has been noted earlier but thus far only dendritic cells, plasma cells, thymocytes and thymic epithelial cells were reported to express EpCAM (46, 145, 146). Unlike in healthy EpCAM⁺ tissue repeated muS110 treatment resulted in a reduction of EpCAM⁺ lymphocytes. Moreover, reduction of EpCAM⁺ B and T cells in peripheral blood samples via redirected lysis *in vivo* or by column/ FACS removal *ex vivo* significantly reduced T cell activation by muS110. A human cell culture system allowed demonstration that addition of only 2% EpCAM⁺ cells triggered T cell activation and cytokine release by MT110, which was comparable in intensity to what has been observed with muS110 in the mouse cell culture system. Of note, MT110 did not induce any T cell activation in human blood samples, unless EpCAM⁺ cells were added. Together, these findings support the notion that muS110-mediated activation of T cells was triggered by EpCAM⁺ lymphocytes in blood and lymphoid organs of mice, and may have been responsible for the acute side effects seen after injection of muS110.

MuS110 could well discriminate between EpCAM found exposed on circulating lymphocytes and the EpCAM embedded in normal epithelial tissues. The absence of any significant damage to normal EpCAM-expressing epithelia by muS110-redirectioned T cells in mice treated with very high doses of muS110 suggests that EpCAM⁺ solid epithelial tissues in mice could not substitute for EpCAM⁺ lymphocytes for activation of T cells in the presence of BiTE antibody muS110. This is in contrast to EpCAM on tumor cells where anti-tumor activity was already evident in mice at doses as low as 2 µg/kg muS110 (85). Should the human EpCAM-specific BiTE antibody MT110 likewise make this distinction, it may have a larger therapeutic window than muS110 in mice. In humans EpCAM⁺ lymphocytes are largely absent. T cells may

only be locally activated if they encounter MT110 that is bound to accessible EpCAM antigen on tumor cells.

6.3.2 Adaptation to repeated injections of muS110

At the beginning, consecutive muS110 administrations slightly intensified the first dose symptoms, as the onset was faster and the duration was longer. However, animals after the fourth muS110 injection tolerated subsequent ones well, even at doses normally lethal when given only once. Thus, dose-dependent side effects were self-limiting and animals adapted to repetitive treatment with muS110.

The cytokine release was also self-limiting and, with the exception of IL-10, much reduced after the second and third injection of muS110. No further cytokine release was detectable after the fourth to seventh injection. Especially the disappearance of IFN- γ , TNF- α and IL-6, known to be the central figures of the cytokine release syndrome, could explain the observed decline of symptoms despite ongoing medication.

One explanation for the transient nature of muS110 induced side effects might be their dependency on EpCAM⁺ lymphocytes. The activating stimulus would decrease gradually by progressive elimination of EpCAM⁺ lymphocytes. As the magnitude of cytokine release correlated with the amount of target cells present, the systemic cytokine secretion would decrease as well. This would in turn result in a reduction of adverse symptoms and recovery from the systemic T cell response. Persistent side effects could be due to a limited T cell activation triggered by the remaining 0.5% EpCAM⁺ lymphocytes, consistent with the *in vitro* data obtained with EpCAM depleted T cells.

However, the immune-suppressive cytokine IL-10 behaved different from all other cytokines in response to a first and second high-dose challenge with muS110 after muS110 mediated eradication of EpCAM⁺ lymphocytes. IL-10 serum concentrations were not decreased but strongly elevated 2 hours after the first high-dose challenge of animals pre-treated with 10 $\mu\text{g}/\text{kg}/\text{day}$ muS110. Induction of IL-10 was not as pronounced in animals pretreated with 2 and 0.4 $\mu\text{g}/\text{kg}/\text{day}$ muS110, respectively. Thus, IL-10 serum levels correlated with the protection from side effects elicited by muS110 challenge. This counter wise behavior of IL-10 was also observed throughout muS110 dose escalation in an efficacy model. The persistent elevation of serum IL-10 concentrations ruled against a mere depletion of EpCAM⁺ target cells as sole cause for increased tolerability, which should have affected all cytokines in a similar way.

Adaptation to repeated anti-CD3 stimulation was also described after the use of anti-CD3 antibodies 145-2C11 and KT3. The cytokine induced syndrome was only observed after the first injections and spontaneously reversible after 2-3 days (101). The initial systemic hyper-activation of the immune system was followed by an immunosuppression. The immunosuppressive abilities of anti-CD3 antibodies are in fact used to prevent and treat allograft rejection or type I diabetes (114).

Our immune system evolved excessive control loops to limit self-damage by its necessarily harsh effector functions and to prevent hyper-activation of the immune system. Some of these mechanisms mediate immunosuppression after administration of anti-CD3 antibodies as well. First, a general short term immunosuppression after anti-CD3 stimulation is partly a result of activation induced down-modulation of the CD3 – TCR surface complex impairing alloantigen induced T cell activation by APCs (109). This down-regulation is completely reversed nine days after a single administration of 145-2C11 (100). Second, a transient depletion of T cells from the peripheral lymphoid organs and the blood can persist for several weeks after a single administration of 145-2C11 and decreases immune functions furthermore (147-150). This lymphocytopenia is resultant from increased adhesiveness of T cells to the vascular epithelium and lysis of antibody-opsonized T cells. A third mechanisms adding to the immunosuppressed state is anergy of the remaining T cells, characterized by diminished capacity to produce IL-2 and proliferate upon re-stimulation *ex vivo* (147-150). Treatment with the anti-mouse CD3 mAb 145-2C11 additionally results in selective inhibition of TH₁- type cytokine secretion upon *in vivo* and *in vitro* re-stimulation, whereas the production of TH₂-type cytokines, e.g. IL-4 is not altered and that of anti-inflammatory cytokines like IL-10 and TGF- β is even boosted (100).

However, short term treatment with anti-CD3 specific antibodies also elicits long term operational tolerance in transplantation and autoimmunity (114). This permanent and active antigen specific unresponsiveness is most probably due to selective expansion and activation of TGF- β dependent regulatory T cells that control pathogenic T cells (151). A consecutive five day treatment with anti-CD3 mAb induced a complete remission of overt diabetes. Belghith et al. showed that TGF- β played a central role in this restoration of peripheral T cell tolerance to pancreatic islet cells. First, the anti-CD3 mAb induced remission was suppressed by administration of a neutralizing anti-TGF- β antibody. Second, isolated CD4⁺ T cells of actively tolerized mice produced TGF- β but hardly other cytokines after *in vitro* re-challenge. The peripheral tolerance was mediated by CD4⁺CD25⁺⁺ regulatory T cells, which were particularly

enriched in the draining pancreatic lymph nodes of tolerized mice (151). Interestingly, no rise in systemic TGF- β levels were found, which stresses the compartmentalization of the tolerance phenomenon (114). However, it was also shown that depletion of T_{reg} and usage of anti-TGF- β antibodies could not totally abrogate immune tolerance suggesting a further, maybe T cell intrinsic level of activation regulation (152).

Chautenaud L. hypothesized that the tolerogenic capacity of anti-CD3 mAbs may develop in two consecutive phases: First, systemic, complete blockade of the pathogenic immune response by T cell depletion, down-modulation of the TCR/ CD3 complex and immune deviation to TH₂ immune response; second, expansion and activation of TGF- β and IL-10 dependent regulatory cells, acting in a more spatially ruled way. Thereby the TH₁ subset is more rendered to anergy whereas the TH₂ cells show proliferation and IL-4 production (153).

Unlike bivalent anti-CD3 mAbs, muS110 treatment did not significantly down-regulate the CD3 antigen on T cells (111). However, it resulted in a transient, peripheral T cell lymphocytopenia. T cell depletion by anti-CD3 antibodies relies on the presence of the Fc part induced complement depending cytotoxicity (CDC) or antibody dependent cell-mediated cytotoxicity (ADCC), which are not mediated by BiTEs. In some cases redirected T cells obtained the BiTE specific antigen from the surface of target cell due to the close cell contact (data not shown) and thus become a target to redirected lysis by themselves. But this concerned only for a very small fraction of T cells. Upregulation of adhesion markers like CD44 on the other hand, was found on more than 80% of all CD8⁺ T cells after a 7 day treatment with muS110. The onset of the observed lymphocytopenia was very fast, so almost all T cells vanished within 2 hours after injection. But unlike after a single dose of 145-2C11, where lymphocytopenia lasted for several weeks, blood T cell numbers were back to baseline level within 48 hours after a single dose of muS110 (100). Total number of CD8⁺ splenocytes was not decreased and the size of all dissected lymph nodes after muS110 treatment even increased (data not shown). Thus, the observed lymphocytopenia was most probably not a result of T cell depletion but redistribution of these cells.

No deviation towards a TH₂ cytokine pattern but a complete suppression of all analyzed cytokines was observed after repeated muS110 treatment. This was partly caused by elimination of EpCAM⁺ target cells and the induced lymphocytopenia. However, the coincidental occurrence of high levels of immunosuppressive IL-10 evidenced another immune regulatory process.

IL-10, also described as a “cytokine synthesis inhibitory factor”, is an anti-inflammatory cytokine and has pleiotropic effects in immune regulation and inflammation (113). It down-regulates the expression of TH₁ cytokines IL-2 and IFN- γ , that of IL-3, TNF- α and GM-CSF. Treatment with the humanized, FcR non-binding anti-CD3 antibody kOKt3yl (Ala-Ala) induced a mild cytokine release syndrome with stronger IL-10 release in ratio to IFN- γ -levels. It increased CD4⁺CD25⁺FoxP3⁺ regulatory T cells numbers, the CD8⁺/CD4⁺ ratio and induced a sub-population of IL-10 secreting CD4⁺ T cells, expressing high levels of surface TGF- β and IL-10, which resembled Tr1 regulatory T cells (115).

Significantly elevated levels of CD4⁺CD25⁺FoxP3⁺ regulatory T cells in splenocytes (10% to 6% of CD4⁺ cells) and a significantly higher CD8⁺/CD4⁺ ratio in blood were also found after muS110 treatment. Together with the prominent appearance of IL-10, this might indicate a similar immune regulatory mechanism for adaptation to repeated muS110 than to kOKt3yl (Ala-Ala) administration. On the other side, no evidence for involvement of TGF- β , which is an important mediator of T cell suppression, was found after muS110 treatment *in vivo* or upon *ex vivo* re-challenges.

T cell activation in the presence of IL-10 can render T cells hypo-responsive, which is observed after administration of 145-2C11. T cell anergy describes a state in which lymphocytes are intrinsically functionally inactivated following an antigen encounter, but remain alive for an extended time in a hypo-responsive state. Functional limitations might occur in cell proliferation, cell differentiation, effector functions and cytokine production (116). There are two main categories of anergy. First, clonal anergy, which develops after incomplete T cell activation mainly in already previously activated T cells. This is an IL-2 reversible growth arrest state and needs no antigen persistence. Second, adaptive tolerance, which arises mostly after stimulation of naive T cells in an environment with high co-inhibition or no co-stimulation, and is not IL-2 reversible. During antigen encounter proliferation and differentiation happens to varying degrees, which is followed by down-regulation of activities (e.g. proliferation, secretion of IL-2, IFN- γ , IL-4) to varying degrees in the face of persistent antigen (116).

Redirected lysis by muS110 *in vivo* involved repeated TCR signaling in the absence of co-stimuli. Almost complete elimination of EpCAM⁺ lymphocytes abrogated the second binding partner in healthy mice over time and T cell activation took place in the presence of high IL-10 concentrations. Hence, reduction of systemic cytokine levels after repeated administration of muS110 could have been a consequence of T cells anergy, possibly imposed by regulatory

T cells. However, under all conditions tested, T cells from low-dose adapted mice were as competent as T cells from untreated mice with respect to proliferation, redirected lysis, and responsiveness to either muS110 (re)stimulation or classical T cell stimuli. Presence or absence of IL-2 did not seem to affect T cell activity. Additionally, potentially induced regulatory T cells were present in all assays used to characterize T cells from adapted mice and hence, should have been able to exert their negative regulatory effects. Therefore, low-dose adaptation to muS110 was not the result of compromised effector functions of cytotoxic T cells.

However, all T cells from adapted mice showed an impaired ability for cytokine secretion upon *in vitro* re-stimulation, which was normalized one week after end of muS110 dosing. Even in the face of a full T cell activating stimulus, T cells from adapted animals did hardly produce cytokines in comparison to those of untreated animals. Additionally, they showed a synchronized, profound proliferation in absence of IL-2. This is in contrast to *in vitro* re-stimulation upon a challenge with anti-CD3 mAbs, where secretion of some cytokines, e.g. IL-4, can be even enhanced (154). Interestingly, T cells from low-dose adapted mice did not require production of inflammatory cytokines, to achieve the same potency of redirected lysis as T cells from vehicle treated mice. This supports the finding that lysis by BiTE-activated T cells depends on cytolytic synapse formation, but not on collateral effects of secreted cytotoxic cytokines or other death receptor ligands (82),(66, 155). Both CD4⁺ and CD8⁺ T cells could well proliferate during redirected lysis but at some point in time, again the ratio appeared to change in favor of CD8⁺ cells.

Taken together, muS110 induced a transient lymphocytopenia but most probably no T cell depletion, no down-regulation of the TCR/ CD3 complex, no immune deviation to TH₂ immune response and no anergy of T cells. However, it resulted in a transient, not IL-2 reversible block of cytokine secretion upon re-stimulation. *In vivo*, administration of muS110 induced a persistent release of IL-10, an expansion of CD4⁺CD25⁺FoxP3⁺ regulatory T cells in the spleen and an increase of the CD8⁺/CD4⁺ T cell ratio in the blood. This might be indicative for the involvement of regulatory cells, which, however, seemed to have no impact on muS110 mediated lysis of EpCAM⁺ target cell. These immune-modulating effects together with the elimination of EpCAM⁺ lymphocytes might be the reason of adaptation to repeated treatment with muS110.

How can such a difference of immunosuppression arise after anti-CD3 stimulation with anti-CD3 antibodies and the BiTE antibody, although their first dose response seemed to be so

similar? No satisfying answer to this question can be given at this point. The concrete differences in T cell activation have to be considered. The BiTE system solemnly relies on the presence of a second binding partner to elicit full T cell activation. The concrete physical properties of target or BiTE necessary to fully activate redirected T cells are not yet known. There seem to be a relation to clustering ability and distance to the cell surface. However, the pre-requisite to full T cell activation are well established for anti-CD3 antibodies.

In vitro, mitogenic activation of T cells by anti-CD3 mAbs is dependent on the interaction of the Fc- part with Fc-receptors (FcR) on accessory cells (152, 153, 156). The lower the affinity of the respective anti-CD3 antibody for FcR, the lower is the induced mitogenic activation and the better is the drug tolerated *in vivo* (IgG2a > IgG1 > IgG2b > IgG3 > IgA > F(ab)₂) (101, 104-108, 157). Full T cell activation could be restored for all formats by the supply of co-stimulatory signal, e.g. CD28 or IL-2 (101, 157). Enhanced *in vivo* T cell activation is caused either indirectly by the inclusion of further cytokine sources, like activated monocytes, and an enlargement of the addressed immune network, or directly by a different quality of the TCR transmitted signal in terms of co-stimuli and receptor clustering. Signals transmitted by the various anti-CD3 antibodies vary in terms of presented co-stimuli (e.g. CD28 on FcR-expressing cells), duration (e.g. terminated by CD3 down-regulation and antibody serum half life) and surface density (e.g. antibody cross-linking). The different quality of the activation signal is translated first, in varying strength of cellular Ca²⁺ influx and second, in varying quantity and quality of phosphorylation of adaptor proteins and receptor tyrosine kinases. All this different events work together to induce a special setting of T cell response in terms of proliferation, TCR down-regulation, activation marker up-regulation and cytokine release, which is in general similar for all anti-CD3 antibodies but subtly differs between the respective isotypes.

Administration of only the F(ab)₂ part of the 145-2C11 mAb for example resulted in down-modulation of the TCR complex but did not induce CD25 up-regulation, lymphokine secretion, T cell proliferation or hypothermia (98). This is thought to be due to the lack of multivalent cross-linking of the CD3 antigen, which impedes development of a functional immune synapse (111). The ability to systemically clear LCMV infection was not reduced after F(ab)₂ fragment administration, although this was observed after administration of intact 145-2C11, whereas protection from diabetes was mediated by both drugs (158). IL-2 secretion upon *in vitro* re-stimulation of T cells as well as *in vitro* CTL function was impaired after administration of both formats for several months. However, exogenous supplied IL-2 could rescue *in*

in vitro CTL function after application of the F(ab')₂ fragment, but not after that of intact mAb (156, 159). Negative effects upon T cell effector function were more prominent in CD4⁺ than in CD8⁺ T cells after application of the F(ab')₂ fragment, but, *vice versa* after administration of the intact anti-CD3 mAb. Therefore, the imposed immune suppression varied directly with the TCR activating signal (156).

Administration of a mAb against CD3, in which the high affinity IgG1 part was replaced by an IgG3 domain with reduced affinity to Fcγ receptors, showed similar results (152). Naive mouse T cells did not proliferate, produce IFN-γ or up-regulate surface activation marker in response to the IgG3 isotype. Administration resulted in immune tolerance and a reduction of TH₁ mediated immunity. No immune deviation from a TH₁ to a TH₂ dominated immune response took place as after injection of 145-2C11. All cytokine level were reduced in a similar way upon *in vitro* re-stimulation. Interestingly, lower binding affinity of the IgG3 isotype to monocytes translated in a less sound T cell anergy. T cells after *in vivo* anti-CD3 stimulation with IgG3 isotype were capable to proliferate and to secrete IL-2 upon *in vitro* re-stimulation. Such T cells *in vivo* stimulated with IgG1 or IgG2a isotypes were not (152).

Interesting results were obtained with CLBT3/4, a non FcR-binding CD3 mAb of the mouse IgA isotype. It induced a rise in intracellular Ca²⁺ levels in T cells comparable to that after anti-human OKT3 (IgG2a) stimulation, however, phosphorylation of LAT was only partly achieved. *In vitro*, it was not mitogenic, did not induce cytokine secretion but caused up-regulation of CD25 and CD69 and down-regulation of the CD3-TCR complex. After *in vivo* administration lymphocytopenia and cytokine release was observed, but T cells were not hypo-responsive after an *ex vivo* re-challenge (104, 157).

Taken together, the nature of secondary binding of anti-CD3 antibodies defines the balance between T cell activation versus suppression and controls thus the induced immune response. There seemed to be a correlation between high affinity of anti-CD3 antibodies to Fc-receptor-expressing cells, strong activation *in vivo* and following profound hyporesponsiveness of T cells to an *ex vivo* re-challenge. The lower the binding to Fc-receptor-expressing cells was during *in vivo* challenge, the lower was the anergic impact on TH₁ cells and CTL after a re-challenge (104, 157). This was not true for antigen specific operational tolerance, which was always imposed independently of the used anti-CD3 antibody format (114). MuS110 induced a new combination of T cell response to CD3 stimulation, as it fully activated T cells but imposed no T cell anergy, which ensures the best anticipated anti-tumor efficacy (Table 8).

Table 8: Effects of different anti-CD3 antibody formats (98), (101, 104-108, 157) (111, 114, 152, 153, 156, 159)

	Format	IgG2a	IgG1	IgG3	F'(ab) ₂	IgA	muS110
In vitro	Mitogenicity	+	+				+
	Cytokine secretion	+	+				+
In Vivo	Down-regulation of CD3-TCR	+	+	+	+	+	
	Up-regulation of CD69/ CD25	+	+			+	+
	Cytokine secretion	+	+			+	+
	Deviation to Th2 cytokine profile	+	+				
	Extra-medullary hematopoiesis	+	+				+
	Operational tolerance	+	+	+	+	+	?
Ex Vivo	T cell hypo-responsiveness	+	+	(+)	+		
	IL-2 reversible hypo-responsiveness			+	+	----	----
	Impaired secretion of all cytokines			+	+	?	+

6.3.3 Efficacy

This unique ability of muS110 was implemented in a special escalating dose-schedule to improve its efficacy. Anti-tumor activity of muS110 was observed at constant doses as low as 2 µg/kg/day. However, the strongest effect was seen in intra-animal dose escalation experiments with a 99% reduction of tumor burden in comparison to untreated control animals, whereby tumor growth was still completely prevented in 5 out of 6 animals 17 days after treatment stop. Only minor side effects, like a small reduction of body weight, were observed despite this high anti-tumor activity.

Co-treatment with a glucocorticoid might be a possibility to even enhance this dose schedule. Glucocorticoids were shown to reduce muS110-induced adverse effects but not BiTE mediated tumor cell lysis (160). Thus, the dose escalation could already start with higher doses of muS110, controlling its adverse effects with mPDS co-treatment at the initial days. As it was shown that mPDS does not hinder adaptation to muS110, BiTE doses can be escalated there-

after. Increased starting dose of this putative model could result in improved anti-tumor efficacy.

The surrogate approach suffered from the presence of EpCAM⁺ lymphocytes in the mouse system, which are absent in the human system. These cells are most probably responsible for the cytokine induced syndrome minimizing the therapeutic window of muS110. On the other hand, their elimination demonstrated discrimination of muS110 between EpCAM found exposed on circulating lymphocytes (or in tumors) and EpCAM embedded in normal epithelial tissues. Should the human EpCAM-specific BiTE antibody MT110 likewise make this distinction, it may have a larger therapeutic window than muS110 in mice. T cells may only be locally activated if they encounter MT110 that is bound to accessible EpCAM antigen on tumor cells. MT110 and muS110 binding to orthologous epitopes might facilitate this possibility (Amann et al., in press).

Glucocorticoid treatment and low dose muS110 adaptation allows the administration of higher BiTE doses without reducing its potency and enlarge therefore the therapeutic window of muS110. Higher doses of muS110 show an exceptionally good efficacy against solid 4T1 tumor, being almost completely able to prevent the outgrowth of these rapid and aggressive tumors. This might more closely resemble the therapeutic window to be expected of MT110 in humans and would promise high clinical potential. Nevertheless, BiTEs address with CD3ε a central protein in the immune response, might induce various cytokines and represent a new technology based on genetic engineering. Thus, MT110 has to be classified as high risk antibody and starting doses for clinical trials will therefore rely not on the NOAEL level, observed in pre-clinical animal models, but on the minimum anticipated biological effect level (MABEL), determined in *in vitro* experiments (161).

7 ABBREVIATIONS

Term or Abbreviation	Description
aa	Amino acid
ADCC	Antibody Dependent Cell-mediated Cytotoxicity
ADP	Adenosindiphosphate
AK	Adenylate Kinase
ATP	Adenosintriphosphate
BiTE	Bispecific T Cell Engager
BSA	Bovine Serum Albumine
CAM	Cell Adhesion Molecule
CBA	Cytometric Bead Array
CD	Cluster of Differentiation
CD3	Part of the T cell receptor, required for signal transduction by the TCR
CD4	Co-receptor for MHC class II, marker for helper T cells
CD8a	Co-receptor for MHC class I, marker for cytotoxic T cells
CD11b	Marker for myeloid and NK cells, subunit of the integrin CR3
CD11c	Marker for myeloid cells, subunit of the integrin CR4
CD16	Fc γ receptor III on neutrophils, NK cells and myeloid cells
CD19	Pan B cells marker
CD25	IL-2 receptor α chain, up-regulated during T cell activation
CD28	Receptor for co-stimulatory signals on T cells, binds to CD80/ 86
CD44	Binds hyaluronic acid and mediates adhesion of leukocytes, upregulated upon T cell activation
CD45	Leukocyte marker
CD45R/B220	Isoform of CD45 on B cells
CD49b	Marker of mouse NK cells, α 2 integrin
CD56	Isoform of neural cell adhesion molecule on NK cells
CD62L	Leukocyte adhesion molecule, mediates rolling interaction with endothelium
CD69	Early activation antigen on macrophages, T, B and NK cells
CD80	Co-stimulator, ligand for CD152 and CD28 on B cells

Term or Abbreviation	Description
CD86	Co-stimulator, ligand for CD152 and CD28 on monocytes, activated B cells and dendritic cells
CD134	Marker of T cell activation, may act as adhesion molecule costimulator, also known as Ox40
CD152	Marker of T cell activation, negative regulator, receptor of CD80 and CD86, also known as CTLA-4
CDC	Complement Dependent Cytotoxicity
CFSE	Carboxy-Fluorescein diacetate, Succinimidyl Ester
CHO	Chinese Hamster Ovary
CT	Cytotox
CTL	Cytotoxic T Lymphocytes
dHFR	diHydro Folate Reductase
DNA	Desoxyribo Nucleic Acid
EC ₅₀	Drug concentration where the half maximal effect is observed
EDTA	Etylenedinitrotetraaceticacid
E -FABP	Epidermal Fatty Acid Binding Protein
EGF	Epidermal Growth Factor
EM	Extracellular Matrix
EpCAM	Epithelial Cell Adhesion Molecule or Epithelial Cell Activating Molecule
E:T	Effector to Target
ELISA	Enzyme Linked Immuno Sorbent Assay
FACS	Fluorescence Activated Cell Sorting
Fc	Constant Fragment of an Antibody
FcR	Fc Receptor
FCS	Fetal Calf Serum
F	Fraction
GMCSF	Granulocyte Macrophage Colony Stimulating Factor
hu	Human
Ig	Immunoglobulin
ICAM-1	IntraCellular Adhesion Molecule -1
IFN	Interferon

Term or Abbreviation	Description
IL	Interleukin
i.p.	Intraperitoneal
i.v.	Intravenous
mAb	Monoclonal Antibody
Lck	Leukocyte specific protein tyrosine kinase
LFA	Leukocyte Functional Antigen
LN _{mes}	Lymph Node <i>mesenteriales</i> ,
LN _{ing}	Lymph Node <i>inguinalis superficialis</i>
LN _{cer}	Lymph Node <i>cervicales</i>
MDC	Myeloid Derived Cells (summarizes all bone marrow derived cells that are not lymphocytes)
MABEL	Minimal Anticipated Biological Effect Level
MHC	Major Histocompatibility Complex
mPDS	Methyl-Prednisolone
mu	Murine
MSD	Meso Scale Discovery
MTD	Maximal Tolerated Dose
MTX	Methotrexate
NEA	Non Essential Amino Acids
NFκB	Nuclear Factor kappa B
NK	Natural Killer
NOAEL	No Observed Adverse Effect Level
PBMC	Peripheral Blood Mononuclear Cells
PBS	Phosphate buffered Saline
PE	Phycoerythrin
PI	Propidium Iodide
Pi3K	Phosphatidylinositol 3 Kinase
PKC	Phosphokinase C
PM	Plasmamembrane
PMA	Phorbol Myristate Acetate
KD	Dissociation Constant

Term or Abbreviation	Description
rhuIL-2	Recombinant human IL-2
RT	Room Temperature
s.c.	Subcutaneous
scFv	Single-chain antibody Fragments variable
SEM	Standard Error of the Mean
siRNA	Small interfering RiboNucleid Acid
SP	Signal Peptide
T _{Naïve/CM}	Naïve or Central Memory T cell (CD62L ⁺ CD127 ⁺)
T _{Int}	Intermediate T cell (CD62L ⁺ CD127 ⁻)
T _{Eff}	Effector T cell (CD62L ⁻ CD127 ⁻)
T _{EM}	Effector Memory T cell (CD62L ⁺ CD127 ⁺)
TCR	T Cell Receptor
TGF-β	Tumor Growth Factor β
TH ₁ or TH ₂	Helper Cell Type 1 or Helper Cell Type 2
TM	Transmembrane
TNF	Tumor Necrosis Factor
TY	Thyroglobulin
V _H or V _L	Variable domains of the Heavy or Light chain

8 ACKNOWLEDGEMENTS

I want to thank the department of bioanalytics for the analysis of BiTE serum concentrations and Grit Lowreczewski for pharmacokinetical calculations. Thanks to the department of BiTE research to provide all used transfected cell lines and BiTE antibodies.

Ich möchte diese Arbeit meiner Großmutter widmen, die in der Zeit meiner Doktorarbeit unheilbar an AML erkrankte und leider deren Fertigstellung nicht mehr miterleben durfte. Drastisch wurde mir vor Augen geführt, wie unendlich wichtig es ist, nicht nur neue Medikamente gegen Krebs zu erfinden, sondern sie auch in den Alltag der Klinik zu bringen und ihre Anwendung so zu Gestalten, dass Patienten damit Leben und nicht nur Überleben können. Ich bin der Firma Micromet dankbar für die Möglichkeit, an der Entwicklung einer neuen Technologie gegen Krebs teilhaben zu können. Mit Stolz erfüllt es mich, MT110 mit auf seinen Weg in die Klinik gebracht zu haben, und so anderen Menschen in einer Situation zu helfen, in der ich selbst bei meiner Großmutter machtlos war.

Während der letzten Jahre hatte ich das Glück von Menschen betreut zu werden, die sich nicht nur durch fachliche, sondern auch durch soziale Kompetenz auszeichnen, und so ein ganz besonderes Arbeitsklima geschaffen haben. Ich danke Bernd und Petra dafür, dass sie mir gezeigt haben wie ein Vorgesetzter für seine Leute einstehen soll, Klaus dafür, dass er einer guten fachlichen Diskussion auch nicht einmal ansatzweise widerstehen kann und Matthias für sein Vertrauen und all die Freiräume, die er mir zugestanden hat. Patrick will ich nicht nur für die Herausforderungen danken, vor die er mich immer wieder stellte und die diese Jahre so spannend gemacht haben, sondern besonders dafür, dass er, wo immer es nötig und möglich war, tatsächlich auch ein Mentor war und mich gefördert hat. Danken will ich ebenfalls meinen Kollegen, namentlich Grit, Eva, Laetitia, Sandra, Sandrine, Annabelle, Susanne, Marco und Larissa, von denen ich vieles gelernt habe und die jederzeit bereit waren, mich zu unterstützen - sogar während meiner „Vormittags – Launen“.

Ein ganz besonderes Dankeschön gilt auch Frau Prof. Weiß und Frau Prof. Jungnickel, die es mir ermöglicht haben, an der LMU zu promovieren.

9 CURRICULUM VITAE

Address: Scheideggerstr. 31
81476 München
Germany
Phone: 0049 89 20342629
Mobile: 0049 179 7456869
Date of birth: 10.04.1980
Nationality: German

Education

6/2005 – 02/2009 Micromet AG, Munich, Germany

Ph.D. Study

Supervisor: Prof. Dr. Patrick Bäuerle

Project: “Primary and secondary pharmacology analyses of bispecific T cell engagers (BiTEs)”

10/1999 – 5/2005 **University of Regensburg, Germany**

Master Degree in Biology

Main subject: Cell biology

Minor subject: Genetics, Botany

Institute of cell biology and plant physiology

Diploma thesis

Supervisor: Prof. Dr. Widmar Tanner

Project: “Oligomerization of plasma membrane proteins of *S.cerevisiae* in connection with Lipid Raft-based protein distribution”

9/1991 – 7/1999 Veit Höser Gymnasium Bogen, Germany

Comprehensive secondary school

10 REFERENCES

1. Herlyn, M., Steplewski, Z., Herlyn, D., and Koprowski, H. Colorectal carcinoma-specific antigen: detection by means of monoclonal antibodies. *Proc Natl Acad Sci U S A*, *76*: 1438-1442, 1979.
2. Baeuerle, P. A. and Gires, O. EpCAM (CD326) finding its role in cancer. *Br J Cancer*, *96*: 417-423, 2007.
3. Sears, H. F., Herlyn, D., Steplewski, Z., and Koprowski, H. Effects of monoclonal antibody immunotherapy on patients with gastrointestinal adenocarcinoma. *J Biol Response Mod*, *3*: 138-150, 1984.
4. Sears, H. F., Atkinson, B., Mattis, J., Ernst, C., Herlyn, D., Steplewski, Z., Hayry, P., and Koprowski, H. Phase-I clinical trial of monoclonal antibody in treatment of gastrointestinal tumours. *Lancet*, *1*: 762-765, 1982.
5. Linnenbach, A. J., Wojcierowski, J., Wu, S. A., Pyrc, J. J., Ross, A. H., Dietzschold, B., Speicher, D., and Koprowski, H. Sequence investigation of the major gastrointestinal tumor-associated antigen gene family, GA733. *Proc Natl Acad Sci U S A*, *86*: 27-31, 1989.
6. Armstrong, A. and Eck, S. L. EpCAM: A new therapeutic target for an old cancer antigen. *Cancer Biol Ther*, *2*: 320-326, 2003.
7. Trzpis, M., McLaughlin, P. M., de Leij, L. M., and Harmsen, M. C. Epithelial cell adhesion molecule: more than a carcinoma marker and adhesion molecule. *Am J Pathol*, *171*: 386-395, 2007.
8. Balzar, M., Winter, M. J., de Boer, C. J., and Litvinov, S. V. The biology of the 17-1A antigen (Ep-CAM). *J Mol Med*, *77*: 699-712, 1999.
9. Chong, J. M. and Speicher, D. W. Determination of disulfide bond assignments and N-glycosylation sites of the human gastrointestinal carcinoma antigen GA733-2 (CO17-1A, EGP, KS1-4, KSA, and Ep-CAM). *J Biol Chem*, *276*: 5804-5813, 2001.
10. Winter, M. J., Cirulli, V., Briaire-de Bruijn, I. H., and Litvinov, S. V. Cadherins are regulated by Ep-CAM via phosphatidylinositol-3 kinase. *Mol Cell Biochem*, *302*: 19-26, 2007.
11. Litvinov, S. V., Velders, M. P., Bakker, H. A., Fleuren, G. J., and Warnaar, S. O. Ep-CAM: a human epithelial antigen is a homophilic cell-cell adhesion molecule. *J Cell Biol*, *125*: 437-446, 1994.
12. Ladwein, M., Pape, U. F., Schmidt, D. S., Schnolzer, M., Fiedler, S., Langbein, L., Franke, W. W., Moldenhauer, G., and Zoller, M. The cell-cell adhesion molecule EpCAM interacts directly with the tight junction protein claudin-7. *Exp Cell Res*, *309*: 345-357, 2005.
13. Guillemot, J. C., Naspetti, M., Malergue, F., Montcourrier, P., Galland, F., and Naquet, P. Ep-CAM transfection in thymic epithelial cell lines triggers the formation of dynamic actin-rich protrusions involved in the organization of epithelial cell layers. *Histochem Cell Biol*, *116*: 371-378, 2001.
14. Litvinov, S. V., Balzar, M., Winter, M. J., Bakker, H. A., Briaire-de Bruijn, I. H., Prins, F., Fleuren, G. J., and Warnaar, S. O. Epithelial cell adhesion molecule (Ep-CAM) modulates cell-cell interactions mediated by classic cadherins. *J Cell Biol*, *139*: 1337-1348, 1997.
15. de Boer, C. J., van Krieken, J. H., Janssen-van Rhijn, C. M., and Litvinov, S. V. Expression of Ep-CAM in normal, regenerating, metaplastic, and neoplastic liver. *J Pathol*, *188*: 201-206, 1999.
16. Cirulli, V., Crisa, L., Beattie, G. M., Mally, M. I., Lopez, A. D., Fannon, A., Ptasznik, A., Inverardi, L., Ricordi, C., Deerinck, T., Ellisman, M., Reisfeld, R. A., and Hayek, A. KSA antigen Ep-CAM mediates cell-cell adhesion of pancreatic epithelial cells: morphoregulatory roles in pancreatic islet development. *J Cell Biol*, *140*: 1519-1534, 1998.
17. Litvinov, S. V., van Driel, W., van Rhijn, C. M., Bakker, H. A., van Krieken, H., Fleuren, G. J., and Warnaar, S. O. Expression of Ep-CAM in cervical squamous epithelia correlates with an increased proliferation and the disappearance of markers for terminal differentiation. *Am J Pathol*, *148*: 865-875, 1996.

18. Schon, M. P., Schon, M., Klein, C. E., Blume, U., Bisson, S., and Orfanos, C. E. Carcinoma-associated 38-kD membrane glycoprotein MH 99/KS 1/4 is related to proliferation and age of transformed epithelial cell lines. *J Invest Dermatol*, 102: 987-991, 1994.
19. Tarmann, T., Dohr, G., Schiechl, H., Barth, S., and Hartmann, M. Immunohistochemical detection of an epithelial membrane protein in rat embryos at different stages of development. *Acta Anat (Basel)*, 137: 141-145, 1990.
20. Schiechl, H. and Dohr, G. Immunohistochemical studies of the distribution of a basolateral-membrane protein in intestinal epithelial cells (GZ1-Ag) in rats using monoclonal antibodies. *Histochemistry*, 87: 491-498, 1987.
21. Klein, C. E., Cordon-Cardo, C., Soehnchen, R., Cote, R. J., Oettgen, H. F., Eisinger, M., and Old, L. J. Changes in cell surface glycoprotein expression during differentiation of human keratinocytes. *J Invest Dermatol*, 89: 500-506, 1987.
22. Winter, M. J., Nagelkerken, B., Mertens, A. E., Rees-Bakker, H. A., Briaire-de Bruijn, I. H., and Litvinov, S. V. Expression of Ep-CAM shifts the state of cadherin-mediated adhesions from strong to weak. *Exp Cell Res*, 285: 50-58, 2003.
23. Osta, W. A., Chen, Y., Mikhitarian, K., Mitas, M., Salem, M., Hannun, Y. A., Cole, D. J., and Gillanders, W. E. EpCAM is overexpressed in breast cancer and is a potential target for breast cancer gene therapy. *Cancer Res*, 64: 5818-5824, 2004.
24. Wurfel, J., Rosel, M., Seiter, S., Claas, C., Herlevsen, M., Weth, R., and Zoller, M. Metastasis-association of the rat ortholog of the human epithelial glycoprotein antigen EGP314. *Oncogene*, 18: 2323-2334, 1999.
25. Munz, M., Kieu, C., Mack, B., Schmitt, B., Zeidler, R., and Gires, O. The carcinoma-associated antigen EpCAM upregulates c-myc and induces cell proliferation. *Oncogene*, 23: 5748-5758, 2004.
26. Munz, M., Zeidler, R., and Gires, O. The tumour-associated antigen EpCAM upregulates the fatty acid binding protein E-FABP. *Cancer Lett*, 225: 151-157, 2005.
27. Flieger, D., Hoff, A. S., Sauerbruch, T., and Schmidt-Wolf, I. G. Influence of cytokines, monoclonal antibodies and chemotherapeutic drugs on epithelial cell adhesion molecule (Ep-CAM) and LewisY antigen expression. *Clin Exp Immunol*, 123: 9-14, 2001.
28. Anderson, R., Schaible, K., Heasman, J., and Wylie, C. Expression of the homophilic adhesion molecule, Ep-CAM, in the mammalian germ line. *J Reprod Fertil*, 116: 379-384, 1999.
29. Al-Hajj, M., Wicha, M. S., Benito-Hernandez, A., Morrison, S. J., and Clarke, M. F. Prospective identification of tumorigenic breast cancer cells. *Proc Natl Acad Sci U S A*, 100: 3983-3988, 2003.
30. Moldenhauer, G., Momburg, F., Moller, P., Schwartz, R., and Hammerling, G. J. Epithelium-specific surface glycoprotein of Mr 34,000 is a widely distributed human carcinoma marker. *Br J Cancer*, 56: 714-721, 1987.
31. Winter, M. J., Nagtegaal, I. D., van Krieken, J. H., and Litvinov, S. V. The epithelial cell adhesion molecule (Ep-CAM) as a morphoregulatory molecule is a tool in surgical pathology. *Am J Pathol*, 163: 2139-2148, 2003.
32. Spizzo, G., Went, P., Dirnhofer, S., Obrist, P., Simon, R., Spichtin, H., Maurer, R., Metzger, U., von Castelberg, B., Bart, R., Stopatschinskaya, S., Kochli, O. R., Haas, P., Mross, F., Zuber, M., Dietrich, H., Bischoff, S., Mirlacher, M., Sauter, G., and Gastl, G. High Ep-CAM expression is associated with poor prognosis in node-positive breast cancer. *Breast Cancer Res Treat*, 86: 207-213, 2004.
33. Spizzo, G., Went, P., Dirnhofer, S., Obrist, P., Moch, H., Baeuerle, P. A., Mueller-Holzner, E., Marth, C., Gastl, G., and Zeimet, A. G. Overexpression of epithelial cell adhesion molecule (Ep-CAM) is an independent prognostic marker for reduced survival of patients with epithelial ovarian cancer. *Gynecol Oncol*, 103: 483-488, 2006.
34. Gastl, G., Spizzo, G., Obrist, P., Dunser, M., and Mikuz, G. Ep-CAM overexpression in breast cancer as a predictor of survival. *Lancet*, 356: 1981-1982, 2000.
35. Fong, D., Steurer, M., Obrist, P., Barbieri, V., Margreiter, R., Amberger, A., Laimer, K., Gastl, G., Tzankov, A., and Spizzo, G. Ep-CAM expression in pancreatic and ampullary carcinomas: frequency and prognostic relevance. *J Clin Pathol*, 61: 31-35, 2008.

36. Stoecklein, N. H., Siegmund, A., Scheunemann, P., Luebke, A. M., Erbersdobler, A., Verde, P. E., Eisenberger, C. F., Peiper, M., Rehders, A., Esch, J. S., Knoefel, W. T., and Hosch, S. B. Ep-CAM expression in squamous cell carcinoma of the esophagus: a potential therapeutic target and prognostic marker. *BMC Cancer*, 6: 165, 2006.
37. Songun, I., Litvinov, S. V., van de Velde, C. J., Pals, S. T., Hermans, J., and van Krieken, J. H. Loss of Ep-CAM (CO17-1A) expression predicts survival in patients with gastric cancer. *Br J Cancer*, 92: 1767-1772, 2005.
38. Seligson, D. B., Pantuck, A. J., Liu, X., Huang, Y., Horvath, S., Bui, M. H., Han, K. R., Correa, A. J., Eeva, M., Tze, S., Belldegrun, A. S., and Figlin, R. A. Epithelial cell adhesion molecule (KSA) expression: pathobiology and its role as an independent predictor of survival in renal cell carcinoma. *Clin Cancer Res*, 10: 2659-2669, 2004.
39. Kim, H. L., Seligson, D., Liu, X., Janzen, N., Bui, M. H., Yu, H., Shi, T., Figlin, R. A., Horvath, S., and Belldegrun, A. S. Using protein expressions to predict survival in clear cell renal carcinoma. *Clin Cancer Res*, 10: 5464-5471, 2004.
40. Went, P., Dirnhofer, S., Salvisberg, T., Amin, M. B., Lim, S. D., Diener, P. A., and Moch, H. Expression of epithelial cell adhesion molecule (EpCam) in renal epithelial tumors. *Am J Surg Pathol*, 29: 83-88, 2005.
41. Piyathilake, C. J., Frost, A. R., Weiss, H., Manne, U., Heimbürger, D. C., and Grizzle, W. E. The expression of Ep-CAM (17-1A) in squamous cell cancers of the lung. *Hum Pathol*, 31: 482-487, 2000.
42. Poczatek, R. B., Myers, R. B., Manne, U., Oelschlager, D. K., Weiss, H. L., Bostwick, D. G., and Grizzle, W. E. Ep-Cam levels in prostatic adenocarcinoma and prostatic intraepithelial neoplasia. *J Urol*, 162: 1462-1466, 1999.
43. Momburg, F., Moldenhauer, G., Hammerling, G. J., and Moller, P. Immunohistochemical study of the expression of a Mr 34,000 human epithelium-specific surface glycoprotein in normal and malignant tissues. *Cancer Res*, 47: 2883-2891, 1987.
44. Schmidt, D. S., Klingbeil, P., Schnolzer, M., and Zoller, M. CD44 variant isoforms associate with tetraspanins and EpCAM. *Exp Cell Res*, 297: 329-347, 2004.
45. Kuhn, S., Koch, M., Nubel, T., Ladwein, M., Antolovic, D., Klingbeil, P., Hildebrand, D., Moldenhauer, G., Langbein, L., Franke, W. W., Weitz, J., and Zoller, M. A Complex of Ep-CAM, Claudin-7, CD44 Variant Isoforms, and Tetraspanins Promotes Colorectal Cancer Progression. *Mol Cancer Res*, 5: 553-567, 2007.
46. Rao, C. G., Chianese, D., Doyle, G. V., Miller, M. C., Russell, T., Sanders, R. A., Jr., and Terstappen, L. W. Expression of epithelial cell adhesion molecule in carcinoma cells present in blood and primary and metastatic tumors. *Int J Oncol*, 27: 49-57, 2005.
47. Went, P. T., Lugli, A., Meier, S., Bundi, M., Mirlacher, M., Sauter, G., and Dirnhofer, S. Frequent EpCam protein expression in human carcinomas. *Hum Pathol*, 35: 122-128, 2004.
48. Herrlich, P., Morrison, H., Sleeman, J., Orian-Rousseau, V., König, H., Weg-Remers, S., and Ponta, H. CD44 acts both as a growth- and invasiveness-promoting molecule and as a tumor-suppressing cofactor. *Ann N Y Acad Sci*, 910: 106-118; discussion 118-120, 2000.
49. Went, P., Vasei, M., Bubendorf, L., Terracciano, L., Tornillo, L., Riede, U., Kononen, J., Simon, R., Sauter, G., and Baeuerle, P. A. Frequent high-level expression of the immunotherapeutic target Ep-CAM in colon, stomach, prostate and lung cancers. *Br J Cancer*, 94: 128-135, 2006.
50. de Bono, J. S., Tolcher, A. W., Forero, A., Vanhove, G. F., Takimoto, C., Bauer, R. J., Hammond, L. A., Patnaik, A., White, M. L., Shen, S., Khazaeli, M. B., Rowinsky, E. K., and LoBuglio, A. F. ING-1, a monoclonal antibody targeting Ep-CAM in patients with advanced adenocarcinomas. *Clin Cancer Res*, 10: 7555-7565, 2004.
51. Naundorf, S., Preithner, S., Mayer, P., Lippold, S., Wolf, A., Hanakam, F., Fichtner, I., Kufer, P., Raum, T., Riethmüller, G., Baeuerle, P. A., and Dreier, T. In vitro and in vivo activity of MT201, a fully human monoclonal antibody for pancarcinoma treatment. *Int J Cancer*, 100: 101-110, 2002.
52. Himmler, G., Loibner, H., Schuster, M., Janzek, E., Stranner, S., and Samonigg, H. Murine monoclonal antibody 17-1A used as vaccine antigen (IGN101): direct induction of anti-

- EpCAM antibodies by vaccination of cancer patients. *Proc Am Soc Clin Oncol*, 22: A732, 2003.
53. Zimmermann, S., Wels, W., Froesch, B. A., Gerstmayer, B., Stahel, R. A., and Zangemeister-Wittke, U. A novel immunotoxin recognising the epithelial glycoprotein-2 has potent antitumoural activity on chemotherapy-resistant lung cancer. *Cancer Immunol Immunother*, 44: 1-9, 1997.
 54. Di Paolo, C., Willuda, J., Kubetzko, S., Lauffer, I., Tschudi, D., Waibel, R., Pluckthun, A., Stahel, R. A., and Zangemeister-Wittke, U. A recombinant immunotoxin derived from a humanized epithelial cell adhesion molecule-specific single-chain antibody fragment has potent and selective antitumor activity. *Clin Cancer Res*, 9: 2837-2848, 2003.
 55. Lindhofer, H., Menzel, H., Gunther, W., Hultner, L., and Thierfelder, S. Bispecific antibodies target operationally tumor-specific antigens in two leukemia relapse models. *Blood*, 88: 4651-4658, 1996.
 56. Schweizer, C., Strauss, G., Lindner, M., Marme, A., Deo, Y. M., and Moldenhauer, G. Efficient carcinoma cell killing by activated polymorphonuclear neutrophils targeted with an EpCAMxCD64 (HEA125x197) bispecific antibody. *Cancer Immunol Immunother*, 51: 621-629, 2002.
 57. Hartung, G., Hofheinz, R. D., Dencausse, Y., Sturm, J., Kopp-Schneider, A., Dietrich, G., Fackler-Schwalbe, I., Bornbusch, D., Gonnermann, M., Wojatschek, C., Lindemann, W., Eschenburg, H., Jost, K., Edler, L., Hochhaus, A., and Queisser, W. Adjuvant therapy with edrecolomab versus observation in stage II colon cancer: a multicenter randomized phase III study. *Onkologie*, 28: 347-350, 2005.
 58. Hempel, P., Muller, P., Oruzio, D., Behr, W., Brockmeyer, C., Wochner, M., Ehnle, S., Riethmuller, R., and Schlimok, G. Combination of high-dose chemotherapy and monoclonal antibody in breast-cancer patients: a pilot trial to monitor treatment effects on disseminated tumor cells. *Cytotherapy*, 2: 287-295, 2000.
 59. Punt, C. J., Nagy, A., Douillard, J. Y., Figer, A., Skovsgaard, T., Monson, J., Barone, C., Fountzilas, G., Riess, H., Moylan, E., Jones, D., Dethling, J., Colman, J., Coward, L., and MacGregor, S. Edrecolomab alone or in combination with fluorouracil and folinic acid in the adjuvant treatment of stage III colon cancer: a randomised study. *Lancet*, 360: 671-677, 2002.
 60. Riethmuller, G., Schneider-Gadicke, E., Schlimok, G., Schmiegel, W., Raab, R., Hoffken, K., Gruber, R., Pichlmaier, H., Hirche, H., Pichlmayr, R., and et al. Randomised trial of monoclonal antibody for adjuvant therapy of resected Dukes' C colorectal carcinoma. German Cancer Aid 17-1A Study Group. *Lancet*, 343: 1177-1183, 1994.
 61. Goel, S., Bauer, R. J., Desai, K., Bulgaru, A., Iqbal, T., Strachan, B. K., Kim, G., Kaubisch, A., Vanhove, G. F., Goldberg, G., and Mani, S. Pharmacokinetic and safety study of subcutaneously administered weekly ING-1, a human engineered monoclonal antibody targeting human EpCAM, in patients with advanced solid tumors. *Ann Oncol*, 18: 1704-1707, 2007.
 62. Herlyn, D., Sears, H. F., Ernst, C. S., Iliopoulos, D., Steplewski, Z., and Koprowski, H. Initial clinical evaluation of two murine IgG2a monoclonal antibodies for immunotherapy of gastrointestinal carcinoma. *Am J Clin Oncol*, 14: 371-378, 1991.
 63. Baeuerle, P., Reinhardt, C., and Kufer, P. BtTE: a new class of antibodies that recruit T-cells. *Drugs Fut*, 33: 1-11, 2008.
 64. Baeuerle, P. A., Kufer, P., and Lutterbuse, R. Bispecific antibodies for polyclonal T-cell engagement. *Curr Opin Mol Ther*, 5: 413-419, 2003.
 65. Wolf, E., Hofmeister, R., Kufer, P., Schlereth, B., and Baeuerle, P. A. BiTEs: bispecific antibody constructs with unique anti-tumor activity. *Drug Discov Today*, 10: 1237-1244, 2005.
 66. Hoffmann, P., Hofmeister, R., Brischwein, K., Brandl, C., Crommer, S., Bargou, R., Itin, C., Prang, N., and Baeuerle, P. A. Serial killing of tumor cells by cytotoxic T cells redirected with a CD19-/CD3-bispecific single-chain antibody construct. *Int J Cancer*, 115: 98-104, 2005.
 67. Yokota, T., Milenic, D. E., Whitlow, M., and Schlom, J. Rapid tumor penetration of a single-chain Fv and comparison with other immunoglobulin forms. *Cancer Res*, 52: 3402-3408, 1992.

68. Mack, M., Riethmuller, G., and Kufer, P. A small bispecific antibody construct expressed as a functional single-chain molecule with high tumor cell cytotoxicity. *Proc Natl Acad Sci U S A*, 92: 7021-7025, 1995.
69. Nagorsen, D., Scheibenbogen, C., Marincola, F. M., Letsch, A., and Keilholz, U. Natural T cell immunity against cancer. *Clin Cancer Res*, 9: 4296-4303, 2003.
70. Boon, T., Cerottini, J. C., Van den Eynde, B., van der Bruggen, P., and Van Pel, A. Tumor antigens recognized by T lymphocytes. *Annu Rev Immunol*, 12: 337-365, 1994.
71. Faroudi, M., Utzny, C., Salio, M., Cerundolo, V., Guiraud, M., Muller, S., and Valitutti, S. Lytic versus stimulatory synapse in cytotoxic T lymphocyte/target cell interaction: manifestation of a dual activation threshold. *Proc Natl Acad Sci U S A*, 100: 14145-14150, 2003.
72. Lee, K. H., Holdorf, A. D., Dustin, M. L., Chan, A. C., Allen, P. M., and Shaw, A. S. T cell receptor signaling precedes immunological synapse formation. *Science*, 295: 1539-1542, 2002.
73. Lee, K. H., Dinner, A. R., Tu, C., Campi, G., Raychaudhuri, S., Varma, R., Sims, T. N., Burack, W. R., Wu, H., Wang, J., Kanagawa, O., Markiewicz, M., Allen, P. M., Dustin, M. L., Chakraborty, A. K., and Shaw, A. S. The immunological synapse balances T cell receptor signaling and degradation. *Science*, 302: 1218-1222, 2003.
74. Cabrera, T., Collado, A., Fernandez, M. A., Ferron, A., Sancho, J., Ruiz-Cabello, F., and Garrido, F. High frequency of altered HLA class I phenotypes in invasive colorectal carcinomas. *Tissue Antigens*, 52: 114-123, 1998.
75. Hicklin, D. J., Wang, Z., Arienti, F., Rivoltini, L., Parmiani, G., and Ferrone, S. beta2-Microglobulin mutations, HLA class I antigen loss, and tumor progression in melanoma. *J Clin Invest*, 101: 2720-2729, 1998.
76. Thomas, D. A. and Massague, J. TGF-beta directly targets cytotoxic T cell functions during tumor evasion of immune surveillance. *Cancer Cell*, 8: 369-380, 2005.
77. Munn, D. H. Indoleamine 2,3-dioxygenase, tumor-induced tolerance and counter-regulation. *Curr Opin Immunol*, 18: 220-225, 2006.
78. Chen, L., Ashe, S., Brady, W. A., Hellstrom, I., Hellstrom, K. E., Ledbetter, J. A., McGowan, P., and Linsley, P. S. Costimulation of antitumor immunity by the B7 counterreceptor for the T lymphocyte molecules CD28 and CTLA-4. *Cell*, 71: 1093-1102, 1992.
79. Brischwein, K., Parr, L., Pflanz, S., Volkland, J., Lumsden, J., Klinger, M., Locher, M., Hammond, S. A., Kiener, P., Kufer, P., Schlereth, B., and Baeuerle, P. A. Strictly target cell-dependent activation of T cells by bispecific single-chain antibody constructs of the BiTE class. *J Immunother* (1997), 30: 798-807, 2007.
80. Kufer, P., Zettl, F., Borschert, K., Lutterbuse, R., Kischel, R., and Riethmuller, G. Minimal costimulatory requirements for T cell priming and TH1 differentiation: activation of naive human T lymphocytes by tumor cells armed with bifunctional antibody constructs. *Cancer Immun*, 1: 10, 2001.
81. Dreier, T., Lorenczewski, G., Brandl, C., Hoffmann, P., Syring, U., Hanakam, F., Kufer, P., Riethmuller, G., Bargou, R., and Baeuerle, P. A. Extremely potent, rapid and costimulation-independent cytotoxic T-cell response against lymphoma cells catalyzed by a single-chain bispecific antibody. *Int J Cancer*, 100: 690-697, 2002.
82. Offner, S., Hofmeister, R., Romaniuk, A., Kufer, P., and Baeuerle, P. A. Induction of regular cytolytic T cell synapses by bispecific single-chain antibody constructs on MHC class I-negative tumor cells. *Mol Immunol*, 43: 763-771, 2006.
83. Kufer, P., Lutterbuse, R., and Baeuerle, P. A. A revival of bispecific antibodies. *Trends Biotechnol*, 22: 238-244, 2004.
84. Bargou, R., Leo, E., Zugmaier, G., Klinger, M., Goebeler, M., Knop, S., Noppeney, R., Viardot, A., Hess, D. A., Schuler, M., Einsele, H., Brandl, C., Wolf, A., Kirchinger, P., Klappers, P., Schmidt, M., Riethmüller, G., Reinhardt, C., Baeuerle, P., and Kufer, P. Tumor Regression in Cancer Patients by Very Low Doses of a T Cell-Engaging Antibody. *Science*, 321: 974-977, 2008.
85. Amann, M., Brischwein, K., Lutterbuese, P., Parr, L., Petersen, L., Lorenczewski, G., Krinner, E., Bruckmeier, S., Lippold, S., Kischel, R., Lutterbuese, R., Kufer, P., Baeuerle, P. A., and

- Schlereth, B. Therapeutic window of MuS110, a single-chain antibody construct bispecific for murine EpCAM and murine CD3. *Cancer Res*, 68: 143-151, 2008.
86. Schlereth, B., Fichtner, I., Lorenczewski, G., Kleindienst, P., Brischwein, K., da Silva, A., Kufer, P., Lutterbuese, R., Junghahn, I., Kasimir-Bauer, S., Wimberger, P., Kimmig, R., and Baeuerle, P. A. Eradication of tumors from a human colon cancer cell line and from ovarian cancer metastases in immunodeficient mice by a single-chain Ep-CAM-/CD3-bispecific antibody construct. *Cancer Res*, 65: 2882-2889, 2005.
87. Bergsagel, P. L., Victor-Kobrin, C., Timblin, C. R., Trepel, J., and Kuehl, W. M. A murine cDNA encodes a pan-epithelial glycoprotein that is also expressed on plasma cells. *J Immunol*, 148: 590-596, 1992.
88. Brischwein, K., Schlereth, B., Guller, B., Steiger, C., Wolf, A., Lutterbuese, R., Offner, S., Locher, M., Urbig, T., Raum, T., Kleindienst, P., Wimberger, P., Kimmig, R., Fichtner, I., Kufer, P., Hofmeister, R., da Silva, A. J., and Baeuerle, P. A. MT110: a novel bispecific single-chain antibody construct with high efficacy in eradicating established tumors. *Mol Immunol*, 43: 1129-1143, 2006.
89. Li, Y., Cockburn, W., Kilpatrick, J. B., and Whitelam, G. C. High affinity ScFvs from a single rabbit immunized with multiple haptens. *Biochem Biophys Res Commun*, 268: 398-404, 2000.
90. Raum, T., Gruber, R., Riethmuller, G., and Kufer, P. Anti-self antibodies selected from a human IgD heavy chain repertoire: a novel approach to generate therapeutic human antibodies against tumor-associated differentiation antigens. *Cancer Immunol Immunother*, 50: 141-150, 2001.
91. Kaufman, R. J. Selection and coamplification of heterologous genes in mammalian cells. *Methods Enzymol*, 185: 537-566, 1990.
92. Smith, K. IL-2 and IL-2 receptor. 1459-1469.
93. Gattoni, A., Parlato, A., Vangieri, B., Bresciani, M., and Derna, R. Interferon-gamma: biologic functions and HCV therapy (type I/II). *Clin Ter.*, 157: 377 - 386, 2006.
94. Sansom, D. M. and Walker, L. S. The role of CD28 and cytotoxic T-lymphocyte antigen-4 (CTLA-4) in regulatory T-cell biology. *Immunol Rev*, 212: 131-148, 2006.
95. Croft, M. Co-stimulatory members of the TNFR family: keys to effective T-cell immunity? *Nat Rev Immunol*, 3: 609-620, 2003.
96. Bachmann, M. F., Wolint, P., Schwarz, K., Jager, P., and Oxenius, A. Functional properties and lineage relationship of CD8+ T cell subsets identified by expression of IL-7 receptor alpha and CD62L. *J Immunol*, 175: 4686-4696, 2005.
97. Alegre, M., Vandenabeele, P., Flamand, V., Moser, M., Leo, O., Abramowicz, D., Urbain, J., Fiers, W., and Goldman, M. Hypothermia and hypoglycemia induced by anti-CD3 monoclonal antibody in mice: role of tumor necrosis factor. *Eur J Immunol*, 20: 707-710, 1990.
98. Alegre, M., Depierreux, M., Florquin, S., Najdovski, T., Vandenabeele, P., Abramowicz, D., Leo, O., Deschodt-Lanckman, M., and Goldman, M. Acute toxicity of anti-CD3 monoclonal antibody in mice: a model for OKT3 first dose reactions. *Transplant Proc*, 22: 1920-1921, 1990.
99. Alegre, M. L., Vandenabeele, P., Depierreux, M., Florquin, S., Deschodt-Lanckman, M., Flamand, V., Moser, M., Leo, O., Urbain, J., Fiers, W., and et al. Cytokine release syndrome induced by the 145-2C11 anti-CD3 monoclonal antibody in mice: prevention by high doses of methylprednisolone. *J Immunol*, 146: 1184-1191, 1991.
100. Wissing, K. M., Desalle, F., Abramowicz, D., Willems, F., Leo, O., Goldman, M., and Alegre, M. L. Down-regulation of interleukin-2 and interferon-gamma and maintenance of interleukin-4 and interleukin-10 production after administration of an anti-CD3 monoclonal antibody in mice. *Transplantation*, 68: 677-684, 1999.
101. Chatenoud, L., Ferran, C., and Bach, J. F. The anti-CD3-induced syndrome: a consequence of massive in vivo cell activation. *Curr Top Microbiol Immunol*, 174: 121-134, 1991.
102. Buysmann, S., Bemelman, F. J., Schellekens, P. T., van Kooyk, Y., Figdor, C. G., and ten Berge, I. J. Activation and increased expression of adhesion molecules on peripheral blood lymphocytes is a mechanism for the immediate lymphocytopenia after administration of OKT3. *Blood*, 87: 404-411, 1996.

103. Miyamoto, T., Fujinaga, T., Yamashita, K., and Hagio, M. Changes of serum cytokine activities and other parameters in dogs with experimentally induced endotoxic shock. *Jpn J Vet Res*, *44*: 107-118, 1996.
104. Parlevliet, K. J., ten Berge, I. J., Yong, S. L., Surachno, J., Wilmink, J. M., and Schellekens, P. T. In vivo effects of IgA and IgG2a anti-CD3 isotype switch variants. *J Clin Invest*, *93*: 2519-2525, 1994.
105. Anasetti, C., Martin, P. J., Storb, R., Appelbaum, F. R., Beatty, P. G., Davis, J., Doney, K., Hill, H. F., Stewart, P., Sullivan, K. M., and et al. Treatment of acute graft-versus-host disease with a nonmitogenic anti-CD3 monoclonal antibody. *Transplantation*, *54*: 844-851, 1992.
106. Alegre, M. L., Peterson, L. J., Xu, D., Sattar, H. A., Jeyarajah, D. R., Kowalkowski, K., Thistlethwaite, J. R., Zivin, R. A., Jolliffe, L., and Bluestone, J. A. A non-activating "humanized" anti-CD3 monoclonal antibody retains immunosuppressive properties in vivo. *Transplantation*, *57*: 1537-1543, 1994.
107. Bolt, S., Routledge, E., Lloyd, I., Chatenoud, L., Pope, H., Gorman, S. D., Clark, M., and Waldmann, H. The generation of a humanized, non-mitogenic CD3 monoclonal antibody which retains in vitro immunosuppressive properties. *Eur J Immunol*, *23*: 403-411, 1993.
108. Cole, M. S., Stellrecht, K. E., Shi, J. D., Homola, M., Hsu, D. H., Anasetti, C., Vasquez, M., and Tso, J. Y. HuM291, a humanized anti-CD3 antibody, is immunosuppressive to T cells while exhibiting reduced mitogenicity in vitro. *Transplantation*, *68*: 563-571, 1999.
109. Chatenoud, L., Baudrihay, M. F., Kreis, H., Goldstein, G., Schindler, J., and Bach, J. F. Human in vivo antigenic modulation induced by the anti-T cell OKT3 monoclonal antibody. *Eur J Immunol*, *12*: 979-982, 1982.
110. Noel, C., Florquin, S., Goldman, M., and Braun, M. Y. Chronic exposure to superantigen induces regulatory CD4+ T cells with IL-10-mediated suppressive activity. *Int. Immunol.*, *13*: 431-439, 2001.
111. Hirsch, R., Gress, R. E., Pluznik, D. H., Eckhaus, M., and Bluestone, J. A. Effects of in vivo administration of anti-CD3 monoclonal antibody on T cell function in mice. II. In vivo activation of T cells. *J Immunol*, *142*: 737-743, 1989.
112. Amann, M., Friedrich, M., Lutterbuese, P., Vieser, E., Lorenczewski, G., Petersen, L., Brischwein, K., Kufer, P., Kischel, R., Baeuerle, P. A., and Schlereth, B. Therapeutic window of an EpCAM/CD3-specific BiTE antibody in mice is determined by a subpopulation of EpCAM-expressing lymphocytes that is absent in humans. *Cancer Immunol Immunother*, *58*: 95-109, 2008.
113. Moore, K. W., de Waal Malefyt, R., Coffman, R. L., and O'Garra, A. Interleukin-10 and the interleukin-10 receptor. *Annu Rev Immunol*, *19*: 683-765, 2001.
114. Chatenoud, L. CD3-specific antibody-induced active tolerance: from bench to bedside. *Nat Rev Immunol*, *3*: 123-132, 2003.
115. Bisikirska, B. C. and Herold, K. C. Use of anti-CD3 monoclonal antibody to induce immune regulation in type 1 diabetes. *Ann N Y Acad Sci*, *1037*: 1-9, 2004.
116. Schwartz, R. H. T cell anergy. *Annu Rev Immunol*, *21*: 305-334, 2003.
117. Hayashi, R., Wada, H., Ito, K., and Adcock, I. M. Effects of glucocorticoids on gene transcription. *Eur J Pharmacol*, *500*: 51-62, 2004.
118. Barnes, P. J. Anti-inflammatory actions of glucocorticoids: molecular mechanisms. *Clin Sci (Lond)*, *94*: 557-572, 1998.
119. Chatenoud, L., Legendre, C., Ferran, C., Bach, J. F., and Kreis, H. Corticosteroid inhibition of the OKT3-induced cytokine-related syndrome--dosage and kinetics prerequisites. *Transplantation*, *51*: 334-338, 1991.
120. Bisikirska, B., Colgan, J., Luban, J., Bluestone, J. A., and Herold, K. C. TCR stimulation with modified anti-CD3 mAb expands CD8+ T cell population and induces CD8+CD25+ Tregs. *J Clin Invest*, *115*: 2904-2913, 2005.
121. Chatenoud, L. and Bluestone, J. A. CD3-specific antibodies: a portal to the treatment of autoimmunity. *Nat Rev Immunol*, *7*: 622-632, 2007.
122. Favier, B., Burroughs, N. J., Wedderburn, L., and Valitutti, S. TCR dynamics on the surface of living T cells. *Int. Immunol.*, *13*: 1525-1532, 2001.

123. Wells, A. D., Gudmundsdottir, H., and Turka, L. A. Following the fate of individual T cells throughout activation and clonal expansion. Signals from T cell receptor and CD28 differentially regulate the induction and duration of a proliferative response. *J Clin Invest*, *100*: 3173-3183, 1997.
124. Viola, A. and Lanzavecchia, A. T cell activation determined by T cell receptor number and tunable thresholds. *Science*, *273*: 104-106, 1996.
125. Saleh, P. J., Khazaeli MB, et al. Phase I trial testing multiple doses of humanized monoclonal antibody (Mab). ASCO Annual Meeting 1998, *abstract no. 1680.*, 1998.
126. Oberneder, R., Weckermann, D., Ebner, B., Quadt, C., Kirchinger, P., Raum, T., Locher, M., Prang, N., Baeuerle, P. A., and Leo, E. A phase I study with adecatumumab, a human antibody directed against epithelial cell adhesion molecule, in hormone refractory prostate cancer patients. *Eur J Cancer*, *42*: 2530-2538, 2006.
127. Schwartzberg, L. S. Clinical experience with edrecolomab: a monoclonal antibody therapy for colorectal carcinoma. *Crit Rev Oncol Hematol*, *40*: 17-24, 2001.
128. Schlereth, B., Quadt, C., Dreier, T., Kufer, P., Lorenczewski, G., Prang, N., Brandl, C., Lippold, S., Cobb, K., Brasky, K., Leo, E., Bargou, R., Murthy, K., and Baeuerle, P. A. T-cell activation and B-cell depletion in chimpanzees treated with a bispecific anti-CD19/anti-CD3 single-chain antibody construct. *Cancer Immunol Immunother*, *55*: 503-514, 2006.
129. Ariel, A., Yavin, E. J., Hershkoviz, R., Avron, A., Franitza, S., Hardan, I., Cahalon, L., Fridkin, M., and Lider, O. IL-2 induces T cell adherence to extracellular matrix: inhibition of adherence and migration by IL-2 peptides generated by leukocyte elastase. *J Immunol*, *161*: 2465-2472, 1998.
130. Green, D. M., Trial, J., and Birdsall, H. H. TNF-alpha released by comigrating monocytes promotes transendothelial migration of activated lymphocytes. *J Immunol*, *161*: 2481-2489, 1998.
131. Blackwell, T. S. and Christman, J. W. Sepsis and cytokines: current status. *Br J Anaesth*, *77*: 110-117, 1996.
132. Panelli, M. C., White, R., Foster, M., Martin, B., Wang, E., Smith, K., and Marincola, F. M. Forecasting the cytokine storm following systemic interleukin (IL)-2 administration. *J Transl Med*, *2*: 17, 2004.
133. Talmadge, J. E., Bowersox, O., Tribble, H., Lee, S. H., Shepard, H. M., and Liggitt, D. Toxicity of tumor necrosis factor is synergistic with gamma-interferon and can be reduced with cyclooxygenase inhibitors. *Am J Pathol*, *128*: 410-425, 1987.
134. Charpentier, B., Hiesse, C., Ferran, C., Lantz, O., Fries, D., Bach, J. F., and Chatenoud, L. [Acute clinical syndrome associated with OKT3 administration. Prevention by single injection of an anti-human TNF monoclonal antibody]. *Presse Med*, *20*: 2009-2011, 1991.
135. Ferran, C., Dy, M., Sheehan, K., Merite, S., Schreiber, R., Landais, P., Grau, G., Bluestone, J., Bach, J. F., and Chatenoud, L. Inter-mouse strain differences in the in vivo anti-CD3 induced cytokine release. *Clin Exp Immunol*, *86*: 537-543, 1991.
136. Florquin, S. and Goldman, M. Immunoregulatory mechanisms of T-cell-dependent shock induced by a bacterial superantigen in mice. *Infect Immun*, *64*: 3443-3445, 1996.
137. Marrack, P., Blackman, M., Kushnir, E., and Kappler, J. The toxicity of staphylococcal enterotoxin B in mice is mediated by T cells. *J Exp Med*, *171*: 455-464, 1990.
138. Matthys, P., Mitera, T., Heremans, H., Van Damme, J., and Billiau, A. Anti-gamma interferon and anti-interleukin-6 antibodies affect staphylococcal enterotoxin B-induced weight loss, hypoglycemia, and cytokine release in D-galactosamine-sensitized and unsensitized mice. *Infect Immun*, *63*: 1158-1164, 1995.
139. Leung, D. Y. and Bloom, J. W. Update on glucocorticoid action and resistance. *J Allergy Clin Immunol*, *111*: 3-22; quiz 23, 2003.
140. Ferran, C., Dy, M., Merite, S., Sheehan, K., Schreiber, R., Leboulenger, F., Landais, P., Bluestone, J., Bach, J. F., and Chatenoud, L. Reduction of morbidity and cytokine release in anti-CD3 MoAb-treated mice by corticosteroids. *Transplantation*, *50*: 642-648, 1990.
141. Newton, R. Molecular mechanisms of glucocorticoid action: what is important? *Thorax*, *55*: 603-613, 2000.

142. Le Naour, F., Andre, M., Greco, C., Billard, M., Sordat, B., Emile, J. F., Lanza, F., Boucheix, C., and Rubinstein, E. Profiling of the tetraspanin web of human colon cancer cells. *Mol Cell Proteomics*, 5: 845-857, 2006.
143. Si, Z. and Hersey, P. Expression of the neuroglandular antigen and analogues in melanoma. CD9 expression appears inversely related to metastatic potential of melanoma. *Int J Cancer*, 54: 37-43, 1993.
144. Litvinov, S. V., Bakker, H. A., Gourevitch, M. M., Velders, M. P., and Warnaar, S. O. Evidence for a role of the epithelial glycoprotein 40 (Ep-CAM) in epithelial cell-cell adhesion. *Cell Adhes Commun*, 2: 417-428, 1994.
145. Borkowski, T. A., Nelson, A. J., Farr, A. G., and Udey, M. C. Expression of gp40, the murine homologue of human epithelial cell adhesion molecule (Ep-CAM), by murine dendritic cells. *Eur J Immunol*, 26: 110-114, 1996.
146. Nelson, A. J., Dunn, R. J., Peach, R., Aruffo, A., and Farr, A. G. The murine homolog of human Ep-CAM, a homotypic adhesion molecule, is expressed by thymocytes and thymic epithelial cells. *Eur J Immunol*, 26: 401-408, 1996.
147. Hirsch, R., Eckhaus, M., Auchincloss, H., Jr., Sachs, D. H., and Bluestone, J. A. Effects of in vivo administration of anti-T3 monoclonal antibody on T cell function in mice. I. Immunosuppression of transplantation responses. *J Immunol*, 140: 3766-3772, 1988.
148. Mackie, J. D., Pankewycz, O. G., Bastos, M. G., Kelley, V. E., and Strom, T. B. Dose-related mechanisms of immunosuppression mediated by murine anti-CD3 monoclonal antibody in pancreatic islet cell transplantation and delayed-type hypersensitivity. *Transplantation*, 49: 1150-1154, 1990.
149. Willems, F., Andris, F., Xu, D., Abramowicz, D., Wissing, M., Goldman, M., and Leo, O. The induction of human T cell unresponsiveness by soluble anti-CD3 mAb requires T cell activation. *Int Immunol*, 7: 1593-1598, 1995.
150. Woodle, E. S., Hussein, S., and Bluestone, J. A. In vivo administration of anti-murine CD3 monoclonal antibody induces selective, long-term anergy in CD8+ T cells. *Transplantation*, 61: 798-803, 1996.
151. Belghith, M., Bluestone, J. A., Barriot, S., Megret, J., Bach, J. F., and Chatenoud, L. TGF-beta-dependent mechanisms mediate restoration of self-tolerance induced by antibodies to CD3 in overt autoimmune diabetes. *Nat Med*, 9: 1202-1208, 2003.
152. Kohm, A. P., Williams, J. S., Bickford, A. L., McMahon, J. S., Chatenoud, L., Bach, J. F., Bluestone, J. A., and Miller, S. D. Treatment with nonmitogenic anti-CD3 monoclonal antibody induces CD4+ T cell unresponsiveness and functional reversal of established experimental autoimmune encephalomyelitis. *J Immunol*, 174: 4525-4534, 2005.
153. Smith, J. A., Tang, Q., and Bluestone, J. A. Partial TCR signals delivered by FcR-nonbinding anti-CD3 monoclonal antibodies differentially regulate individual Th subsets. *J Immunol*, 160: 4841-4849, 1998.
154. Donckier, V., Flament, V., Gerard, C., Abramowicz, D., Vandenabeele, P., Wissing, M., Delvaux, A., Fiers, W., Leo, O., Velu, T., and et al. Modulation of the release of cytokines and reduction of the shock syndrome induced by anti-CD3 monoclonal antibody in mice by interleukin-10. *Transplantation*, 57: 1436-1439, 1994.
155. Gruen, M., Bommert, K., and Bargou, R. C. T-cell-mediated lysis of B cells induced by a CD19xCD3 bispecific single-chain antibody is perforin dependent and death receptor independent. *Cancer Immunol Immunother*, 53: 625-632, 2004.
156. Hirsch, R., Archibald, J., and Gress, R. E. Differential T cell hyporesponsiveness induced by in vivo administration of intact or F(ab')2 fragments of anti-CD3 monoclonal antibody. F(ab')2 fragments induce a selective T helper dysfunction. *J Immunol*, 147: 2088-2093, 1991.
157. Meijer, R. T., Yong, S. L., ten Berge, I. J., van Lier, R. A., and Schellekens, P. T. Non FcR-binding murine antihuman CD3 monoclonal antibody is capable of productive TCR signalling and induces proliferation in the presence of costimulation. *Clin Exp Immunol*, 123: 511-519, 2001.
158. von Herrath, M. G., Coon, B., Wolfe, T., and Chatenoud, L. Nonmitogenic CD3 antibody reverses virally induced (rat insulin promoter-lymphocytic choriomeningitis virus) autoimmune diabetes without impeding viral clearance. *J Immunol*, 168: 933-941, 2002.

-
159. Hirsch, R., Bluestone, J. A., Bare, C. V., and Gress, R. E. Advantages of F(ab')₂ fragments of anti-CD3 monoclonal antibody as compared to whole antibody as immunosuppressive agents in mice. *Transplant Proc*, *23*: 270-271, 1991.
 160. Brandl, C., Haas, C., d'Argouges, S., Fisch, T., Kufer, P., Brischwein, K., Prang, N., Bargou, R., Suzich, J., Baeuerle, P. A., and Hofmeister, R. The effect of dexamethasone on polyclonal T cell activation and redirected target cell lysis as induced by a CD19/CD3-bispecific single-chain antibody construct. *Cancer Immunol Immunother*, *56*: 1551-1563, 2007.
 161. Liedert, B., Bassus, S., Schneider, C. K., Kalinke, U., and Lower, J. Safety of phase I clinical trials with monoclonal antibodies in Germany--the regulatory requirements viewed in the aftermath of the TGN1412 disaster. *Int J Clin Pharmacol Ther*, *45*: 1-9, 2007.